

NUCLEASE-BASED EDITING IN THE PORCINE GENOME: A STRATEGY TO
FACILITATE PORCINE-TO HUMAN XENOTRANSPLANTATION

James R. Butler

Submitted to the faculty of the University Graduate School
in partial fulfillment of the requirements
for the degree
Doctor of Philosophy
in the Department of Medical and Molecular Genetics,
Indiana University

December 2017

Accepted by the Graduate Faculty, of Indiana University, in partial
fulfillment of the requirements for the degree of Doctor of Philosophy.

A. Joseph Tector, MD PhD.
Chair

Kenneth E. White, Ph.D.
Chair

Doctoral Committee

C. Max Schmidt, MD Ph.D.

18 April, 2017

Milan Radovich, Ph.D.

© 2017

James R. Butler

ACKNOWLEDGEMENTS

I express the utmost gratitude to Dr. A. Joseph Tector for giving me the opportunity to undertake the present inquiry under his guidance. Similarly, I am thankful for the camaraderie, discussion and assistance provided by Dr. Greg Martens, Dr. Matthew Tector, Joseph M. Ladowski, Dr. Richard Sidner, Dr. Zheng-yu Wang, Dr. Luz Reyes, Dr. Jose Estrada, Dr. Ping Li, Dr. Rafael Santos, Dr. Andy Lutz, Dr. Ray Chihara, and Sue Downey. I am indebted to my council members Drs. Kenneth E. White, C. Max Schmidt, and Milan Radovich, for providing invaluable counsel and direction. I am also grateful for support from the Indiana University Departments of Surgery and Medical and Molecular Genetics. This work was directly supported by Indiana University Health Transplant Division Department of Surgery, and grants awarded from the Association for Academic Surgery, and The American Society of Transplant Surgeons. Lastly, I am grateful for the patience and support provided by my family members.

James R. Butler

NUCLEASE-BASED EDITING IN THE PORCINE GENOME: A STRATEGY TO
FACILITATE PORCINE-TO HUMAN XENOTRANSPLANTATION

Solid organ transplantation is severely limited by a shortage of available donor allografts. Pig-to-human xenotransplantation offers a potential solution to this growing problem. For xenotransplantation to achieve clinical relevance, both immunologic and physiologic barriers must be understood. Genetic modification of pigs has proven to be a valuable means of both studying and eliminating these barriers. The present body of work describes a method for greatly increasing the efficiency and precision of genome editing within the porcine genome. By combining non-integrating selection and homologous recombination of exogenous oligonucleotides, a method for rapidly creating genetic modification without reliance on phenotypic sorting was achieved. Furthermore this work employs the technique of CRISPR/Cas9-directed mutagenesis to create and analyze several new animal models of porcine-to-human xenotransplantation with respect to both immunologic and physiologic parameters. First, Isoglobotrihexosylceramide -a controversial glycan to the field of xenotransplantation- was studied in a knockout model and found not to affect human-anti-porcine humoral reactions. Second, a new combination of glycan modifications is described that significantly lowers the human-anti-porcine humoral immune response. This model animal suggests that glycan-deletion alone will be sufficient to promote clinical application, and that conventional immunosuppression will be successful in mediating the human cellular response. Finally,

two potential *physiologic* barriers to xenotransplantation are studied in genetically modified model animals. Xenogenic consumption of human platelets was studied across hepatic and renal organ systems; xenogenic platelet consumption was reduced by glycan modifications to the porcine *liver* while human platelet sequestration was not identified in the study of *renal* endothelium. Porcine FcRN –an essential receptor expressed in kidneys to maintain serum proteostasis- was studied as a final potential barrier to pig-to-human renal transplantation. Because albumin is the primary driver of serum oncotic pressure, the protein-protein interaction of endogenous porcine FcRN and human albumin was studied. Porcine FcRN was found capable of binding human albumin under physiologic parameters. In summary, the results of the present work suggest that the salient barriers to clinical xenotransplantation have been removed and that porcine-to-human renal transplantation may soon offer an answer to the current organ shortage.

A. Joseph Tector M.D. Ph.D., Co-Chair

Kenneth E White, PhD., Co-Chair

TABLE OF CONTENTS

LIST OF TABLES	x
LIST OF FIGURES	xi
LIST OF ABBREVIATIONS	xiii
CHAPTER ONE: Introduction to Xenotransplantation and Genome Modification	1
CRISPR/Cas9 Nuclease	3
The origins of CRISPR	3
The path towards gene-targeted animals	5
Early nuclease technology	7
CRISPR at work	8
Evolving strategies of porcine gene-modification	9
Random Integration	11
Somatic Cell Nuclear Transfer	11
Homologous Recombination	12
Nuclease Editing	14
Zinc Finger and TALEN Nuclease	16
Off-target effects	17
Nuclease-based transgene delivery	18
CHAPTER TWO: Efficient generation of targeted and controlled mutational events in porcine cells using nuclease-directed homologous recombination	22
INTRODUCTION	22
MATERIALS AND METHODS	24
Porcine aortic cell isolation and culture	24
Creation of an immortalized AEC line	25
Cas9 guide RNA and DNA oligonucleotide assembly	25
Transfection and cell sorting by non-integrating selection	26
Analysis of phenotype-specific mutation efficiency	26
Analysis of genotypic mutation efficiency	27
HDR-directed mutagenesis	28
Analysis of HDR-directed genome editing	29
Genetic knock-in with homology-directed repair	30
RESULTS	31
Phenotype-specific mutation efficiency is increased with non-integrating selection ...	31
Genotypic mutation efficiency is increased with non-integrating selection	31
HDR-directed genome editing	33
Genetic knock-in with homology-directed repair	36
DISCUSSION	39
CHAPTER THREE: Silencing the porcine iGb3s gene does not affect Gal α 3Gal levels or measures of anticipated pig-to-human and pig-to primate acute rejection.	45
INTRODUCTION	45
MATERIALS AND METHODS	50
Knockout constructs	50
Selection and Genotyping	50
Somatic cell nuclear transfer (SCNT)	51
A3GalT2 locus silence verification	51

α Gal Phenotype analysis	52
Tissue staining and confocal microscopy.....	52
Antibody binding	53
Complement-mediated cytotoxicity	54
Glycosphingolipid analysis.	55
RESULTS	56
Gene knockout pigs.....	56
α -Gal phenotype analysis.....	58
Tissue staining and confocal microscopy.....	60
Antibody binding	60
Antibody-dependent complement-mediated cytotoxicity	62
Glycosphingolipid Analysis	64
DISCUSSION.....	67
CHAPTER FOUR: Silencing porcine genes significantly reduces human-anti-pig cytotoxicity profiles: an alternative to direct complement regulation.	71
INTRODUCTION	71
MATERIALS AND METHODS.....	75
Construction of hCD55 Plasmid	75
Production of Genetically modified animals.....	76
Antibody binding	76
Antibody-mediated complement-dependent cytotoxicity	77
Statistics	78
Tissue staining and confocal microscopy.....	78
RESULTS	80
DISCUSSION.....	86
CHAPTER FIVE: Modified glycan models of pig-to-human xenotransplantation do not enhance the human-anti-pig T cell response.....	89
INTRODUCTION	89
MATERIALS AND METHODS.....	92
Modified Porcine Cell Construction	92
Preparation of Stimulator Populations	93
Preparation of Responder Populations	93
BrdU ELISA based Mixed lymphocyte reaction (MLR) assay	93
Immunosuppressive treatment during MLR	94
RESULTS	96
Creation of modified porcine cells.....	96
BrdU ELISA based Mixed lymphocyte reaction (MLR) assay	97
Effect of Immunosuppression on xenogenic human CD4 T cell proliferation in vitro	101
DISCUSSION.....	103
CHAPTER SIX: The fate of human platelets exposed to porcine renal endothelium: a single-pass model of platelet uptake in domestic and genetically modified porcine organs.	107
INTRODUCTION	107
MATERIALS AND METHODS.....	112
Creation of genetically modified pigs.....	112

Isolation and staining of autologous (donor animal) platelets for perfusion.....	112
Isolation and staining of human platelets.....	113
Procurement and preparation of porcine organs	113
Perfusion of organs.....	114
Measuring of Fluorescence	115
Confocal for Biopsy	115
In Vitro Platelet Up-Take.....	116
Confocal analysis of endothelial lines.....	117
RESULTS	119
DNA sequencing analysis of the cloned pigs.....	119
Analysis of human platelet uptake	120
DISCUSSION.....	127
CHAPTER SEVEN: Silencing porcine CMAH and GGTA1 genes significantly reduces xenogeneic consumption of human platelets by porcine livers.	131
INTRODUCTION	131
MATERIALS AND METHODS.....	134
Genetically modified pigs	134
Platelet Isolation and Staining.....	134
Perfusion of Livers	135
Measuring Xenogeneic Human Platelet Consumption	136
Staining and Confocal Microscopy	136
RESULTS	138
Analysis of in Vitro Human Platelet Uptake.....	138
Analysis of Ex Vivo Perfusion with Human Platelets	140
DISCUSSION.....	145
CHAPTER EIGHT: Conserved FcRN-albumin interactions across species: implications for porcine-to-human renal xenotransplantation.....	148
INTRODUCTION	148
MATERIALS AND METHODS.....	153
Intravital 2-photon microscopy	153
Fluorescent labeling of human albumin	153
Porcine kidney preparation and microcopy.....	154
In vitro proximal tubule cell analysis.....	154
Kinetics analysis of FcRN-Albumin interaction	155
In vivo evaluation of proteinuria	156
RESULTS	157
DISCUSSION.....	164
CLOSING REMARKS.....	166
REFERENCES	169
CURRICULUM VITAE	

LIST OF TABLES

Table 1.1: Nuclease Classes.....	15
Table 1.2: The creation of pigs carrying unique genetic alterations.....	20
Table 4.1: Interpretation of Flow Cytometric Crossmatch values for allograft allocation.....	74

LIST OF FIGURES

Figure 1.1: The growing gap between Unites States solid organ waitlist patients and available organs.	2
Figure 1.2: Gene Knockout strategies.....	13
Figure 2.1: Non-integrating (NI) selection enhances nuclease mediated phenotypic and genotypic mutation efficiency.....	32
Figure 2.2: Design and use of exogenous DNA oligomers in nuclease-mediated genome editing.....	34
Figure 2.3: Homology-directed repair by short exogenous oligomers facilitates increased gene silencing.	36
Figure 2.4: Locus-specific transgene delivery to the porcine genome facilitated by nuclease-targeted homology driven insertion.	38
Figure 2.5: Nuclease-based genetic insertion strategy.....	41
Figure 3.1: Illustration of alpha Gal and iGb3.....	47
Figure 3.2: Nuclease-driven silencing of the isoglobotrihexosylceramide 3 synthase production in porcine tissue and cells.....	57
Figure 3.3: Ib4 binding profiles of iGb3s knockout pig cells.....	59
Figure 3.4: Confocal analysis of IB4 binding to iGb3s knockout pig tissues.....	60
Figure 3.5: Baboon and human antibody binding profiles of iGb3s knockout pig cells.....	61
Figure 3.6: Antibody-mediated complement-dependent cytotoxicity of baboon and human sera against GGTA1-null or A3GalT2/GGTA1-null cells.....	63
Figure 3.7: Liquid chromatography analysis of kidney tissue from wild type and A3GalT2-null animals.	66
Figure 4.1: Phenotypic silence of porcine carbohydrate genes.....	81
Figure 4.2: Transgenic expression of hCD55 on porcine tissue and cells.....	82
Figure 4.3: Human antibody binding directed towards porcine cells.	83
Figure 4.4: Human antibody-mediated complement-depended cytotoxicity to porcine cells.	84
Figure 4.5: Antibody-mediated complement-depended cytotoxicity is related to human IgM levels.	85
Figure 5.1: Targeted Genetic Disruptions.....	96
Figure 5.2: Stimulation Indices of allogeneic and xenogeneic mixed lymphocyte reactions.....	98
Figure 5.3: Stimulation Indices of allogeneic and xenogeneic mixed lymphocyte reactions in the presence of dexamethasone.	100
Figure 5.4. Effect of Immunosuppression agents on human T cell proliferation.	102
Figure 6.1: Porcine Von Willebrands Factor A1 Domain.	110
Figure 6.2: Genotype of Genetically Modified Pigs.....	120
Figure 6.3: A single pass model of platelet uptake.....	122
Figure 6.4: Biopsy Samples from human platelet perfusion.....	124
Figure 6.5: Confocal Imaging of In vitro Uptake.	126
Figure 7.1: Human platelet accumulation by GGTA1 ^{-/-} CMAH ^{-/-} , GGTA1 ^{-/-} , ASGR1 ^{-/-} and WT liver sinusoidal endothelial cells in vitro.	139

Figure 7.2: A Continuous-pass model for the xenogenic consumption of human platelets by modified porcine livers.....	141
Figure 7.3: A single-pass model of human platelet uptake for GGTA1 ^{-/-} CMAH ^{-/-} and ASGR1 ^{-/-} livers.....	143
Figure 8.1: FcRN mediated albumin absorption at the proximal tubule.....	150
Figure 8.2: FcRn receptor sequence is highly conserved across species.....	151
Figure 8.3: Human albumin in the porcine kidney: filtered and absorbed.	158
Figure 8.4: Surface plasmon resonance analysis of FcRn-albumin kinetics.	160
Figure 8.5: Urine protein over time in a pig-to-primate model of xenotransplantation.....	162

LIST OF ABBREVIATIONS

α Gal	Alpha 1,3-galactose
AA	Amino acid
AMR	Antibody-mediated rejection
ANOVA	Analysis of variance
A3GalT2	Gene encoding Alpha 1,3-Galactosyltransferase 2
cDNA	cDNA
CD55	Gene encoding complement decay accelerating factor ('hDAF')
CRISPR	Clustered Regularly Interspaced Short Palindromic Repeats,
Cas9	CRISPR associated protein 9
CMAH	Gene encoding Putative cytidine monophosphate-N-Acetylneuraminic acid hydroxylase-like protein
DAPI	4',6-diamidino-2-phenylindole
DSB	Double-Strand Break (relevant to DNA cleavage)
DEG	Differentially expressed genes
DNA	Deoxyribonucleic acid
DRG	Dorsal root ganglia
EcoRI	Escherichia coli RI endonuclease
FBS	Fetal bovine serum
gDNA	Genomic DNA
GGTA1	Gene encoding Alpha-1,3-galactosyltransferase
GFP	green fluorescent protein
GTKO	GGTA1 biallelic knockout
HR	Homologous recombination
HDR	Homology-directed repair
H&E	Hematoxylin and eosin
iGB3	isoglobotrihexosylceramide, or isogloboside 3
IHC	Immunohistochemistry
IL-6	Interleukin 6
IRES	Internal ribosome entry site
mRNA	Messenger ribonucleic acid
Neu5Gc	N-Glycolylneuraminic acid
NHEJ	Non homologous end joining
PAM	Protospacer adjacent motif
P	Passage
PBS	Phosphate-buffered saline
PCR	Polymerase chain reaction
PFA	Paraformaldehyde
PBMC	Peripheral blood mononuclear cells
PI	Propidium iodide
RNA	Ribonucleic acid
SCNT	Somatic cell nuclear transfer
sgRNA	Single-guide RNA (combines tracrRNA and crRNA)
TALEN	Transcription activator-like effector nucleases
qRT-PCR	Quantitative reverse transcription polymerase chain reaction

RHD	Relative homology domain
SDS	Sodium dodecyl sulfate
SDS-PAGE	SDS polyacrylamide gel electrophoresis
SEM	Standard error of the mean
TAD	Transactivation domain
TNF- α	Tumor Necrosis Factor Alpha
WT	Wild type
ZFN	Zinc Finger Nuclease

CHAPTER ONE: Introduction to Xenotransplantation and Genome Modification

The treatment for end stage organ failure has been transformed by solid organ transplantation. Unfortunately today, a growing shortage of donor allografts severely limits the reach of this treatment. The solid organ waitlist has over 180,000 patients in the United States, and each year this number continues to grow, matched against a relatively static supply of available organs for transplant (Figure 1.1). Every 14 minutes, someone is added to the renal transplant list alone. Not considering those patients that are deemed too sick to be placed on the waiting list, 13 patients die each day while waiting for a kidney transplant. Xenotransplantation, the transplantation of organs across species, has been proposed as a potential solution to this growing problem. Owing to certain gestational, immunologic and physiologic properties, pigs have been identified as the best potential surrogate organ donor. However, for pig-to-human xenotransplantation to be realized as a treatment, several important immunologic and physiologic barriers must be studied and overcome. Genetic modification of porcine models has proven valuable to the study of porcine-to-human xenotransplantation. Recent advances in genetic engineering, coupled with somatic cell nuclear transfer has greatly sped up the process of model animal creation. Moving from model to treatment will require improvements to the efficiency and precision of these tools; this is a central pursuit in the present body of work.

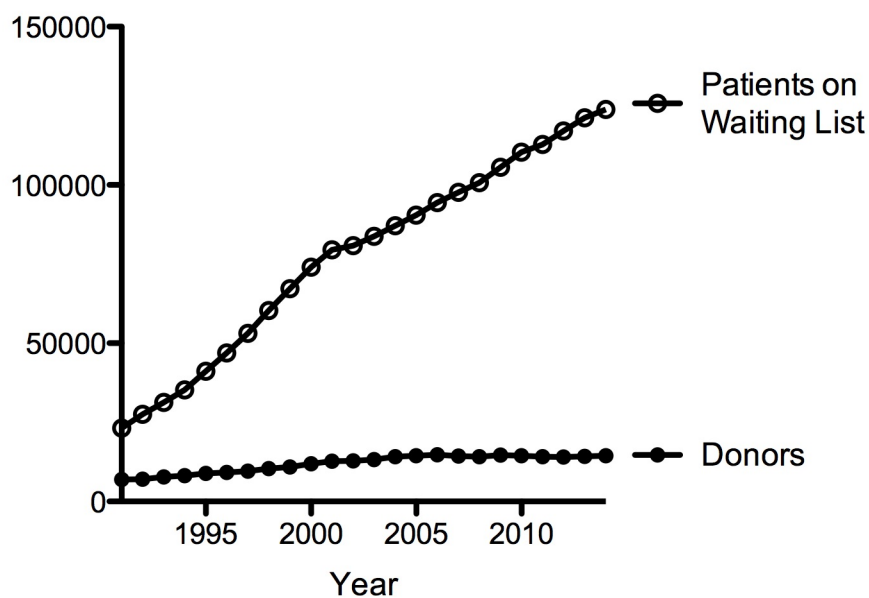


Figure 1.1: The growing gap between United States solid organ waitlist patients and available organs.

The gap between available organs for transplant and patients on the solid organ transplant list has existed since the beginning of organ transplantation. Despite attempts to utilize available solid organs more liberally, this gap continues to grow. Today there are more than 180,000 patients on the transplant waitlist in the United States alone; for many patients each day this will mean death without transplantation. Not captured in these figures are the many patients evaluated at transplant centers but unlisted due to prioritization of healthier recipients in the face of systemic organ shortages.

CRISPR/Cas9 Nuclease

Though genetic engineering has a long history, the present work is uniquely indebted to the CRISPR/Cas9 platform of genome modification; as such, these tools are deserving of a dedicated introduction. Few scientific revolutions have offered greater potential to both research and therapy than the advent of CRISPR genome-editing. CRISPR gene-targeting represents three advantages relative to previous tools. First, the flexibility in target-design coupled with recent advances in genomic sequencing allows for unparalleled ease in gene-targeting. Second, CRISPR allows investigators to effect multiple site-specific alterations concurrently. Third, the versatility of the platform offers a wide repertoire of effects to achieve complete control over the targeted loci. The potential applications of CRISPR-engineering range from plants to animals, infectious disease to cancer. At the most elemental level, CRISPR has sped the pace of creating new animal models for the study of human disease. Moving quickly from model to potential treatment, pig-to-human xenotransplantation offers one of the most immediate opportunities for clinical application of this technology: an answer to the growing shortage of available organs for transplant.

The origins of CRISPR

Since its recent discovery, CRISPR technology has steadily been distinguishing itself as the greatest medical breakthrough to come from prokaryotes since Alexander Fleming noticed a contaminant strain of *Penicillium notatum* clearing *Staphylococcus* cultures. With an equal amount of serendipity, CRISPR can trace its prokaryotic origins to a

Danish yogurt company. There, scientists were working to promote viral resistance in *Streptococcus thermophilus*, a bacterium needed for yogurt production; they observed that short palindrome sequences -mirror images within the DNA separated by a short spacing sequence- provided acquired immunity against foreign genetic elements. In bacteria, foreign DNA is digested and inserted into the CRISPR locus, from which CRISPR RNA (crRNA) is made.[1] These short RNA sequences then associate with homologous –presumably foreign- sequences in the genome. When the homologous genomic sequence is followed by an appropriate ‘protospacer-adjacent motif’ (PAM) at the 3’ end, the Cas9 endonuclease creates a DSB. (Figure 1.2 A₁) The PAM spacer helps prevent the CRISPR-locus itself from being targeted.[2] In 2007 they published their findings that *clustered regularly interspaced short palindromic repeats* (CRISPR) and *CRISPR-associated proteins* [Cas] were adaptable agents of prokaryotic immunity. [3]

Over the next several years in laboratories across the world, the mechanisms of this system underwent a series of pivotal discoveries that would help recognize CRISPR as a potential agent of DNA manipulation. [4-8] In August of 2012 the CRISPR/Cas9 system was realized as a programmable platform for targeted genome editing.[9] By February of the following year, CRISPR/Cas9 was successfully used to introduce targeted genetic manipulation in a range of mammalian species, including the human genome.[10]

The path towards gene-targeted animals

CRISPR/Cas9 technology currently represents the most advanced method of effecting genetic alteration; its importance is best understood in context with the recent history of mammalian genome editing. Capecchi, Smithies, and Evans first developed methods to create targeted alterations in the mouse genome more than 20 years ago.[11] By discovering that mammalian cells could incorporate exogenous DNA into their genome through a process of *homologous recombination*, they were able to produce the first site-specific mutations. Although tedious –about 1 in 1,000 attempts would succeed[12]- this process represented a paradigm shift for somatic cell genetics. When these results were reproduced in embryonic stem cells (ES), followed by injection of modified cells directly into a pre-implanted blastocyst, the first gene-targeted mice were created.

Pigs offer multiple advantages over mice as models for human research due to their morphologic, physiologic, immunologic and gestational properties.[13, 14] Similarly, pigs have been identified as the most suitable surrogate for human allografts in Xenotransplantation.[15] Unfortunately porcine ES cells are not available.[16] Because of this -and the supposition that somatic differentiation was unidirectional- the creation of gene-targeted pigs was considered impossible. This barrier was eliminated in 1997 when a mammary epithelial cell was fused with an enucleated egg. By this process, a somatic cell metamorphosed into an embryonic cell capable of producing a cloned sheep.[17] This process of somatic cell nuclear transfer (SCNT) has now become of central importance to the field of xenotransplantation. In the continued absence of reliable pig embryonic stem cells, gene-targeted pigs are created from modified somatic cells. In 2000, SCNT produced the first wild-type clonal pigs;[18] two years later, the first gene-

targeted pig was cloned from cells edited by the same process of *homologous recombination* that had been used to create model mice.[19]

Early nuclease technology

Site-specific endonuclease technology actually predates the CRISPR/Cas9 system by several years and began shifting attention away from homology-driven gene targeting by 2002.[20] Endonucleases are DNA-cutting enzymes that create a double strand break (DSB) in DNA. Nuclease-driven DSBs are subsequently repaired by non-homologous end joining (NHEJ). Because NHEJ is a relatively low fidelity process, the repaired DNA often includes small insertions or deletions that result in a null phenotype. By artificially tethering an endonuclease to sequence-specific DNA binding proteins such as transcription activator-like effectors or zinc-fingers, targeted genetic mutation could be delivered to the mammalian genome.[21] In 2011 zinc-finger nucleases (ZFNs) were utilized to create true knockout pigs in 5 months instead of 36 months.[22]

The discovery of CRISPR/Cas9 as a *naturally occurring* sequence-targeting nuclease system offers an opportunity to capitalize on efficiencies forged over millions of years in bacterial evolution. In bacteria, foreign (viral) DNA is digested and inserted into the CRISPR locus, from which CRISPR RNA (crRNA) is transcribed. Short crRNA combine with trans-activating RNA which then act as mobile guides that scour the entire genome for their DNA homologs, marking unwanted viral inserts. When the homologous genomic sequence is followed by an appropriate 3' *protospacer-adjacent motif* (PAM), the Cas9 endonuclease is recruited and creates a DSB. The most commonly used system originates from *Streptococcus pyogenes*, which has a 3' PAM sequence of NGG, where N represents any nucleotide.[9] This system allows for the creation of a mutation event in any porcine genomic sequence consisting of GN₁₉NGG. This process may be reappropriated to target any loci in any genome by simply introducing exogenous guide

RNA sequences together with Cas9 to the nuclei. In this way, genome-editing has quickly become fast, reliable and affordable.

CRISPR at work

Applications of the CRISPR platform for genome editing are now pervasive. The use of tissue-specific promoters to drive Cas9 expression allows CRISPR to target virtually any loci in a tissue-specific manner. Recently, cardiac-specific[23] and lung-specific²¹ applications have been described, this will allow for the rapid creation of new models of heart and lung disease. Coupled with the plasticity of CRISPR gene-targeting, this may eventually offer a method to achieve targeted and sustained control of even the most challenging genetic problems, like the heterogeneous nature of pancreatic or non-squamous cell lung carcinomas.

Today, one of the most immediate applications for CRISPR technology is pig-to-human xenotransplantation. As new models move closer to clinical relevance, CRISPR-modified pigs now offer a potential answer to the single largest problem facing the field of transplantation: a growing shortage of transplantable organs. CRISPR technology has greatly sped the process of creating genetically modified pigs. In 2014, CRISPR was used to silence 3 separate porcine genes in a single reaction, creating pigs of multiple genetic modifications within a single pregnancy.[24] Later that year, a Class 1 MHC-null pig was created, representing the simultaneous silencing of 7 porcine alleles within a single reaction.[25] The number of concurrently targeted loci within the porcine genome has since increased as high as 62.[26] CRISPR's ability to efficiently target multiple loci has

also facilitated the recent discovery of triple-gene knockout pigs that exhibit very low levels of human antibody binding.[27] As described within the present body of work, measures of human-anti-porcine humoral immunity can now be reduced to levels comparable with allograft transplantation;[28] clinical xenotransplantation is closer than ever. Although the full potential of CRISPR genome-editing is almost certainly not yet realized, it represents a technology worth watching for both researchers and clinicians.

Evolving strategies of porcine gene-modification

A central hypothesis of the present work is that *gene-knockout* pigs hold great promise for creating donor animals that will be suitable for clinical xenotransplantation. Specifically, this work privileges the study of gene-modifications that affect the porcine *glycome*. The immunologic potential of carbohydrate profiles has been recognized since the early 1900s when De Landsteiner received the Nobel Prize for characterizing ABO blood groups in his study of allogenic blood transfusion. Later understood to be driven by the ABO glycosyltransferase on chromosome 9q34.1, this enzyme creates glycoproteins that are among the most important antigens in allograft matching. Because these glycosyltransferases imprint *many* proteins through post-translational modification their immunologic significance is leveraged. Similarly, species-specific glysylation patterns have the potential to create powerful sources of xenoantigens that –if unmodified- would prohibit successful xenotransplantation. The present work recognizes the importance of two important carbohydrate xenoantigens to which humans have xenoreactive antibodies: gal- α -(1,3)-gal, and N-glycolylneuraminic acid (Neu5Gc). These xenoantigens are

produced by enzymes that are present in humans and pigs, but in humans, gene activity has been silenced during the course of evolution. α -1,3-galactosyltransferase (GGTA1) produces the Gal α (1,3) Gal epitope, and the development of GGTA1^{-/-} pigs eliminated 70-85% of the xenoreactive antibodies that humans have as a barrier to xenotransplantation. The cytidine monophosphate-N-acetylneuraminic acid hydroxylase (CMAH) gene produces N-Glycolylneuraminic acid (Neu5Gc). The creation of GGTA1^{-/-} CMAH^{-/-} pigs has further reduced human antibody binding to the point where the crossmatch of pigs with humans is more favorable than a primate-to-human crossmatch. [29] As described later in the present body of work, the CRISPR/Cas9 system has now been used to simultaneously silence 3 glycome-modifying porcine genes; the majority of *humans* now exhibit very low levels of antibody binding to cells from this triple knockout pig.

Although it is our belief that the present findings will help solidify the clinical relevance of carbohydrate *knockout* models, this approach has not always been favoured by the field. As aforementioned, the creation of gene-targeted pigs has traditionally been slow and tedious because of the lack of identifiable embryonic stem cells (ES) in the pig, the reliance upon homologous recombination to create targeted gene deletions, and the subsequent need for lengthy breeding programs to create homozygous knockout pigs. In this climate it was difficult to efficiently create true knockout animals. Because of these barriers, human transgene delivery into the porcine genome has been the dominant strategy of pig-to-human xenotransplantation research. The difficult road towards efficient porcine knockout model creation is best understood by examining recent strategies to remove the first-discovered porcine xenoantigen: α Gal (GGTA1).

Random Integration

Initially, due to the absence of pig ES, creating a true genetic knockout pig was not feasible. In this era, attention focused on transgenic methods to regulate α Gal expression. The process of ‘competitive glycosylation’ involved inserting a gene for a fucosyltransferase or sialyltransferase; [30] by depleting the common acceptor substrate N-acetyllactosamine, α Gal was competitively replaced with less immunoreactive oligosaccharides. At the genomic level, one such method placed a human cDNA fucosyltransferase -under CMV and H2K-b promoters- into the pig genome by embryo microinjection. [31] Despite variable and mosaic expression patterns, this method was successful in *reducing* α Gal expression.

Somatic Cell Nuclear Transfer

One of the early barriers to creating genetically modified pigs was the biologic tenet that cellular differentiation is unidirectional. This dogma was rewritten in 1997 when a mammary epithelial cell was used to create an embryonic cell. [17] Fused with an enucleated egg, a somatic sheep cell was redesigned to become an embryonic cell capable of producing a cloned sheep. This process of somatic cell nuclear transfer (SCNT) has now become of central importance to the field of xenotransplantation. In the absence of pig embryonic stem cells, genetically modified pigs are created directly from somatic cell modification; by 2000, SCNT was successfully used to clone pigs. [18, 19]

Homologous Recombination

With new ability to create clonal animals from somatic cell nuclear donors, the field shifted focus from microinjection of randomly integrating transgenes towards site-directed mutagenesis. The first of these gene-targeting strategies was homologous recombination (Figure 1.2B). In 2002, Lai et al used a gene trap-targeting vector, pGalGT, for homologous replacement of the endogenous GGTA1 allele;[19] after antibiotic selection and SCNT, 4 single-allele knockout pigs were created. Later that year, Phelps et al. accelerated the production of a double α Gal knockout pig by employing three consecutive rounds of cloning instead of backcross breeding.[32] In this process, heterozygous fetal fibroblasts were isolated from a pregnancy and subjected to a second ATG-targeting knockout vector with antibiotic selection. After enrichment for α Gal - cells by *C. difficile* toxin A, the second allele was found to be serendipitously disrupted by a rare spontaneous mutation. Aside from this one spontaneous mutation, antibiotic selection markers complicated homologous recombination strategies; the obligatory insertion of exogenous genes of antibiotic resistance limited clinical application of these animals.

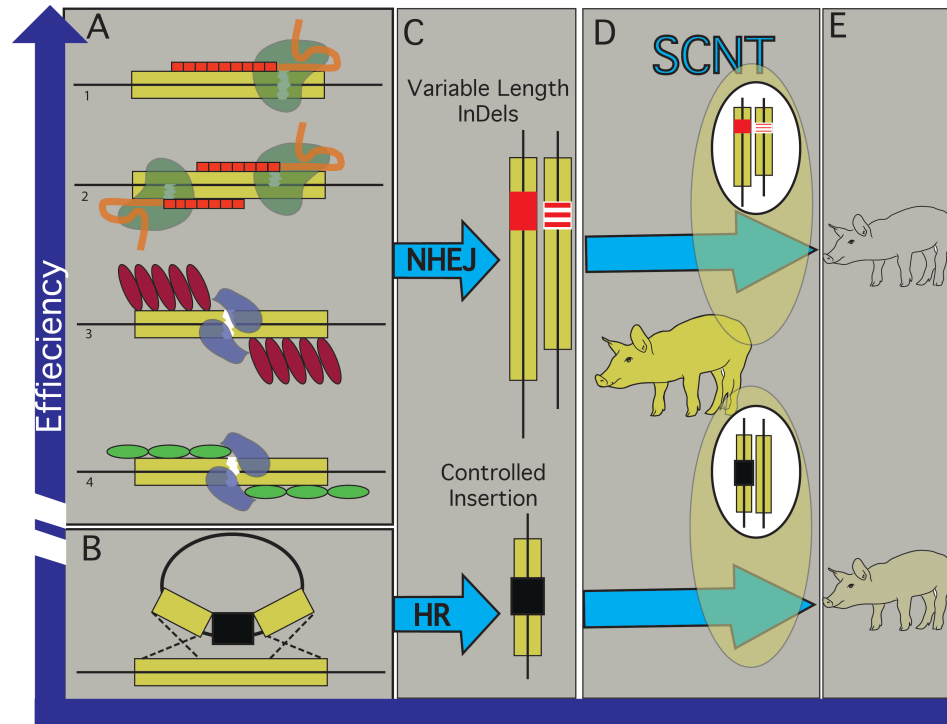


Figure 1.2: Gene Knockout strategies.

A depicts site-specific nuclease-based editing tools. **A₁**: CRISPR targets Cas9 to create a double stranded break. **A₂**: The Nickase system targets a mutant Cas9 to create two adjacent single-strand breaks. **A₃**: TALENs dimerize two FokI units to create a double strand break. **A₄**: Zinc Fingers similarly dimerize two FokI units to create a double strand break. **B** depicts homologous recombination technique. A donor plasmid is built with homologous arms flanking an exogenous selection marker. **C** depicts the resulting mutation events. DSBs are repaired by error-prone NHEJ to create variable-length insertions or deletions. This may simultaneously affect both alleles. Homologous recombination targets cell division, where the donor plasmid homology arms cross over with the genomic DNA, disrupting the loci by inserting an exogenous marker. **D** Somatic cell nuclear transfer (SCNT) uses the mutated cell to create a clonal animal. **E** Due to low

efficiency, HR most often affects one allele, while with appropriate selection, nuclease-based approaches may create a biallelic knockout within a single reaction.

Nuclease Editing

Site-specific nuclease technology shifted attention away from homology-driven recombination knockout. Table 1.1 compares the 4 nuclease classes. Broadly speaking, these strategies involve creating a double-strand break (DSB) by targeting a bacterial nuclease to a specific genomic sequence. Nuclease-driven DSBs are subsequently repaired by the error-prone process of non-homologous end joining (NHEJ). The product often includes small deletions or insertions that yield missense or nonsense mutations and a null phenotype. (Figure 1.2C-E) Alternatively, homology-directed repair (HDR) offers the opportunity to control the mutation event.[33] By co-transfecting a site-specific nuclease with oligonucleotides or donor sequences containing locus-specific homology to the DSB site, a specific insertion may be created.[34] Regardless of repair pathway, the introduction of DSBs can increase the random recombination frequency from 1 event per 10^6 cells to 1 in 5 cells.[35]

Table 1.1: Nuclease Classes

	ZFNs	TALENs	CRISPR	Nickase
Nuclease	FokI	FokI	Cas9	mCas9
gDNA Targeting Mechanism	Zinc-finger protein	Transcription activator-like effector	sgRNA	sgRNA
Target Design Requirements	G-rich	Begin with T; end with A	GN19/NGG	2(GN19/NGG)
Specific Length of Target Site	18-36 bp	30-40bp	22bp	22bp
Mutation Rate*	Low (10%)	High (20%)	High (20-75%)	High (20%)
Off-target Effects	High	Low	Variable**	Very Low
Cytotoxicity	High	Low	Variable	Very Low
Size	1KB	1KB	4.2KB	4.2KB
Commercial Cost per Target	\$4,000-7,000	\$3,3600-\$5,000	\$500	\$500

ZFN, zinc-finger nuclease. TALEN, Transcription activator-like effector nuclease. CRISPR, clustered regularly interspaces short palindromic repeat. Cas9, CRISPR-associated protein 9. gDNA, genomic DNA. sgRNA, single guide RNA. N, any nucleotide. *Mutation rates reported are variable across the literature and depend on cell-type and delivery method, they are commonly defined as the frequency of insertion or deletion without respect to phenotype. ** CRISPR/Cas9 off-target rates may be controlled during the design of sgRNA targets by bioinformatics query against the genome of interest.[36] Commercial cost calculated based on Biocompare data (Biocompare, San Francisco, CA. USA).

Zinc Finger and TALEN Nuclease

In 2010, Zinc Finger Nucleases (ZFN) offered the first of the site-directed approaches used in the porcine genome. [37] ZFNs are fusions of a nonspecific DNA cleavage motif with a sequence-specific zinc finger protein. (Figure 1.2A₄) The nuclease activity is a derivative of the FokI bacterial restriction endonuclease, capable of creating a single strand break. ZFNs operate in concert by dimerizing two DNA-binding domains with two FokI enzymes to produce DSBs with 18bp targeting specificity. The subsequent damage response pathway of NHEJ afford ZFNs their mutagenic potential. (Figure 1.2C) In 2013 ZFN were used to create a biallelic knockout of both the α Gal and CMAH genes in vitro prior to SCNT; this set an important precedent of using endonuclease technology to remove two xenoantigens from a wild-type genome within 7 months.[38]

Transcription activator-like effector nucleases (TALENs) were introduced to the porcine genome in 2011, and function like ZFNs to create DSBs by tethering the FokI endonuclease to DNA binding domains.[39] (Figure 1.2A₃) In 2013, TALENs were used to create biallelic GGTA1 knockout pigs. In this process, the targeting efficiency of TALEN-directed mutagenesis has been reported with efficiencies reaching 73.1% with a 27.8% rate of biallelic knockout.[40] TALENs may be distinguished from ZFNs by their ease of design, decreased cost, and marginally improved targeting frequencies.

Off-target effects

Understanding the potential for off-target effect of nuclease-based genomic editing is essential as new porcine models become clinically relevant. An off target effect is created when a mutation event occurs outside the targeted locus. Early recognition of this phenomenon began with ZFN-cytotoxicity, presumably caused by target sequence homology to multiple and unintended loci. Because the active ZFN is a dimer with each 3-Finger side recognizing 9 bps, the combination should recognize a unique 18bp sequence. However, due to symmetry at the FokI interface, homodimerization is possible, which reduces the specificity to 9bp. [35] Successful strategies to avoid this have been adopted and include an altered FokI incapable of homodimerization and the creation of a highly-specific 5-finger ZFN. [41] Conversely, it has recently been suggested that *shortening* the guide RNA molecule for Cas9 may increase CRISPR site specificity.[42]

A second approach to limiting off-target endonuclease effect is the adoption of ZFN and Cas9 Nickases. By inactivating one of the ZFN monomers or mutating Cas9, Nickase strategy relegates the endonuclease capable of inflicting only single strand breaks.[43, 44] In both scenarios, the resulting single strand break favors the HDR repair pathway over NHEJ. Because single strand breaks are often repaired without error, off target hits are overwhelmingly silent.[45] Nickase-driven mutagenesis remains possible by *co-transfecting* a ZFN nickase with a homologous oligonucleotide or *co-localizing* two independent Cas9-nickases. (Figure 1.2 A₂) Off-target limits for CRISPR/Cas9 sgRNA can be incorporated into the design process by using bioinformatics to query possible off-target binding sites; avoiding guide sequences that bind to multiple regions within the genome and limiting possible off-targets to non-coding regions can

significantly reduce background.[36] Even in the absence of these specificity-enhancing techniques, recent studies employing whole-genome sequencing suggest very low rates of off-target effects of conventional endonuclease technique.[46] Importantly, off-target effects have not limited the ability to employ nuclease based editing tools for the creation of healthy donor animals through SCNT.

Nuclease-based transgene delivery

As reported later within the present work, nuclease-created DSBs also have the ability to facilitate efficient transgene delivery. By co-transfecting a site-specific nuclease with an exogenous gene flanked by locus-specific homology arms to the DSB site, an exogenous sequence may be successfully inserted. (Chapter Two) This combines the initial process of HR with modern nuclease-based editing to exponentially increase both the frequency and specificity of transgene insertion. Where once, a randomly integrated transgene was the only tool, nuclease-based techniques now offer simultaneous ability to insert and delete genetic material. Genetic engineering has transitioned from random addition of genes and expression cassettes to site-specific deletion or addition of genetic material.

The pace of genetic engineering has changed rapidly over the past five years. Understanding the capability of nuclease-based editing has led to a dramatic increase in the productivity of our field. As displayed in Table 1.2, the published numbers of genetically unique animals is increasing dramatically. Where once it took 36 months to create a biallelic knockout animal, multiple-gene knockout animals can be reliably produced within 6 months.[47] These tools have brought xenotransplantation closer to

the clinic than it has ever been. Described within the present work, a triple knockout animal has now been created that exhibits a negative antibody-mediated complement-dependent crossmatch on the majority of patients currently on a solid organ waitlist (Chapter Four). One of the greatest achievements in transplant medicine was the early adoption of calcineurin inhibitors; by controlling the early immunologic injury, it revolutionized allotransplantation into a reliable treatment. The central aim of the present body of work is that we may soon come to recognize nuclease-based genetic engineering as the catalyst that turns xenotransplantation into a clinical reality.

Table 1.2: The creation of pigs carrying unique genetic alterations.

First Author (Year)	Modification	Technique
Fodor (1994) [48]	Human CD59 +	Random integration (H2kb-hCD59 DNA for embryo injection)
Cozzi (1995) [49]	Human CD55 +	Random integration (6.5 kilobase DNA construct with the 4kb hDAF)
Osman (1997) [50]	Human GLA +	Random integration (pH2kb-hHT)
Costa (1999) [31]	Human H-transferase +	Random integration (H2Kb-HT construct)
Diamond (2001) [51]	Human CD46 +	Random integration (60kb genomic construct with CD46)
Miyagawa (2001) [52]	Human GnT-III +	Random integration (pCX vector-GnT-III)
Lai (2002) [19]	GGTA1 -/+	Homologous recombination
Phelps (2003) [32]	GGTA1 -/-	Homologous recombination, back cross
Klose (2005) [53]	Human TRAIL +	Random integration (TRAIL in pUCH2XXS-TRAIL)
Wu (2007) [54]	Human DAF and MCP +	Random integration
Dieckhoff (2008) [55]	PERV siRNA	Random integration (pLVTHM-pol2 with shRNA)
Phelps (2009) [56]	Porcine CTLA4-Ig +	Random integration (pCTLA4-Ig with CHS and CH3 linker of IgG1)
Peterson (2009) [57]	Human thrombomodulin +	Random integration (hTM in pEGFP-N1)
Weiss (2009) [58]	HLA-E/Human Beta-2-microglobulin +	Random integration (HLA-B7 in pCR2.1-TOPO)
Oropeza (2009) [59]	Human A20 +	Random integration (pCAGGSEhA20-IRESNEO)
Yazaki (2009) [60]	Endo-B-Galactosidase + and Human CD55 +	Random integration (pCAG-hDAF-p(A)) and (pCAGGS/GT+EdnoGalC-neo)

Hara (2010) [61]	CIITA-DN +	Random integration
Seol (2010) [62]	Human Fas Ligand +	Random integration (pcDNA/FasL)
Cho (2011) [63]	Human TNFRI-Fc +	Random integration (shTNFRI-Fc)
Yeom (2012) [64]	Human heme oxygenase 1 +	Random integration (SV40-hHO-I)
Wheeler (2012) [65]	Human CD39 +	Random integration (H2Kb-hCD39)
Klymiuk (2012) [66]	LEA29Y +	Random integration (LEA29Y in B-cell specific expression vector)
Lutz (2013) [38]	GGTA1 ^{-/-} CMAH ^{-/-}	ZFN
LI (2014) [47]	GGTA1 ^{-/-} CMAH ^{-/-} IGb3S ^{-/-}	CRISPR/Cas9
LI (2014) [47]	GGTA1 ^{-/-} CMAH ^{-/-}	CRISPR/Cas9
LI (2014) [47]	GGTA1 ^{-/-}	CRISPR/Cas9
LI (2014) [47]	GGTA1 ^{-/-} IGb3S ^{-/-}	CRISPR/Cas9
Reyes (2014) [25]	GGTA1 ^{-/-} ; SLA-1,-2,-3 ^{-/-}	CRISPR/Cas9
Paris (2015) [67]	ASGR1 ^{-/-}	TALEN
Estrada (2015) [24]	GGTA1 ^{-/-} CMAH ^{-/-} B4GalNT2 ^{-/-}	CRISPR/Cas9

+ denotes transgene expression. ^{-/-} denotes biallelic knockout. ^{-/+} denotes heterozygote knockout.

**CHAPTER TWO: Efficient generation of targeted and controlled mutational events
in porcine cells using nuclease-directed homologous recombination.**

INTRODUCTION

As discussed within the previous chapter, the clustered randomly integrating spaced palindromic repeats and associated Cas9 protein (CRISPR/Cas9) platform has revolutionized the process of creating targeted genetic modification. Capitalizing on the error-prone nature of DNA repair, CRISPR-targeted DNA damage delivers phenotype-altering insertions and deletions. When coupled with the success of somatic cell nuclear transfer (SCNT), this has produced the ability to efficiently create model organisms at an unprecedented pace.[21] Improvements in the efficiency and precision of this platform will increase our ability to develop novel clinical applications. These techniques also hold great promise for the future of clinical xenotransplantation and cell-based therapies for cancer or immunodeficient pathology. However, to fully realize the potential of nuclease editing tools, the efficiency and precision of their application must be optimized.

Recent success using nuclease editing to efficiently create new model swine has relied on a phenotypic selection strategy of genetically modified cells for use in animal cloning that involves somatic cell nuclear transfer.[24, 47] Occasionally, cell types that are useful in animal cloning cannot be selected on the basis of the desired phenotype; these lines ultimately require genomic analysis to isolate the desired mutants. In this territory, even small improvements in efficiency can reduce the time and cost of identifying appropriately modified cells. To this end, the targeted introduction of

restriction enzyme binding sites into the genome offers an important selection tool; restriction digest of clonal cell populations can reliably identify genomic modification.

Herein we describe a process by which nuclease-driven genomic editing in pigs can be enhanced by a non-integrating selection strategy. We describe the introduction of short exogenous DNA sequences to offer control over the mutational event and aid in genotype selection. Furthermore, we show that the use of very short 5' homology sequences can affect locus-specific transgene delivery to the porcine genome. These methods increase the precision and efficiency of nuclease-based genome editing. Their application will aid broadening applications for nuclease technology by unfettering their use from phenotypic selection.

MATERIALS AND METHODS

Porcine aortic cell isolation and culture

The animals used in this study were approved by the Institutional Biosafety and Institutional Animal Care and Use Committee of Indiana University School of Medicine. Porcine primary aortic endothelial cells (AEC) were isolated from wild-type porcine aorta after euthanasia. The posterior lumbar arteries were ligated and the aortic lumen was filled with 0.025% of collagenase type IV from *Clostridium histolyticum* (Sigma, St. Louis, MO), placing vascular clamps on proximal and distal ends. This sample was incubated at 37 °C for 35 min. Enzyme activity in the perfusate was immediately quenched by the addition of 1/10 volume new born calf serum. The perfusate was centrifuged at 400 *g* for 10 min at room temperature. The cell pellet was saved and resuspended in RPMI medium supplemented with 0.02% (w/v) EDTA. The cell suspension was centrifuged again at 400 *g* for 10 min at 4 °C. The pellet was resuspended in EC culture medium (RPMI medium supplemented with 10% fetal bovine serum (v/v), 100 µg/ml endothelial cell-specific growth factor, penicillin, streptomycin, and amphotericin B). After seven days, endothelial cells were purified from culture by staining with chicken anti-Pig CD31 (Invitrogen, Grand Island, NY) and positive sorting using a FACS Aria II (Becton Dickinson, San Jose, CA).

Creation of an immortalized AEC line.

Porcine immortalized cell lines were generated as described previously [68]. Briefly, primary AECs from domestic pigs were isolated as described above. After a 3-day culture, AECs were infected for 24 hours with lentiviral supernatant, containing lentiviral vector in which a c-DNA expresses the large and small T antigen of SV40 (Applied Biological Materials Inc, Richmond, BC, Canada). Single-cell clones were isolated and amplified.

Cas9 guide RNA and DNA oligonucleotide assembly

The clustered randomly interspaced palindromic repeats and associated protein 9 (CRISPR/Cas9) nuclease system was employed to introduce targeted double strand breaks (DSB) within the porcine genome. A single-guide RNA was designed to target the porcine GGTA1 gene beginning at position 293654066 of NC_010443.4. A pair of oligonucleotides for the targeted site were designed and checked using ZiFiT Targeter Version 4.2 software (<http://zifit.partners.org/ZiFiT/>). These oligonucleotides (forward: 5'CACCGAGAAAATAATGAATGTCAA3', reverse: 5'AAACTTGACATTCATTA-TTTTCTC3') were annealed to generate short double-strand DNA fragments which were ligated to BbsI-linearized Cas9 vectors pX330-U6-Chimeric_BB-CBh-hSpCas9 or pSpCas9[14]-2A-GFP plasmids which were a gift from Feng Zhang (Addgene plasmid #42230 and 48138 respectively).[10, 69]

Transfection and cell sorting by non-integrating selection

Porcine AECs were transfected by electroporation using the Neon transfection system (Life Technologies, Grand Island NY, USA) according to the manufacturer's instruction. Concentrations of Cas9-expressing plasmid and cell number remained constant at 2 μ g/1e6 cells per transfection. Cas9 expression vectors differed only by the presence or absence of GFP. Cells were cultured for 24 hours in antibiotic free culture media. After 24 hours, cells transfected with a GFP expressing vector were sorted for fluorescence using a FACS Aria II (Becton Dickinson, San Jose, CA). A gate was established to retain the brightest cells; this was limited to <3% of the total population. All cells were retained in culture for 14 days after sorting, at which point the absence of transient GFP expression was confirmed in the experimental group by flow cytometric analysis using an Accuri C6 flow cytometer (Accuri, Ann Arbor, MI, USA). For comparison, a column selection strategy was simultaneously employed as described by Li et al.[24] Briefly, this approach involved co-transfection with CRISPRs designed to inactivate both the CMAH and GGTA1 genes without a GFP selection, followed by column selection with anti-Neu5Gc antibody (Sialix, Vista, CA, USA) on day 14, to remove Neu5Gc (CMAH gene product) positive cells; the effect on GGTA1 gene mutation was then observed.

Analysis of phenotype-specific mutation efficiency.

The phenotype-specific mutational efficiency was analyzed by measuring expression of the Gal α (1,3)Gal epitope (GGTA1 gene product). Cells were stained with Alexa Fluor 488 conjugated *Griffonia simplicifolia* IB4 (Invitrogen, Grand Island, NY, USA) to

examine gene expression function. Unlabeled cells were used as a negative control. Flow cytometric data were collected using Accuri C6 flow cytometer (Accuri, Ann Arbor, MI, USA), analysis was performed with FlowJo software version 8.8.7 (Treestar Inc., Ashland, OR).

Analysis of genotypic mutation efficiency

Cells were analyzed to determine genotypic mutation efficiency at a second porcine locus by sequencing of clones after nuclease delivery and cell sorting by fluorescence. To show the applicability of our strategy across loci, a second porcine locus was targeted for this analysis. A gRNA sequence was designed to target the FGL2 gene beginning at position 113115686 of NC_010451.3 (5'-GAAGCTGTCGAACTGGTGC-3'). Porcine AECs were transfected by electroporation using the Neon transfection system (Life Technologies, Grand Island NY, USA) according to the manufacturer's instruction. Concentrations of Cas9-expressing plasmid and cell number remained constant at 2 μ g/1e6 cells per transfection. Cas9 expression vectors differed only by the presence or absence of GFP. Cells were cultured for 24 hours in antibiotic free culture media. After 24 hours, cells transfected with a GFP expressing vector were sorted for fluorescence using a FACS Aria II (Becton Dickinson, San Jose, CA). A gate was established to retain the brightest cells; this was limited to <3% of the total population. Individual cells from the retained population were expanded clonally and genomic DNA was obtained from each colony using a GeneElute Mammalian Genomic DNA Miniprep Kit (Sigma-Aldrich, St. Louis, MO, USA). Polymerase chain reaction amplification of the targeted

region for analysis was accomplished using the primers: forward 5'-CCCGCCCTTTTCTGAGAACAA-3', reverse 5'-GGTGACAGCAGTCCATTCCT-3'. Pwo SuperYield DNA polymerase (Roche Applied Science, Indianapolis, IN, USA) was used, and PCR conditions for GGTA1 were as follows: 94 °C, 2 min; 94 °C, 15 s; 54.7 °C, 30 s; and 72 °C, 30 s for 15 cycles; 94 °C, 15 s; 54.7 °C, 30 s; 72 °C, 30 s with additional 5 s each cycle for 25 cycles; and a final extension step of 72 °C for 5 min. Sequence was analyzed by Sanger reaction.

HDR-directed mutagenesis

In the context of improved nuclease-directed mutation efficiencies, we endeavored to test whether we could use exogenous DNA oligonucleotides to facilitate nuclease-mediated HDR in porcine aortic endothelial cells. DNA oligonucleotides for short HDR were designed with homology to the genomic sequence at the nuclease-targeted cut site. Single strand DNA (ssDNA) oligomers were designed with homology to the genomic sense (forward) and antisense (reverse) strand. Total length of HDR oligos were 30bp and 50 bp. Double-strand DNA (dsDNA) was created by annealing sense and antisense oligomers. In all sequences, the translation start codon was replaced with EcoRI restriction enzyme to facilitate downstream analysis. In addition, single-stranded RNA oligonucleotide was designed analogous to the 50bp sense homology sequence. All oligonucleotides were ordered from Integrated DNA technologies (Coralville, Iowa, USA). At the time of nuclease-delivery, exogenous template DNA was delivered at either a 1uM or 5uM concentration. Cells were kept in culture for 14 days at which point they

were analyzed and sorted for phenotypic mutation events. Mutation-positive cells were retained and expanded clonally. 100 clones from each experimental group were obtained for genomic analysis.

Analysis of HDR-directed genome editing.

Genomic DNA was isolated from clonal cultures of mutated cells using a GeneElute Mammalian Genomic DNA Miniprep Kit (Sigma-Aldrich, St. Louis, MO, USA). Polymerase chain reaction amplification of the targeted rejoin for analysis was accomplished using the primers: forward 5'-CCTTAGTATCCTTCCCAACCCAGAC-3', reverse 5'-GCTTTCTTTACGGTGTGTCAGTGAAT-3.' Pwo SuperYield DNA polymerase (Roche Applied Science, Indianapolis, IN, USA) was used, and PCR conditions for GGTA1 were as follows: 94 °C, 2 min; 94 °C, 15 s; 54 °C, 30 s; and 72 °C, 45 s for 15 cycles; 94 °C, 15 s; 54 °C, 30 s; 72 °C, 45 s with additional 5 s each cycle for 25 cycles; and a final extension step of 72 °C for 5 min. HDR-directed editing efficiency was determined by restriction digestion and confirmed by sanger sequence. HDR templates were designed to introduce an EcoRI restriction site at the GGTA1 transcription start site; successful HDR was confirmed with EcoRI restriction enzyme digestion and subsequently verified by sanger sequence. GraphPad Prism 5 (GraphPad Software, La Jolla, CA, USA) was used for data analysis between experimental cohorts. Two-tailed Student's t-test and one-way ANOVA were performed. Significant differences were considered at $P < 0.05$.

Genetic knock-in with homology-directed repair

Given the relatively high efficiency of short HDR inserts, we tested whether we could apply nuclease-driven, HDR-mediated insertion into the porcine genome to drive locus-specific transgene expression. By using a short 5' homology sequence, exogenous insertion of promoter elements may be avoided; when coupled with antibiotic selection, this has the capacity to limit off-target insertion. Two gRNAs were constructed to excise the porcine thrombomodulin gene (NCBI ID: 100157642), one targeting the ATG translation start site and the other targeting the region immediately 5' to the translation stop site (5'-CACCGAGGAGCAGAACGCGGAGCA-3' and 5'-CACCGGTCTGTGGCCAGATGCCA-3' respectively). A 'landing pad' for HDR-transgene delivery was constructed with 50bp homology in the 5' and 360bp in the 3' region. In between these homology arms, promoterless transcripts for GFP and Puromycin were inserted using the 2A linker as described by Lee et al.[70]. Cells were transfected with 2.5µg of each nuclease vector and 2µg of landing pad. 48 hours after transfection, cells were selected with puromycin. Individual clones were picked and analyzed for locus-specific insertion by PCR, transgene expression of GFP fluorescence was detected by flow cytometry performed using an Accuri C6 flow cytometer (Accuri, Ann Arbor, MI, USA).

RESULTS

Phenotype-specific mutation efficiency is increased with non-integrating selection

Expression of a fluorescence protein on the Cas9 vector created a useful non-integrating selection marker. Expression of GFP was detectable at 24 hours post transfection but was silent at both 7 and 14 days post transfection. GFP positivity on the Cas-9-expressing vector allowed for selective exclusion of 97% of the transfected population. After population sorting and expansion in culture, this method was successful in increasing nuclease-delivered mutation efficiency for both primary and immortalized porcine aortic endothelial cells (Figure 2.1A). Flow cytometric selection by this marker increased phenotype-silencing mutation rates from 3.5 to 82% in primary porcine aortic endothelial cells. Similar efficiency was achieved in an immortalized cell line.

Genotypic mutation efficiency is increased with non-integrating selection

Sixty-two clones were isolated from a population undergoing conventional CRISPR/cas9 transfection and 68 clones were isolated from a population subjected to GFP selection by sorting after 24 hours for the top 3% brightest cells. Sanger sequencing indicated 7 (11.29%) of the unselected clones and 65 (95.58%) of the GFP-sorted clones contained mutations in the targeted region (Figure 2.1B).

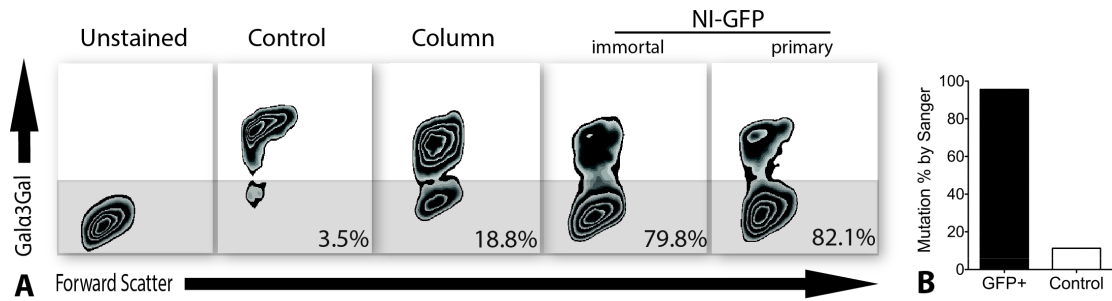


Figure 2.1: Non-integrating (NI) selection enhances nuclease mediated phenotypic and genotypic mutation efficiency.

To test the ability of a plasmid-based selection marker to increase the efficacy of nuclease-mediated gene silencing in porcine cells, a plasmid expressing guide RNA, Cas9 and GFP was compared to a control plasmid expressing guide RNA and Cas9 alone. The column-based selection method described by Li et al.[24] was also compared for reference. The Guide RNA was targeted to the GGTA1 porcine locus and gene expression was determined by flow cytometer 14 days after transfection (A). The genotypic frequency of insertion or deletion event delivered by these two plasmids was also queried at a second porcine locus, revealing that the non-integrating selection marker facilitated a genotypic mutation event with 96% efficiency (B). Histograms are representative of all experiments preformed in triplicate.

HDR-directed genome editing

Exogenous template-mediated HDR offers the ability to precisely control gene modifications to enable a new level of specificity in the modification of genomic sequences for experimental and therapeutic application. In the context of improved nuclease-directed mutation efficiencies, we queried whether we could use exogenous DNA oligonucleotides (Figure 2.2A) to facilitate nuclease-mediated HDR in porcine aortic endothelial cells. We found that relatively short template sequences, when introduced at the time of nuclease-delivery, could effect HDR-mediated editing with remarkable efficiency. HDR-mediated template insertion was achieved at a rate of 11-38%, with a biallelic insertion rate of 6-22% as verified by restriction digest and Sanger sequence (Figure 2.2C-D).

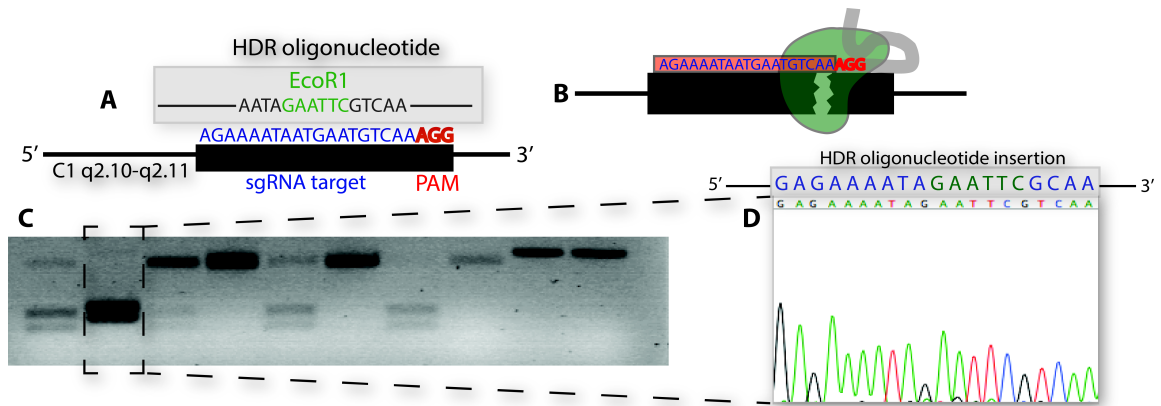


Figure 2.2: Design and use of exogenous DNA oligomers in nuclease-mediated genome editing.

Short exogenous DNA oligonucleotides were designed with homology to a CRISPR-targeted cut site at the GGTA1 translation start site within the porcine genome. All oligomers were designed to replace the GGTA1 start codon with the EcoRI restriction enzyme sequence (A). These oligomers were co-transfected at the time of nuclease delivery and were present during the creation of targeted DNA damage (B). To determine the insertion of exogenous template sequences by homology-directed repair, genomic DNA from clonal populations was amplified at the GGTA1 locus and then subjected to restriction enzyme digest and Sanger sequence (C-D).

As shown in figure 2.3, ssDNA was more effective at inducing mutation than dsDNA. In addition, the presence of short exogenous template sequences increased the aggregate mutational event rate, defined as the sum of phenotype-altering mutation effected by NHEJ and HDR. As can be seen by phenotypic analysis, the presence of short exogenous sequences for HDR, increased the frequency of biallelic mutational events; in the absence of template mediated mutation, a sanger-verified heterozygote population remains weakly positive by flow cytometry (Figure 2.3 Control).

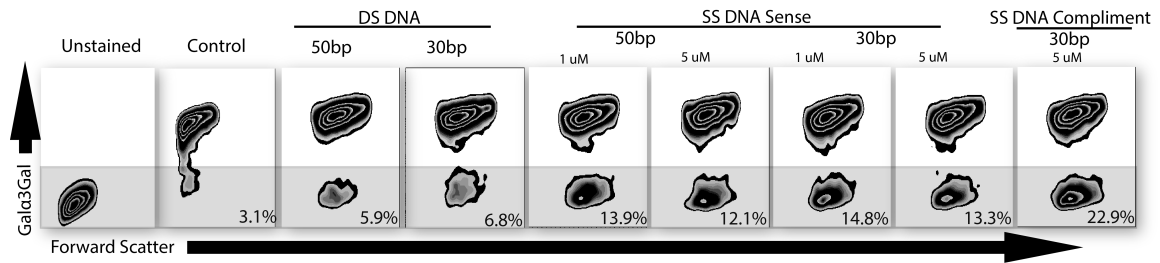


Figure 2.3: Homology-directed repair by short exogenous oligomers facilitates increased gene silencing.

To test the ability of short exogenous DNA sequences to direct homology-mediated repair of nuclease-induced genome cleavage, oligomers were designed with homology to a nuclease cut site within the porcine genome. Exogenous oligomers ranged in size from 30bp to 50bps and were either single or double stranded. They were delivered in concentration of 1uM or 5uM at the time of nuclease transfection, gene expression was determined by flow cytometer after 14 days. A control group received no exogenous oligomer. Double stranded oligomers (DS DNA) were less likely to promote phenotype-silencing mutation than single stranded oligomers (SS DNA). Furthermore, the template strands complimentary to the strand recognized by the CRISPR guide RNA, appeared to have the best efficiency. Histograms are representative of all experiments performed in triplicate.

Genetic knock-in with homology-directed repair

Due to the successful integration of very short DNA templates, we designed a 50bp 5' homology arm for locus-specific transgene delivery to the porcine genome. This leading homology strand for HDR-mediated transgene insertion was devoid of promoter elements

and positioned at the porcine thrombomodulin gene translation start site. 48 hours after cotransfection with nuclease and exogenous transgenes, 15 individual clones were isolated from puromycin selection. The 50bp 5' homology arm successfully directed transgene insertion to the porcine thrombomodulin loci in 15/15 (100%) of the selected clones. (Figure 2.4A) In all fifteen of these colonies, the endogenous thrombomodulin promoter facilitated expression of the two inserted exogenous genes (Figure 2.4B).

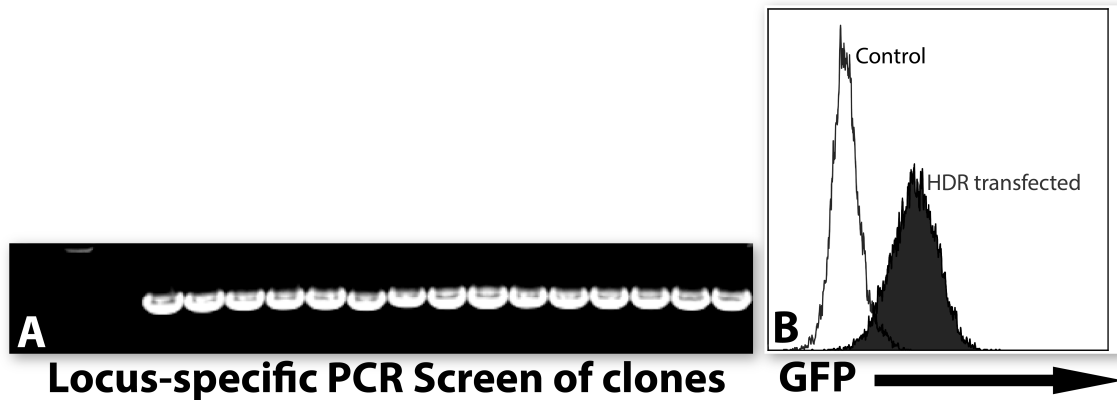


Figure 2.4: Locus-specific transgene delivery to the porcine genome facilitated by nuclease-targeted homology driven insertion.

Given the observed efficiency of short homology directed repair (HDR) templates, we tested whether nuclease-mediated insertion by HDR could drive locus-specific transgene expression in the porcine genome. Two promotorless exogenous genes –puromycin resistance gene and GFP- were placed 3' to a very short homology sequence which was designed 5' to a nuclease cut site. The cut site targeted the porcine thrombomodulin translation start codon, and the exogenous homology sequence contained no promoter elements. After cotransfection with nuclease and transgenic DNA, site-specific insertion was queried by PCR utilizing a forward primer 5' to the homology sequence region and a reverse primer within the transgene. After selection by puromycin 15/15 (100%) of clones exhibited locus-specific insertion (A). Phenotypic expression of GFP was analyzed by flow cytometer; all colonies exhibited GFP expression by the endogenous porcine thrombomodulin promoter (B).

DISCUSSION

Though various nuclease-based approaches have been employed to silence genes within the porcine genome, CRISPR/Cas9 offers several advantages over previous techniques; making it the best choice for optimization efforts. Chief among these advantages is the ease of its programmability. CRISPR utilizes a relatively flexible targeting system.

Relying on short RNA signals to guide the nuclease, CRISPR is capable of recognizing - and editing- any loci that contains a GN19NGG sequence where N refers to any nucleotide. Although even the length of guide target has recently proven flexible, the genomic target sequence for editing *must* have the NGG on its 3' end. This sequence is termed the protospacer adjacent motif (PAM). In bacteria –where CRISPR exists as an adaptive agent of defense against viral DNA- the PAM is present in the DNA to be degraded but not on the RNA that will target it. For CRISPR to work in bacteria, both a targeting RNA sequence and a nuclease-recruiting RNA sequence must hybridize. By artificially creating a chimera of these two entities, a fully functional targeting system can be created for use across many genomes; this structure is termed the single-guide RNA (sgRNA). For genome-editing purposes, functional sgRNA may be synthesized exogenously or they may be transcribed from an inserted plasmid. Once inside the cell, they serve as a mobile guide, capable of directing targeted genomic modification. The independent mobility of both sgRNA and Cas9 offers another advantage to the CRISPR/Cas9 system. Because sgRNA are independent of the Cas9 nuclease, which is free to associate and dissociate with multiple sgRNAs, CRISPR may be multiplexed. Multiplexing CRISPR has made it possible to effect many genetic modifications within a

single transfection. In 2015 Li et al described the use of multiplexed CRISPR technology to target multiple genes within a single reaction and produce pigs of multiple different genetic backgrounds within in a single pregnancy.

Multiplexed or not, the essential common component of CRISPR editing strategies involves creating a targeted double strand break (DSB) in the genome. This is done by a cleavage domain of the Cas9 endonuclease. As shown in figure 2.5, Cas9-induced DSBs are repaired by one of two mechanisms: nonhomologous end-joining (NHEJ) or homology directed repair (HDR). NHEJ is a well-characterized endogenous DNA repair pathway that is responsible for repairing insults to the host genome. NHEJ relies on DNA ligase IV to repair DSBs; because the fidelity of this enzyme is relatively low, NHEJ is said to be ‘error-prone.’ NHEJ often results in the presence of insertion or deletion mutations within repaired DNA. In this way CRISPR-directed DSBs provide an efficient means of silencing a gene, simply by disrupting the translational reading frame. An alternative approach to repairing CRISPR-induced DSBs involves the process of HDR. HDR requires the insertion of exogenous DNA templates that have homology to the CRISPR target. We show within this report that exogenous ‘donor template’ sequences are capable of inserting themselves into the porcine genome by relying on host genome repair mechanisms. In this way HDR-mediated DNA repair can be utilized as a means to introduce specific mutations or to insert exogenous sequences into the targeted loci.

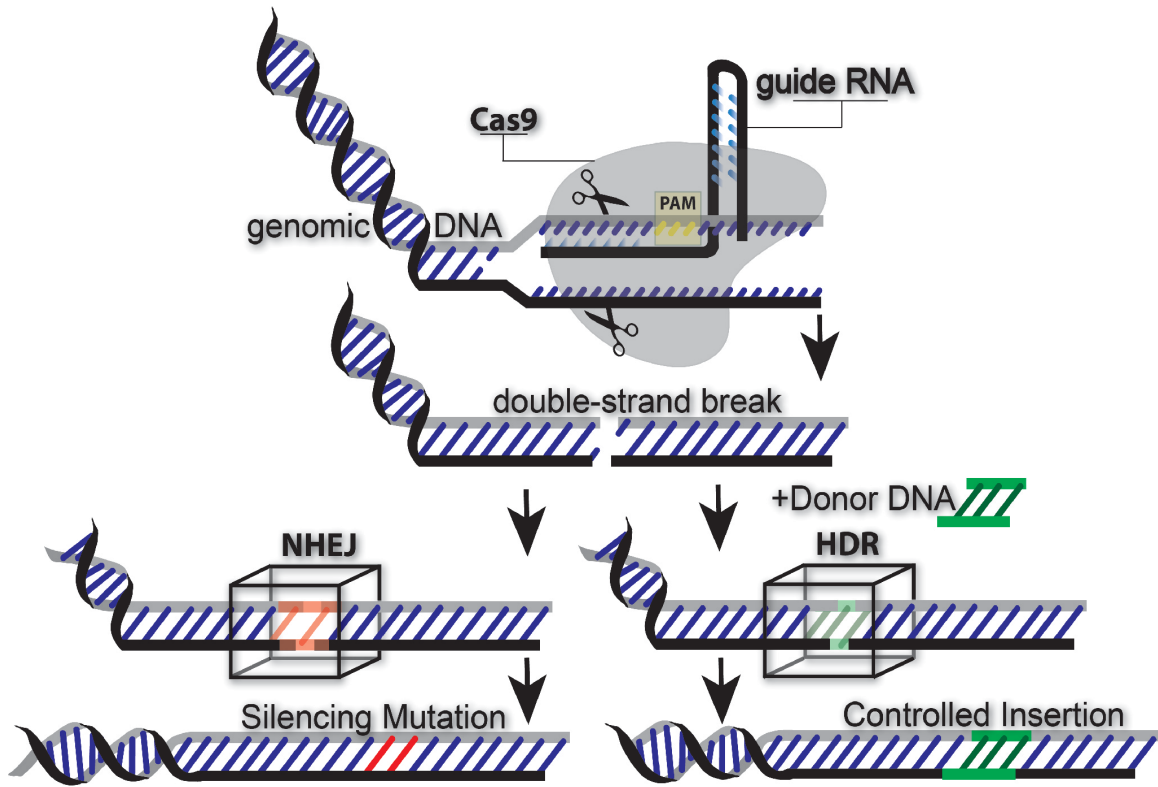


Figure 2.5: Nuclease-based genetic insertion strategy.

CRISPR-induced double-strand breaks in genomic DNA may be repaired through one of two processes. The first involves the error-prone process of NHEJ. Owing to its relative low fidelity, frame-shifting point mutations may be introduced that create a null phenotype at that locus (figure left). Alternatively, HDR requires the presence of a homologous donor DNA template (figure right). In this process, simple homologous recombination occurs to repair the double-strand break; a highly homologous template may harbor salient exogenous (mutagenic) template, thereby introducing a controlled mutation or transgene.

The advent of the CRISPR/Cas9 system has dramatically increased the accessibility of nuclease-based genome editing. Applying these tools to the porcine genome also offers potential *therapeutic* application; genetically modified pigs –as surrogate organ donors- are increasingly becoming recognized as a potential solution to the growing shortage of transplantable organs.[15, 21, 71-73] However, for the potential of nuclease-based tools to be fully realized, cost-effective and efficient methods of improving cas9-mediated editing must be pursued. Although multiple efforts are underway to increase nuclease-efficiency,[74-76] plasmid-delivery of cas9 and single-guide RNAs typically offer a 1-10% mutational efficiency. [69, 77, 78]

This study represents the first efforts to specifically query Cas9 efficiency within the porcine genome. The results suggest that the use of a transiently expressed selectable marker on the nuclease-delivery plasmid enables enrichment of mutated cells. Similarly, by introducing targeted restriction enzyme sites into our mutational event, we show that restriction digest of clonal cell populations can reliably identify genomic modification. Given the high insertion efficiencies reported here, this strategy offers the ability to significantly reduce the time and cost required to create -and identify- modified cells.

Recently Schumann et al. have reported similar increases in mutational efficiency by directly transfecting Cas9 protein and pre-prepared ribnucleoprotein guides at a 20uM concentration. [75] Although this strategy warrants great attention, we offer comparable results in the present study with a plasmid-based platform; this avoids the need to isolate ribonucleotide proteins and Cas9 exogenously.

Xenotransplantation of genetically modified porcine organs is increasingly close to clinical application. In the context of human trials, the mechanisms of genome editing must move beyond efficiency to also incorporate great precision. The inclusion of very short oligonucleotide templates by nuclease-directed HDR offers this precision. Specifically, controlling the mutational event by short exogenous templates offers an avenue to achieve biallelic homozygosity (Figure 2.5). By accepting only mutations that possess mutations with allelic homozygosity, we may limit the possibility of downstream chromosomal allele recovery by crossing over as described first by Orr-Weaver and Szostak.[79] One potential strategy to *further* increase the rate at which we achieve this precision could be to inhibit NHEJ during the mutation period. Although not applied within the present study, recent use of pharmacologic agents that inhibit mammalian NHEJ has demonstrated increases in HDR-mediated repair pathways, [76, 80] making this strategy a potential companion technique for the present work.

Finally, nuclease-mediated HDR with exogenous DNA can move beyond enhancing the frequency and control of mutational events. It is reasonable to apply this technique to create meaningful codon substitutions, replace or remove whole exons, and as shown within this report, insert entire transgenes. Although it remains uncertain which -if any- human transgenes will be necessary to promote porcine-to-human xenotransplantation, the ability to place transgenes precisely into the porcine genome is a great advantage.

Taken together, our results suggest that nuclease-driven genome editing can be enhanced by a non-integrating selection strategy. The introduction of short exogenous DNA sequences both offers control over the mutational event and aids genotype

selection. Furthermore, the use of a very short homologous sequence is able to guide precision transgene insertion to the porcine genome. This process has the potential to limit off-target insertion and facilitates transgene expression by an endogenous promoter. These studies collectively represent a cost-effective repertoire for enhancing the application of CRISPR/cas9 system within the porcine genome. Their application will aid broadening applications for nuclease technology in the understanding and treatment of surgical disease.

CHAPTER THREE: Silencing the porcine iGb3s gene does not affect Gal α 3Gal levels or measures of anticipated pig-to-human and pig-to primate acute rejection.

INTRODUCTION

With the enhanced efficiency of porcine genome engineering as described in the previous chapters, attention was turned to utilizing these processes to create and analyze new animal models of xenotransplantation. Theoretically, enzymes that affect glycosylation patterns may alter cross-species immunogenicity of the transcriptome on an *organismal* level through post-translational glycosylation. As such, initial priority was given to the porcine glycome, rather than the proteome. Gal α 1,3Gal (α Gal) is a disaccharide synthesized in pigs but not in humans and old world monkeys. [81] (Figure 3.1A) Primarily, α -GAL is formed by the catalytic activity of the enzyme α -galactotransferase (GGTA1) by which galactose is added to Gal1–4GlcNAc structures present on glycoproteins or glycosphingolipids. [82] (Figure 3.1C) In humans the GGTA1 gene is inactive and humans develop antibodies when exposed to α -GAL epitopes.[83] Following xenotransplantation, α -GAL antibodies promote hyperacute rejection (HAR). [84] To address the issue of α -Gal epitopes, GGTA1 null animals have been generated in order to eliminate the α -GAL epitope and eliminate HAR. [19, 22, 32, 85-87] However, a residual amount of α -GAL epitope reactivity has been recognized in biallelic GGTA1 knockout pig cells and implicated as a possible contributor to chronic rejection of GGTA1^{-/-} organs seen in non-primate models of xenotransplantation. [88-90] One reason suggested for this is that the α -GAL epitope can be biosynthesized by other members of

the galactotransferase enzyme family. (Figure 3.1C) In particular the enzyme isoglobotrihexosylceramide synthase (iGb3S) is known to generate the gal α 1,3gal disaccharides epitopes on glycosphingolipids by the addition of galactose to lactosyl ceramide. (Figure 3.1B) In a similar manner to GGTA1, the human genome includes iGb3s (NM001080438) and the gene is thought to be silent due to several mutations that prevent the formation of iGb3. [91].

Studies in other animals demonstrate that iGb3 levels are species specific. In rat thymus, iGb3 levels are moderate whereas in mouse and human thymus iGb3 is undetectable. [93] Moreover, iGb3 is tissue specific. iGb3 is not detectable in brain, liver, kidney, spleen, thymus, testis, lung, stomach, intestine, eye, spinal cord, and plasma of mice but is detected in murine dorsal root ganglia (DRG). [93] Further studies demonstrate that in mice iGb3 is an immune modulatory glycosphingolipid, whereby iGb3 binds to CD1d and is presented to the T-cell receptor (TCR) of invariant natural killer T (iNKT) cells. [94, 95] In addition, iGb3-primed bone marrow-derived dendritic cells exert a significant iNKT cell-mediated anti-tumor activity. [96] Consequently, both tissue- and species-specific differences in iGb3 levels make information gained from rodent models difficult to translate into the porcine-human or porcine-primate xenotransplant models. [93]

This translation is made more difficult because iGb3s gene expression does not match iGb3 epitope levels. In mice, iGb3s gene expression is ubiquitous within mouse tissues but iGb3 is detected only in the DRG. This disparity is potentially due to translational regulation or because of continuous flux in glycosphingolipid pathways. In particular iGb3 is a substrate for iGb4 synthase which converts iGb3 to iGb4. iGb4 does not contain the terminal Gal α (1,3)gal epitope.

Consequently, there is a conflict regarding the importance of iGb3/iGb3s in the literature. [91, 97] Within the context of pig-to-primate xenotransplantation, some argue for the importance of iGb3 while others have failed to detect iGb3 in porcine tissues. [98, 99] To address this we have generated iGb3s gene (A3GalT2) knockout pigs in a GGTA1^{-/-} background and compared α -GAL epitope expression, antibody binding

profiles, and antibody-mediated complement depended cytotoxicity between GGTA1^{-/-} and GGTA1^{-/-}/A3GalT2^{-/-} double knockout pigs.

MATERIALS AND METHODS

Knockout constructs

Bicistronic CRISPR sgRNA expression vectors co-expressing the Cas9 gene were designed as described by Li et al. [67] to bind and cleave the GGTA1 gene beginning at position 293654066 of NC_010443.4 (forward: CACCGCGAAAATAATGAATGTCAA) and A3GalT2 gene beginning at position 83572809 of NCBI reference NC_010448.3 (forward: CACCGCGCTGGCAGGACGTGTCCA). Porcine liver-derived cells were cultured as previously described [38] and co-transfected with both of the above CRISPR vectors using the Neon transfection system (Life Technologies, Grand Island NY, USA) according to the manufacturer's instruction.

Selection and Genotyping

CRISPR-transfected cells were subjected to a-Gal counter-selection process, as described by Li et al., [67] to enrich for a mutation-positive population. Genomic DNA from counter-selected cells and the derivative clonal animals was obtained by GeneElute Mammalian Genomic DNA Miniprep Kit (Sigma-Aldrich, St. Louis, MO, USA). PCR amplification of targeted-genes was performed using primers and conditions previously described. [67]

Somatic cell nuclear transfer (SCNT)

All the animals used in this study were approved by the Institutional Biosafety and Institutional Animal Care and Use Committee of IUPUI. SCNT was performed as described by Estrada et al., [100] using in vitro matured oocytes (DeSoto Biosciences Inc, St. Seymour, TN.). Cumulus cells were removed from the oocytes by pipetting in 0.1% hyaluronidase. Only oocytes with normal morphology and a visible polar body were selected for SCNT. Oocytes were incubated in manipulation media (Ca-free NCSU-23 with 5% FBS) containing 5 $\mu\text{g}/\text{mL}$ bisbenzimidazole and 7.5 $\mu\text{g}/\text{mL}$ cytochalasin B for 15 min. Oocytes were enucleated by removing the first polar body plus metaphase II plate, and one cell was injected into each enucleated oocyte. Couples were fused and activated simultaneously by two DC pulses of 180 V for 50 μsec (BTX cell electroporator, Harvard Apparatus, Holliston, MA, USA) in 280mM Mannitol, 0.1mM CaCl_2 , and 0.05mM MgCl_2 . Activated embryos were placed back in NCSU-23 medium with 0.4% bovine serum albumin (BSA) and cultured at 38.5 $^{\circ}\text{C}$, 5% CO_2 in a humidified atmosphere for about one hour, before being transferred into the recipient. Recipients were synchronized oviducal gilts on their first day of estrus.

A3GalT2 locus silence verification

The genome of iGb3S knockout animals was analyzed at the A3GalT2 locus by sanger sequence to confirm the presence of biallelic gene-silencing events. Because the dorsal root ganglion (DRG) has been shown to exhibit the highest levels of iGb3S expression, porcine dorsal root ganglion isogloboside-3-synthase levels were determined in control

and knockout pigs using a commercially available ELISA kit as per manufacturer's instructions (#MBS7205937, www.MyBiosource.com).

α Gal Phenotype analysis

Pig tissue and cells were collected in accordance with Institutional Review Board and Institutional Animal Care and Use Committee approved protocols. GGTA1-null and A3GalT2/GGTA1-null and WT PBMCs, Lymph node cells (LNC) and Splenocytes were isolated from mature animals after euthanasia. Cells were stained with isolectin GS-IB4 Alexa Fluor 488 conjugate (Life technologies, Carlsbad, CA USA) to examine the presence of the α Gal epitope. Unlabeled cells were used as a negative control and WT cells served as positive control. Fluorescence detection was performed using an Accuri C6 flow cytometer (Accuri, Ann Arbor, MI, USA). Analysis of the median was performed with FlowJo version 8.8.7 (Treestar Inc., Ashland, OR). Results were reported in median fluorescence intensity (MFI).

Tissue staining and confocal microscopy

Tissues were procured from mature A3GalT2/GGTA1-null and GGTA1-null pigs after euthanasia. Frozen sections of kidney were prepared. Mounted tissues were blocked in Odyssey blocking buffer (Li-Cor Biosciences, Lincoln, NE USA) in HBSS for 1 hour. The slides were then fixed in paraformaldehyde for 10 minutes. Tissues were stained with isolectin GS-IB4 Alexa Fluor 488 conjugate (Life technologies, Carlsbad, CA USA)

to visualize the presence of α -Gal [19]. Tissues were also stained with goat anti-Pig CD31 1:100 (R and D systems, Minneapolis, MN) to visualize the endothelial surface [101], followed by three PBS washes and bovine anti-goat IgG DyLight 649 (Jackson Immuno Research Laboratories Inc., West Grove, PA). Tissues were incubated for 1 hour at 4°C and washed three times with 0.1% HBSS Tween DAPI (Invitrogen, Carlsbad, CA) was added to all slides for 1 minute as a nuclear stain [75] followed by two 0.1% HBSS tween washes. Tissues were mounted in ProLong Gold (Invitrogen, Carlsbad, CA). Confocal microscopy was accomplished using an Olympus FV1000 (Olympus America Inc., Center Valley PA, USA). All confocal settings were set to isotype control levels. Tissue staining of PBMC for confocal analysis was also performed as above.

Antibody binding

GGTA1-null and A3GalT2/GGTA1-null PBMCs were isolated and assessed for viability using trypan blue. Approximately 200,000 PBMCs of each group were incubated with 25% heat inactivated human sera from 10 healthy human and baboon donors for 1 hour at 4°C. Samples were then washed three times with HBSS. Human IgG and IgM were detected individually with anti-human secondary antibodies conjugated to Alexa Fluor 488 (Jackson ImmunoResearch Laboratories Inc., West Grove, PA) for 1 hour at 4°C. PBMCs were washed three times in HBSS. Fluorescence detection was performed using an Accuri C6 flow cytometer (Accuri, Ann Arbor, MI, USA). Analysis of the median was performed with FlowJo version 8.8.7 (Treestar Inc., Ashland, OR), and results were reported in median fluorescence intensity.

Complement-mediated cytotoxicity

The assay was performed as described by Diaz et al. [102] with slight modifications. In a 96-well V-bottom assay plate, 100 μ l of serially diluted, heat inactivated human or baboon serum was mixed with a 100 μ l aliquot of PBMC from either a GGTA1-null pig or A3GalT2/GGTA1-null pig. The final concentration of PBMC in each well was 1×10^6 /ml and serum concentration varied by dilution (50%, 17%, 6%, 2%, 0.6%, 0.2% and .07%). The assay was incubated for 30 mins at 4°C. After incubation, plates were centrifuged for 6 min (400x g), decanted and washed with HBSS; this step was repeated twice. Baby Rabbit complement (Cedarlane, Burlington, NC, USA) was diluted 1:15 in HBSS and 140 μ l was added to each well and incubated for 30 mins at 37°C. PBMCs were labeled with a fluorescein diacetate (FDA) 1 μ g/ml in acetone and propidium iodide (PI) prepared at a concentration of 50 μ l/ml in phosphate-buffered saline (PBS). After incubation in complement, the samples were transferred from 96 well to flow tubes containing 100 μ l HBSS and 10 μ l FDA/PI. Analysis was completed by flow Cytometry. The percentage of dead cells (PI+, FDA-), damaged cells (PI+, FDA+) and live cells (PI-, FDA+) was determined by quadrant analysis. PI-/FDA- events were excluded from analysis. Background spontaneous cytotoxicity was determined by analyzing cells not exposed to human sera. Values for cytotoxicity are subsequently reported after correction by this background value using the following equation: %cytotox = (%cytotoxExp - %cytotoxSpont)/ (100 -%cytotoxSpont) where %CTXexp is the percentage of dead cells under the experimental condition.

Glycosphingolipid analysis.

Sample Collection: GGTA1^{-/-} animals are known to exhibit reduced levels of α -series glycosphingolipids which facilitates more resolute detection of iGb3 by HPLC. For this reason, porcine kidney samples were collected from GGTA1^{-/-} A3GalT2^{-/-} double knock out (DKO) and wild type pigs at Indiana University Medical School, USA under IACUC approved protocol. [47, 67] Samples were flash frozen in liquid nitrogen and stored at -80°C prior to shipping under dry ice to DP at University of Oxford Department of Pharmacology, UK. **Glycosphingolipid Extraction:** Glycosphingolipids were extracted by chloroform/methanol extraction as per Svennerholm and Fredman [101] and solid phase purification (SepPac C18) as previously described. [103] **Ceramide glycanase digestion:** Extracted and purified glycosphingolipids were digested to release carbohydrates, using 50 mU ceramide glycanase at 37 °C for 18 hours as previously described. [104] **Carbohydrate labeling:** The ceramide-glycanase-released oligosaccharides were labeled with anthranilic acid, as previously described. [103] **Normal Phase HPLC:** Anthranilic acid labeled oligosaccharides were separated by normal phase high performance liquid chromatography and detected by fluorescence, as previously described. [103]

RESULTS

Gene knockout pigs

Porcine, liver-derived cells transfected with the bisstronic sgRNA/Cas9 knockout vectors for GGTA1 and A3GalT2 genes exhibited biallelic gene-silencing mutational events; IB4 lectin-conjugated beads facilitated the isolation of successfully mutated cells. These cells were used to create healthy clonal animals by SCNT. The genotype of animals used in this analysis exhibited an A3GalT2/GGTA1-null or a GGTA1-null background and have been previously published by Li et al.[67] Sanger sequencing of genomic DNA obtained from knockout animals used within this study confirmed biallelic frame-shift mutational events, indicating gene silencing at the iGb3s locus. (Figure 3.2A) As show in figure 3.2B, iGb3 synthase expression was silenced; dorsal root ganglion iGb3s production was reduced from 1.7 ± 0.4 ng/mg protein in WT pigs to 0.14 ± 0.08 ng/mg protein in A3GalT2^{-/-} pigs ($p= 0.005$); mutation within the A3GalT2 locus rendered iGb3s levels that were not statistically greater than the background zero standard ($p=0.18$).

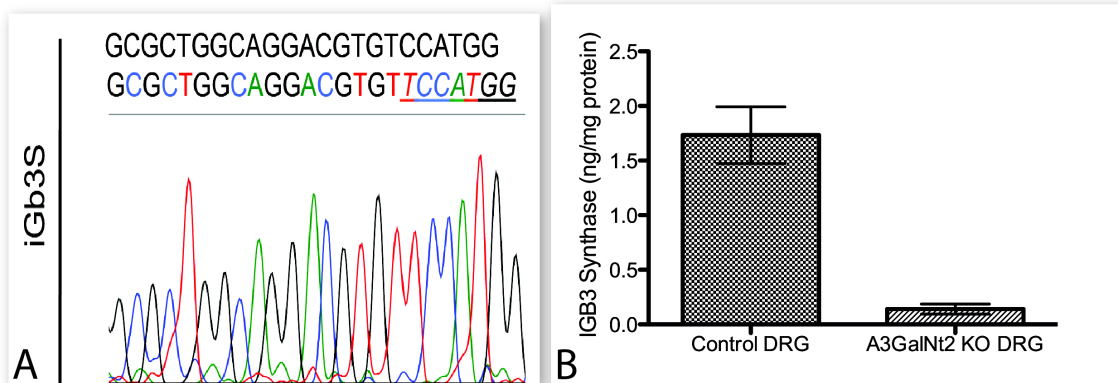


Figure 3.2: Nuclease-driven silencing of the isoglobotrihexosylceramide 3 synthase production in porcine tissue and cells.

Tissue and cells isolated from WT and A3GalT2-null animals were immediately frozen for DNA and protein analysis. **A** Sanger sequence analysis of A3GalT2^{-/-} animal genomic DNA that documents frame-shift gene silencing events in a biallelic pattern. **B** The results of a commercially available ELISA analysis documents successful disruption of iGb3s production in KO animals; iGb3S detection was significantly reduced ($p=0.005$) to levels of background absorbance in A3GalT2^{-/-} animals; iGb3s levels in A3GalT2^{-/-} pigs were not statistically greater than the background zero standard ($p=0.18$).

α -Gal phenotype analysis

Gal α 3Gal epitope expression, measured by IB4 binding, was not significantly different on cells or tissue from A3GalT2/GGTA1-null or a GGTA1-null animals. At the cellular level this was true for spleen cells, lymph node cells and PBMCs; histograms for IB4-stained cells from A3GalT2/GGTA1-null and GGTA1-null animals overlay the corresponding unstained controls (Figure 3.3).

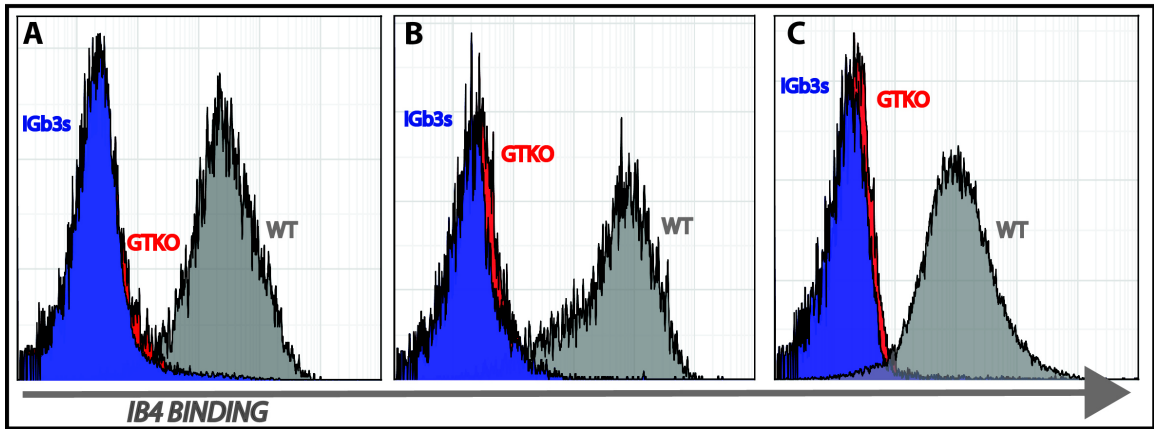


Figure 3.3: IB4 binding profiles of iGb3s knockout pig cells.

Spleen cells, Lymph node cells and PBMCs, from wild-type (WT), GGTA1-null (GTKO) or A3GalT2/GGTA1-null (iGb3) animals were incubated with a fluorescent-conjugated IB4 lectin probe to detect α Gal carbohydrate profiles. For each frame, blue represents A3GalT2/GGTA1-null cells, red represents GGTA1-null cells and grey is a WT positive control. IB4 binding was not significantly affected by silencing the iGb3s gene. **A** represents IB4 binding profiles of spleen cells **B** represents IB4 binding profiles of lymph-node cells **C** represents IB4 binding profiles of PBMCs. In all panels, knockout animal histograms overlay unstained negative controls.

Tissue staining and confocal microscopy

Confocal microscopy analysis showed no visible changes to IB4 binding at the tissue level between A3GalT2/GGTA1-null and GGTA1-null kidneys (Figure 3.4).

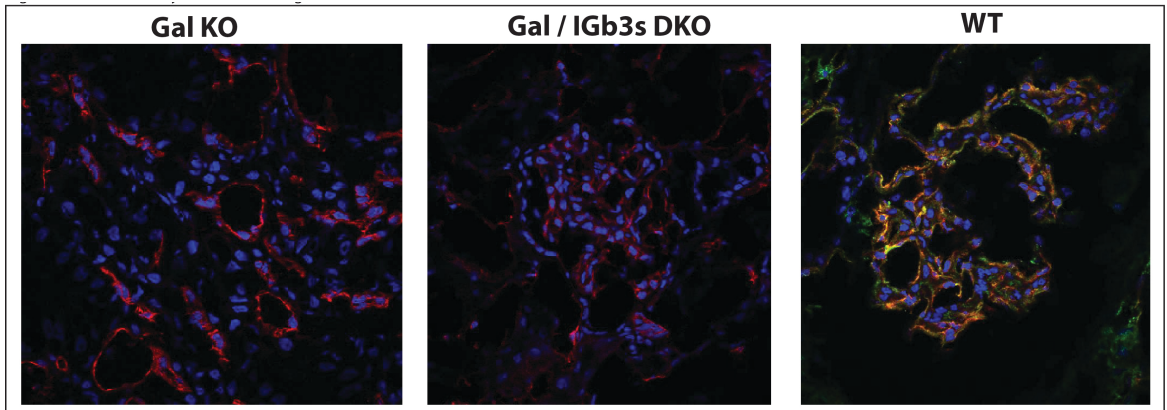


Figure 3.4: Confocal analysis of IB4 binding to iGb3s knockout pig tissues.

Sections of kidney tissue were obtained from mature WT, GGTA1-null or A3GalT2/GGTA1-null pigs after euthanasia. These tissues were stained with IB4 lectin [19] to show Gal α 3Gal expression level, anti-CD31 [101] endothelial marker and a DAPI [75] nuclear stain.

Antibody binding

IgG and IgM antibody binding from baboon sera and human sera was unchanged between PBMCs from A3GalT2/GGTA1-null and GGTA1-null animals (Figure 3.5).

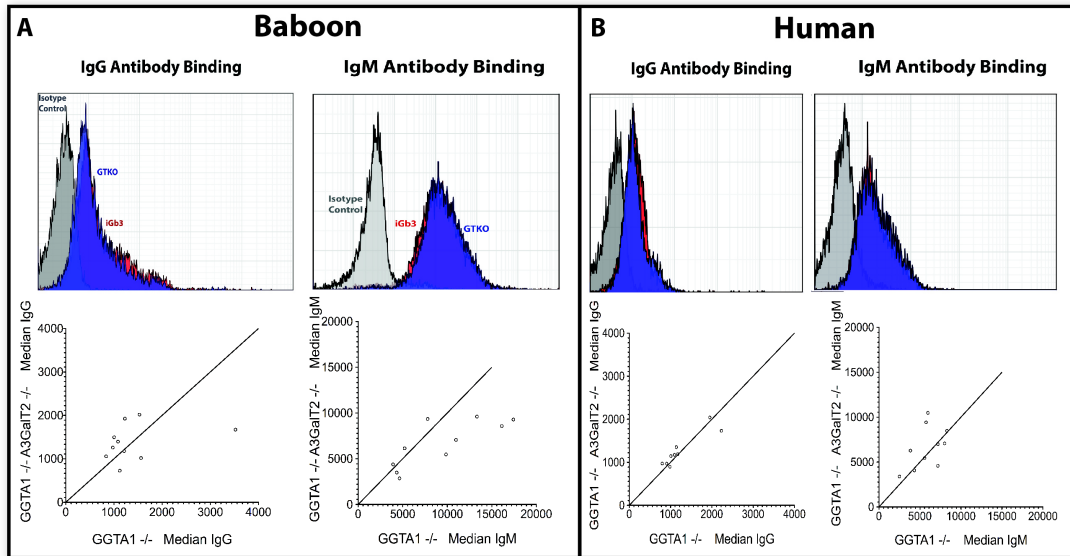


Figure 3.5: Baboon and human antibody binding profiles of iGb3s knockout pig cells.

Baboon and human sera were incubated with PBMCs from swine containing inactivated GGTA1, or GGTA1 and A3GalT2 genes. Secondary fluorescent antibodies were used to detect IgG and IgM binding to the cells with median fluorescence intensity being evaluated (MFI). T-test statistical analysis was used to analyze the difference between genotype cohorts; baboon and human IgG and IgM binding was not statistically affected by silencing the iGb3s gene. For each frame, blue represents A3GalT2/GGTA1-null cells, red represents GGTA1-null cells and grey is an isotype control. **A** represents patterns of IgG and IgM binding to baboon sera. A representative histogram (above) is paired with an aggregate plot of all 10 sera analyzed (below). The diagonal line indicates equivalent binding to both single and double knockout cells. **B** represents patterns of IgG and IgM binding to human sera. A representative histogram (above) is paired with an aggregate plot of all 10 sera analyzed (below). The diagonal line indicates equivalent binding to both single and double knockout cells.

Antibody-dependent complement-mediated cytotoxicity

Similarly, antibody-mediated complement-dependent cytotoxicity, was not reduced by the silencing of the iGb3s gene (Figure 3.6). The lysis profiles of PBMCs from A3GalT2/GGTA1-null and GGTA1-null animals were equivalent when subjected to baboon sera and human sera.

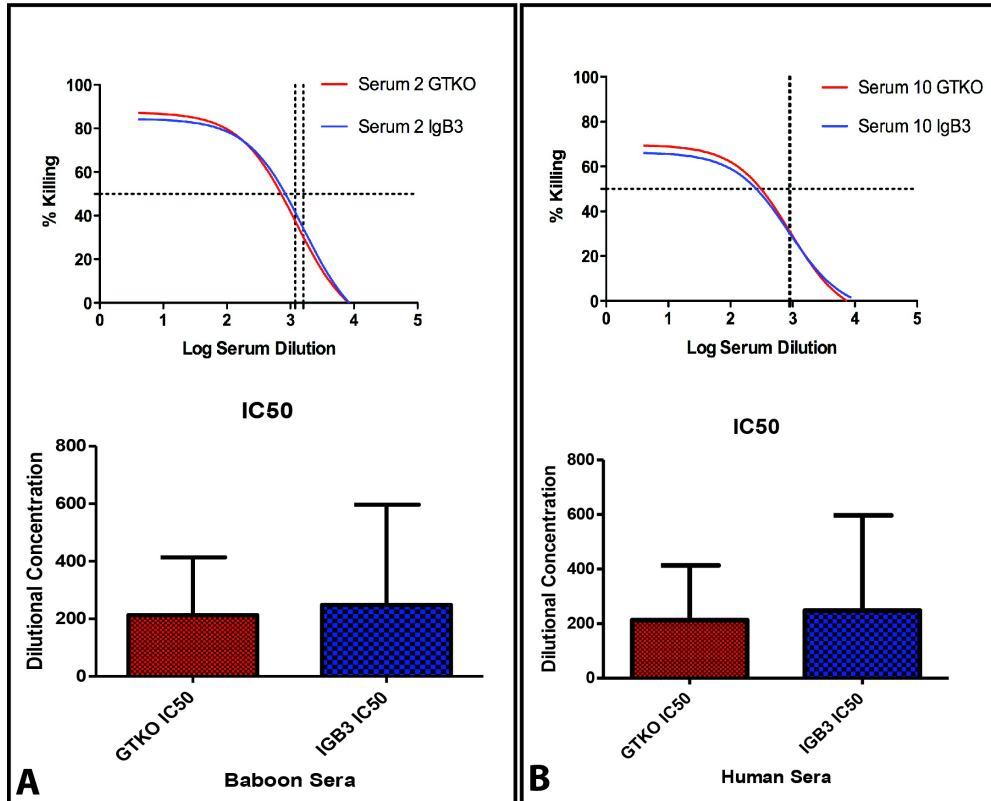


Figure 3.6: Antibody-mediated complement-dependent cytotoxicity of baboon and human sera against GGTA1-null or A3GalT2/GGTA1-null cells.

PBMCs were isolated from GGTA1-null or A3GalT2/GGTA1-null pigs. These were subjected to heat-inactivated baboon and human sera as a source of antibody.

Complement-mediated cell-lysis was induced by the addition of rabbit complement and measured in a live/dead dual-labeling assay. Example curves for antibody-mediated complement-dependent cytotoxicity against GGTA1-null [101] or A3GalT2/GGTA1-null cells [75], are above aggregate median dilutional cytotoxicity at which point sera effected 50% cell death. T-test statistical analysis was used to analyze the differences between genetic cohorts; complement-mediated lysis was not statistically affected by silencing the iGb3s gene. **A** represents baboon sera toxicity **B** represents human sera toxicity.

Glycosphingolipid Analysis

Although silencing the porcine iGb3s gene did not affect patterns of IB4-binding, antibody binding, or antibody-mediated cytotoxicity, the glycosphingolipid profile of these animals was altered. HPLC analysis of tissue obtained from GGTA1^{-/-}A3GalT2^{-/-} animals evidenced a unique glycosphingolipid profile compared to the wild type animals. In particular, iGb3 was not detected in renal tissue from wild type or DKO pigs. iGb3 elutes between Gb3 and GM3 and no appropriate peak was observed. (Figure 3.7A,B) Detection of iGb3 is difficult because of the abundance of Gb3 and GM3 in wild type pigs, which limits resolution between peaks. This is particularly challenging when GM3 is high as seen in wild type pigs (Figure 3.7A). In DKO pigs there was a significant reduction in α -series glycosphingolipids that include GM3 which makes detection of iGb3 easier. This reduction in GM3 is probably related to the GGTA1 gene deletion rather than deletion of A3GalT2. A similar loss of GM3 is reported in α -gal null mouse tissues. [93] Despite the reduction of GM3 detection of iGb3 was not detectable. Gb3 levels were slightly increased in DKO pigs which hindered iGb3 detection. Typically iGb3 can be detected at 1% of Gb3 levels in the absence of GM3. Because both Gb3 and GM3 were present in DKO pig kidney detection of iGb3 is significantly challenging. Our failure to detect iGb3 in wild type porcine kidneys is in accordance with previous studies of iGb3 in pigs, using linear ion-trap mass spectrometry detection, that was unable to detect iGb3 in pig heart, liver, kidney and pancreas. [97] In contrast to iGb3 quantification we did observe a potential reduction in the levels of iGb4 in kidneys from DKO pigs, when compared to wild type controls. iGb3 is converted to iGb4 by the enzyme iGb4 synthase. iGb4 elutes between GM2 and Gb4. (Figure 3.7B) Moreover,

iGb4 was potentially identified, suggesting a rapid conversion of iGb3 to iGb4, which would explain the absence of iGb3 in wild type pig kidneys. In kidneys from DKO pigs iGb4 was not detected. Because iGb4 peaks are unaffected by GGTA1 silencing -as the synthetic pathway is independent of Alpha-1,3-galactosyltransferase and employs a unique precursor, the A3GalT2 locus is implicated in this observation. [93] This suggests the direct reduction of substrate iGb3 relating to iGb3 synthase gene deletion. (Figure 3.1D) [93]

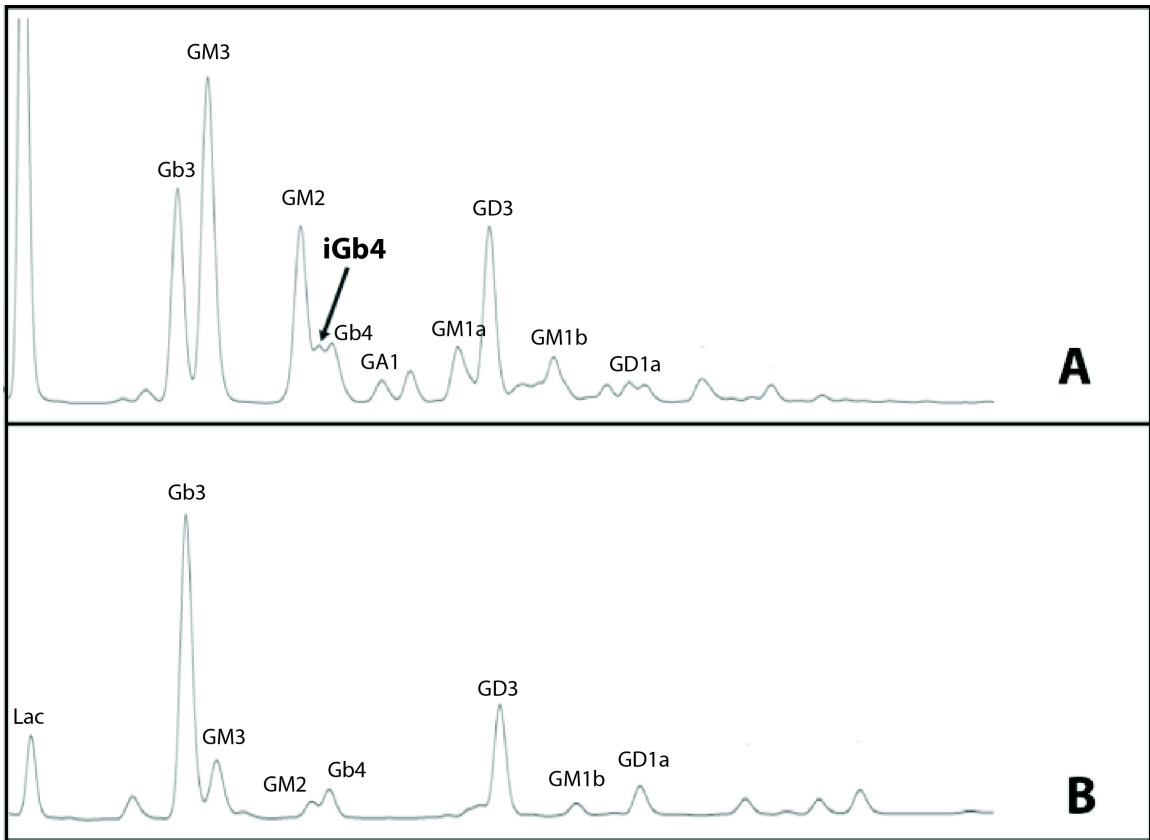


Figure 3.7: Liquid chromatography analysis of kidney tissue from wild type and A3GalT2-null animals.

A represents elution patterns from WT kidney sample and **B** represents elution patterns from A3GalT2-null sample. iGb4 elutes just before Gb4 in a WT, and the triplet peak in the WT pig becomes a doublet in the A3GalT2- null sample. This is indicative of upstream silencing of the iGb3s enzyme. Inversion of the ratio between GM2 and GB4 further suggests substrate shunting towards GB4 production in the absence of functional iGb3s in A3GalT2^{-/-} animals.

DISCUSSION

As discussed within chapter one, the shortage of donor organs is the most pressing problem in clinical transplantation. [105] Xenotransplantation of pig organs is becoming an immunologically realistic solution to this problem. [47] However, to achieve clinical relevance, the major drivers of immune-mediated, antibody-mediated rejection (AMR), must be understood and eliminated. [106] Over the course of evolution, humans and primates have inactivated the α -1,3-glycosyltransferase-1 (GGTA1) gene and form antibodies to α -GAL epitopes within xenotransplanted porcine organs. The biallelic (GGTA1) knockout pig represented the first successful step towards ‘humanizing’ porcine organs for xenotransplant. Nevertheless, porcine-baboon xenotransplant studies using GGTA1^{-/-} pig cells have demonstrated residual α -Gal antibody formation and chronic cytotoxicity, suggesting additional sources for α -Gal epitopes. An alternative cause for α -gal biosynthesis is the enzyme isoglobotrihexosylceramide synthase (iGb3s). Some groups have suggested that iGb3s may function to replace a residual amount of α -GAL epitope in GGTA1^{-/-} animals, whereas others argue against such a role. [91, 107] To address any ambiguity, this study directly investigated the role of iGb3 by creating and comparing GGTA1^{-/-} pigs with GGTA1/A3GalT2^{-/-} double KO pigs. Our results show that there is no meaningful contribution to α -GAL levels by iGb3s. Although there is a very small trend (Figure 3.2) towards lower α -GAL expression in the iGb3s-null animal cells, this difference was not appreciated at the tissue level (Figure 3.3) and both antibody binding and cytotoxicity remained unchanged by inactivating iGb3s (Figure 3.4). We are cognizant that IB4 binding to iGb3 is reduced when compared to α -GAL and so the

staining might not be a true reflection of iGb3 levels. [108] However, IB4 does bind to iGb3 and the purpose of this study was to determine comparative reductions in IB4 binding associated with iGb3s silencing. Although the absolute levels of iGb3 are not reflective of IB4 staining, there was no significant reduction in staining associated with deletion of iGb3s gene.

A lack of measured role for iGb3s in acute rejection is not unexpected. Anti α -Gal reactive antibodies are found in GGTA1 KO pigs and mice with no discernable acute or chronic reaction. [109-112] This is probably because anti α -Gal antibodies can differentiate between α -GAL carbohydrate epitopes associated with lacNAc (GGTA1) and LacCer (iGb3) core structures. [107] Most preformed antibodies recognize LacNAc form of α -GAL rather than the LacCer form, even though the terminal disaccharide is identical. Millard *et al.* do report an iGb3 specific antibody from GGTA1^{-/-} mice that argues in favor of a role for iGb3s. [107] However, the specificities to antibodies produced by Milland *et al.* has been questioned because the over expression of iGb3s is likely to generate more than just iGb3 and will generate pol-GAL glycosphingolipids such as Gal α 1,3Gal α 1,3Gal α 1,3Gal α 1,3Gal β 1,4Glc β 1,1Cer. [113] Moreover, translation of murine studies to porcine-human xenotransplantation is problematic. In particular GGTA1 gene null mice are known to have lower levels of natural anti α -Gal antibodies when compared to humans and old world primates. In the study by Malland *et al.* mice were immunized against α -Gal in order to generate antibodies. [107] Consequently, it is not unexpected that the mice would generate antibodies that recognized iGb3 like epitopes. In contrast, neither humans nor baboons were immunized against α -Gal, therefore antibody binding to porcine PBMC cells from GGTA1^{-/-} and GGTA1^{-/-}

/A3GalT2^{-/-} pigs was minimal. Consequently, immunological quantification of iGb3 is uncertain.

In order to better understand the role of iGb3 levels in hyper acute rejection we performed glycosphingolipid analysis by NP-HPLC of kidneys from wild type and DKO pigs in order to detect iGb3. In wild type pigs iGb3 was below detectable limits. This is in accordance with previous studies of iGb3 in pigs using linear ion-trap mass spectrometry detection, whereby iGb3 was undetectable in pig heart, liver, kidney and pancreas. [97] The absence of detectable iGb3 can be explained by a rapid conversion of iGb3 to iGb4 by iGb4 synthase. (Figure 3.1D) In wild type pigs iGb4 was potentially detected as a peak eluting between GM2 and Gb4. Confirmation that this peak accurately represents iGb4 requires digesting the sample with a specific hexosaminidase to convert iGb4 to iGb3. For this study digestion was not performed, because the focus is on potential sources of residual α -Gal epitope and iGb4 does not contain a terminal α -gal epitope. However, by monitoring renal glycosphingolipid profiles in A3GalT2 knock out pigs we did observe a general disruption of glycosphingolipid metabolism and no iGb4 peak; suggesting that deletion of iGb3 synthase reduces the iGb3 substrate for iGb4 synthase.

In conclusion, our data suggests that iGb3s is not a contributor to AMR in pig-to-primate or pig-to-human xenotransplantation. Although, iGb3s gene silencing significantly changed the renal glycosphingolipid profile, the effect on Gal α 3Gal levels, antibody binding, and cytotoxic profiles of baboon and human sera on porcine peripheral blood mononuclearcytes (PBMCs) was neutral. In contrast, recently created triple xenoantigen KO pigs have reduced xenoreactive antibody binding and suggest that

further work should continue to focus on genomic editing for the reduction of non- α Gal xenoantigens and xenopeptides. [38, 47, 106, 114]

CHAPTER FOUR: Silencing porcine genes significantly reduces human-anti-pig cytotoxicity profiles: an alternative to direct complement regulation.

INTRODUCTION

Continuing my inquiry into the immunologic importance of the porcine *glycome* in pig-to-human xenotransplantation, this chapter describes a comparison between two novel model animals for the study of pig-to-human xenotransplantation. As described in the previous chapter, the unmodified porcine glycome has great potential to limit clinical application of solid xenotransplantation by effecting antibody-mediated rejection. Genetically modified porcine organs offers an answer to this problem. Although strategies of genetic modification have ‘humanized’ the porcine model *towards* clinical relevance, acceptable levels of human anti-porcine cytotoxicity have not previously been described. Most notably, these approaches have aimed at *either* antigen reduction or human transgene expression. The object of this study was to evaluate the relative effects of both antigen reduction and direct complement regulation on the human-anti-porcine complement dependent cytotoxicity response.

As aforementioned, the use of genetically modified porcine organs for clinical transplantation has not progressed to the clinic because of antibody-mediated rejection (AMR) that occurs shortly following graft reperfusion. AMR is mediated by the binding of xenoreactive antibodies to antigens on the porcine endothelial cell (EC) surface, followed by complement activation leading to EC injury. Two genetic engineering strategies in donor pigs have been employed to minimize the impact of xenoreactive

antibodies on xenograft survival. The deletion of endothelial xenoantigens such as the Gal[alpha]1–3gal epitope (α Gal) as well as the insertion of human complement regulatory protein (hCRP) transgenes have been used in pigs to limit EC injury. [115] Human CD55, also known as decay accelerating factor, is the most widely utilized hCRP transgene. It acts downstream to antibody binding by limiting the ability of C3b to potentiate complement-mediated EC damage. It has previously been shown that when expressed in porcine cells, this transgene limits human and primate antibody mediated complement-dependent cytotoxicity. [116] As a strategy to limit antibody-mediated damage, these proteins have proven valuable within the relatively high antigen background of wild type or α Gal-negative pigs. Recently, the antigen barrier has been significantly reduced by the sequential identification and removal of two more xenoantigens produced by the CMAH and B4GalNT2 genes. [47]

There are two main forms of sialic acid in mammals N-acetylneuraminic acid (Neu5Ac) and N-glycolylneuraminic acid (Neu5Gc). The CMAH gene is responsible for the creation of Neu5Gc. This gene was deleted during the course of evolution in humans because it conferred a protective advantage against a prevailing malaria strain. [117] The net result is that humans produce antibodies that react with Neu5Gc on the surface of pig cells. Deletion of the GGTA1 and CMAH gene produced pigs whose cells had less human antibody binding than chimpanzee cells. [29]

Byrne and McGregor used serum from primates that had rejected GGTA1^{-/-} pig hearts to screen a cDNA library from GGTA1^{-/-} pig endothelial cells to identify an enzyme, Beta-1,4-N-Acetyl- Galactosaminyl Transferase 2 (B4GALNT2), that produces a glycan to which humans and non-human primates have antibodies. [118, 119] Although

it is not yet clear which glycan is affected by the B4GALNT2 enzyme, deleting the porcine genes for B4GALNT2 in addition to GGTA1 and CMAH reduced human antibody binding to pig peripheral blood mononuclear cells (PBMCs), to the point where early antibody mediated rejection would not be expected. [47]

In xenotransplantation like allotransplantation, the risk of antibody-mediated rejection can be assessed by crossmatch analysis. A crossmatch involves placing recipient serum onto donor PBMCs. In allotransplantation, only IgG and not IgM, is considered. The reaction was initially a cellular cytotoxicity assay using fluorescent dyes, but has more recently been performed using flow cytometry to assess the degree of antibody binding. [120] Flow cytometry readout is expressed as median fluorescence intensity (MFI), and generally MFI background (cells only) is around 2,000. As described in Table 1, this value would represent a completely negative crossmatch. Crossmatches with MFIs between 2,000-5000, indicate donor specific antibody is present but at levels that are unlikely to create clinical issues. Crossmatches with MFIs between 5,000-9,500 are acceptable for transplant, but sometimes necessitate treatment with either plasmapheresis or IVIG. A flow crossmatch with elevated MFIs $> 9,500$ would result in a positive cellular dependent cytotoxicity crossmatch. At these levels, the risk of AMR prohibits clinical application even within the context of desensitization protocols.

Table 4.1: Interpretation of Flow Cytometric Crossmatch values for allograft allocation

MFI*	Clinical interpretation for allograft allocation
≤ 2,000	Background fluorescence (negative crossmatch)
2000-5,000	Acceptable for transplant without recipient desensitization
5,000- 9,500	IVIG or Plasmapheresis recommended before transplant [121]
> 9,500	Positive Crossmatch with high risk of early AMR** graft loss

*MFI, median fluorescence intensity; **AMR, antibody-mediated rejection

Human complement regulatory transgenes have proven ability to limit porcine endothelial cell damage in the presence of antibody binding. The purpose of this work was to examine the benefit of a hCRP transgene within a lower antigenic background than has previously been studied. Furthermore, we describe the first characterization of the effect of silencing the B4GalNT2 gene on human antibody-mediated cytotoxicity.

MATERIALS AND METHODS

Construction of hCD55 Plasmid

All restriction and modification enzymes used were purchased from Thermo Scientific (Vilnius, Lithuania) unless otherwise stated. First step was the conversion of our plasmids to the Multisite Gateway® (MG) system (Life Technologies, Carlsband, CA). The pCXEGFP expression cassette was excised with *XmaCI*+*SalI* digestion from the pMGEGFP5'3'MARHyg2272 and its resulting arms were blunted by T4 polimerase treatment in order to insert the blunted MG conversion cassette OrfA (Life Technologies). The resulting pMG5'3'MARHyg2272rev-OrfAPLrev destination vector presented 2 matrix attachment regions (MAR) of the chicken lysozyme [122] flanking the OrfA cassette on a pBlueScriptIIS+ backbone (Stratagene, Cedar Creek, TX). The ubiquitous hybrid promoter of pCAGGS expression vector was chosen for our experiments, obtaining the pCAGGS-hCD55 expression cassette. [123, 124] The hCD55 Entry clone was obtained cloning pCAGGS-hCD55/*PstI* S1nuclease-treated+*SalI* fragment (3363 bp) into the Entry clone pENTRL1L2-OligoSacISalluni (previously obtained in our laboratory) digested with *SalI*+*SmaI* restriction enzymes. After *MunI* recognition site deletion by T4 polymerase treatment, the resulting pENTRL1L2-CXhCD55del*MunI* Entry clone was finally exchanged with the pMG5'3'MARHyg2272rev-OrfAPLrev using the LR Clonase® enzyme mix (Life Technologies).

Production of Genetically modified animals

Genetically modified pigs were created utilizing a CRISPR/Cas9 approach and somatic cell nuclear transfer as previously described.[24] Briefly, bicistronic CRISPR sgRNA expression vectors co-expressing the Cas9 gene were designed to target the GGTA1, CMAH and B4GalNT2 genes within the first exon. A human CD55-expressing cassette was designed for hCRP transgene introduction. After transfection and selection, modified cells served as nuclear donors for somatic cell nuclear transfer (SCNT) to create clonal animals. Animals were grown to maturity and blood was obtained by peripheral venous sample. All the animals used in this study were approved by the Institutional Biosafety and Institutional Animal Care and Use Committee of IUPUI.

Antibody binding

Peripheral blood was obtained by venous sample from CMAH^{-/-} GGTA1^{-/-}, hDAF+ CMAH^{-/-} GGTA1^{-/-}, and CMAH^{-/-} GGTA1^{-/-} B4GalNT2^{-/-} animals. Peripheral blood mononuclearcytes (PBMCs) were isolated by Ficoll-Paque centrifugation (GE Health, Uppsala, Sweden) and assessed for viability using Trypan blue. 200,000 PBMCs of each group were incubated with 25% heat inactivated human sera from 10 healthy human donors for 1 hour at 4°C. Samples were then washed three times with Hank's Buffered Salt Solution (HBSS). Human IgG and IgM were detected individually with anti-human secondary antibodies conjugated to Alexa Fluor 488 (Jackson ImmunoResearch Laboratories Inc., West Grove, PA) for 1 hour at 4°C. PBMCs were washed three times in HBSS. Fluorescence detection was performed using an Accuri C6 flow cytometer

(Accuri, Ann Arbor, MI, USA). All experiments were performed in triplicate. Analysis of the median was performed with FlowJo version 8.8.7 (Treestar Inc., Ashland, OR) n=10.

Antibody-mediated complement-dependent cytotoxicity

The assay was performed as described by Diaz et al. [102] with slight modifications. In a 96-well V-bottom assay plate, 100 μ l of serially diluted heat inactivated human serums from ten healthy volunteers ages 21-63 was mixed with a 100 μ l aliquot of PBMC from either a CMAH^{-/-} GGTA1^{-/-}, hDAF+ CMAH^{-/-} GGTA1^{-/-} or CMAH^{-/-} GGTA1^{-/-} B4GalNT2^{-/-} animal. Although lytic assays for allograft screening utilize a process to remove IgM antibodies from recipient sera, IgM was left intact within these assays to determine the highest potential killing. The final concentration of PBMC in each well was 1×10^6 /ml and serum concentration varied by dilution (100%, 50%, 17%, 6%, 2%, 0.6%, and 0.2%). The assay was incubated for 30 mins at 4°C. After incubation, plates were centrifuged for 6 min (400x g), decanted and washed with HBSS; this step was repeated twice. Heat inactivation of human sera prevents the variable presence of complement within stored sera from affecting results. Baby Rabbit complement, a common stable substitute for human complement, (Cedarlane, Burlington, NC, USA) was diluted 1:15 in HBSS and 140 μ l was added to each well and incubated for 30 mins at 37°C. PBMCs were labeled with a fluorescein diacetate (FDA) 1 μ g/ml in acetone and propidium iodide (PI) prepared at a concentration of 50 μ l/ml in phosphate-buffered saline (PBS). After incubation in complement, the samples were transferred from 96 well to flow tubes containing 100 μ l HBSS and 10 μ l FDA/PI. Analysis was completed by

flow Cytometry. The percentage of dead cells (PI+, FDA-), damaged cells (PI+, FDA+) and live cells (PI-, FDA+) was determined by quadrant analysis. PI-/FDA- events were excluded from analysis. Background spontaneous cytotoxicity was determined by analyzing cells not exposed to human sera. Values for cytotoxicity are subsequently reported after correction by this background value using the following equation: $\% \text{cytotox} = (\% \text{cytotoxExp} - \% \text{cytotoxSpont}) / (100 - \% \text{cytotoxSpont})$ where %CTXexp is the percentage of dead cells under the experimental condition.

Statistics

Flow cytometric results were reported in mean fluorescence intensity (MFI) values for each human serum subjected to both test group PBMC for IgG and IgM assays.

Antibody-mediated complement-dependent cytotoxicity data was plotted into a non-linear regression model, by taking the log of each of the seven serum dilution against the corresponding percentage of cytotoxicity to estimate serum DC50. The comparison of cytotoxicity and antibody binding cohorts was performed using a two-tailed student's t-test. P-values < 0.05 were considered statistically significant. All experiments were performed in technical and biological triplicate.

Tissue staining and confocal microscopy

Tissue and PBMCs were procured from hDAF+ CMAH^{-/-} GGTA1^{-/-} piglet after euthanasia. Mounted samples were blocked in Odyssey blocking buffer (Li-Cor Biosciences, Lincoln, NE USA) in HBSS for 1 hour. The slides were then fixed in

paraformaldehyde for 10 minutes. Samples were stained with hCD55-phycoerythrin conjugate (Santa Cruz Biotechnology, Inc. Santa Cruz, CA) to visualize the presence of the hDAF. Tissues were incubated for 1 hour at 4°C and washed three times with 0.1% HBSS. DAPI (Invitrogen, Carlsbad, CA) was added to all slides for 1 minute as a nuclear stain followed by two 0.1% HBSS washes. Samples were mounted in ProLong Gold (Invitrogen, Carlsbad, CA). Confocal microscopy was accomplished using an Olympus FV1000 (Olympus America Inc., Center Valley PA, USA). All confocal settings were set to isotype control levels.

RESULTS

Genetic modification of porcine cells and SCNT produced healthy pigs. Cells from CMAH^{-/-} GGTA1^{-/-} (DKO), hDAF+ CMAH^{-/-} GGTA1^{-/-} (DKO CD55+), and CMAH^{-/-} GGTA1^{-/-} B4GalNT2^{-/-} [125] animals exhibited the expected glycan-null phenotypes (Figure 4.1). The DKO CD55+ animals achieved hCRP transgene expression (Figure 4.2). As expected, human IgG and IgM antibody binding levels were unchanged between the DKO and the DKO CD55+ animals. Human IgG and IgM antibody binding were significantly lower to the TKO animal. As displayed in figure 4.3, Median IgG and IgM MFI values for DKO cells were 3917.1 (SEM=1057.1) and 5615.2 (SEM= 1270.3) respectively. IgG and IgM values for TKO cells dropped to 1952.4 (SEM= 226.1) and 3185.9 (SEM= 379.4) respectively. This represented a 49.1% (p= 0.012) reduction in IgG and 43.2% (p= 0.002) reduction in IgM binding when compared to the DKO background. The new reduction in antibody binding brings a pig-to-human crossmatch within ranges associated with matched allograft allocation. (Table 4.1) Compared to the DKO, human anti-porcine cytotoxicity was reduced by 8% with the addition of a hCRP (p=.046). As displayed in figure 4.4, it was reduced by 54.3% with silencing the B4GalNT2 gene (p=.0002). Reductions in cytotoxicity to the TKO animal varied between human sera. The magnitude of reduction to complement-mediated cytotoxicity was directly proportional to reductions in human IgM binding when compared across individual sera (Figure 4.5).

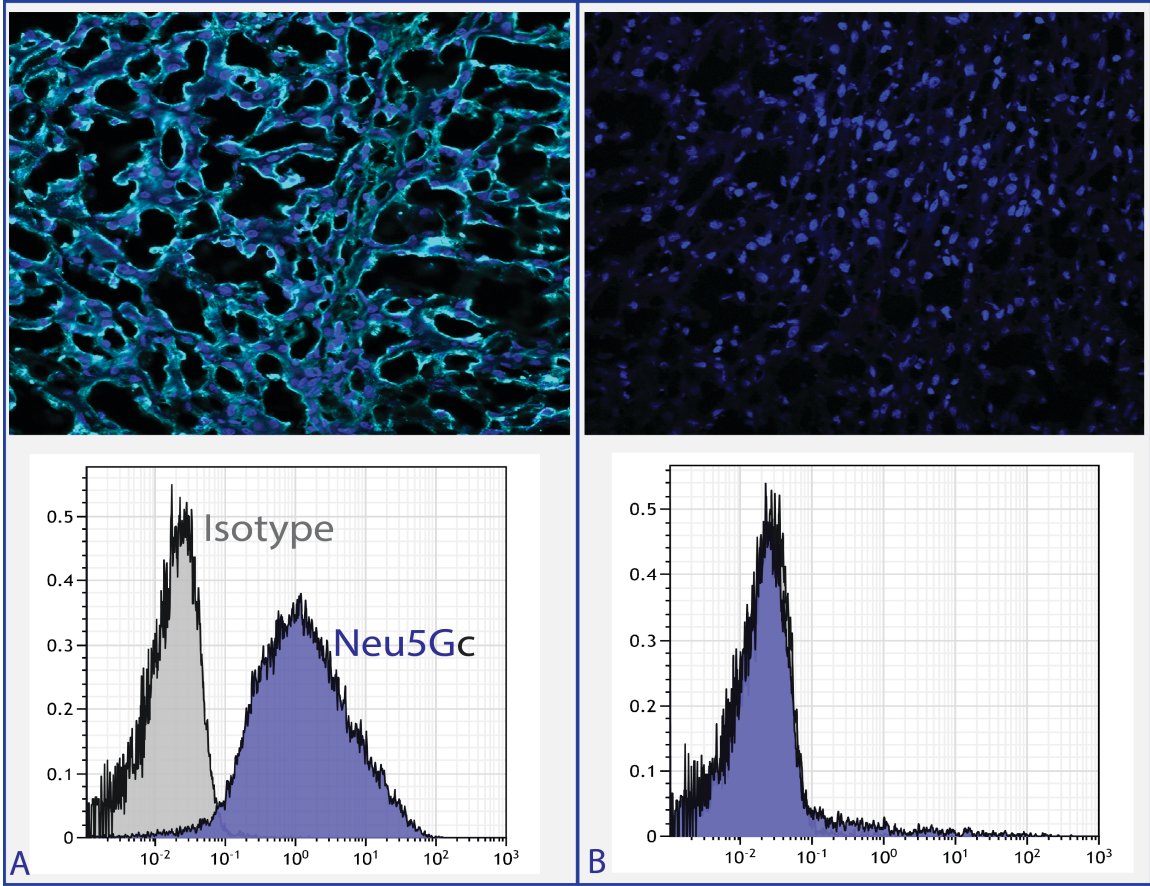


Figure 4.1: Phenotypic silence of porcine carbohydrate genes.

A: Confocal analysis of Porcine WT Liver tissue stained with DAPI and HD (above); flow cytometric analysis of PBMCs from Porcine WT PBMCs stained for Neu5Gc and Isotype control (Below). **B:** Confocal analysis of Porcine CMAH Liver tissue stained with DAPI and Anti-Neu5gc (above); flow cytometric analysis of PBMCs from Porcine WT PBMCs stained for Neu5Gc and Isotype control (below).

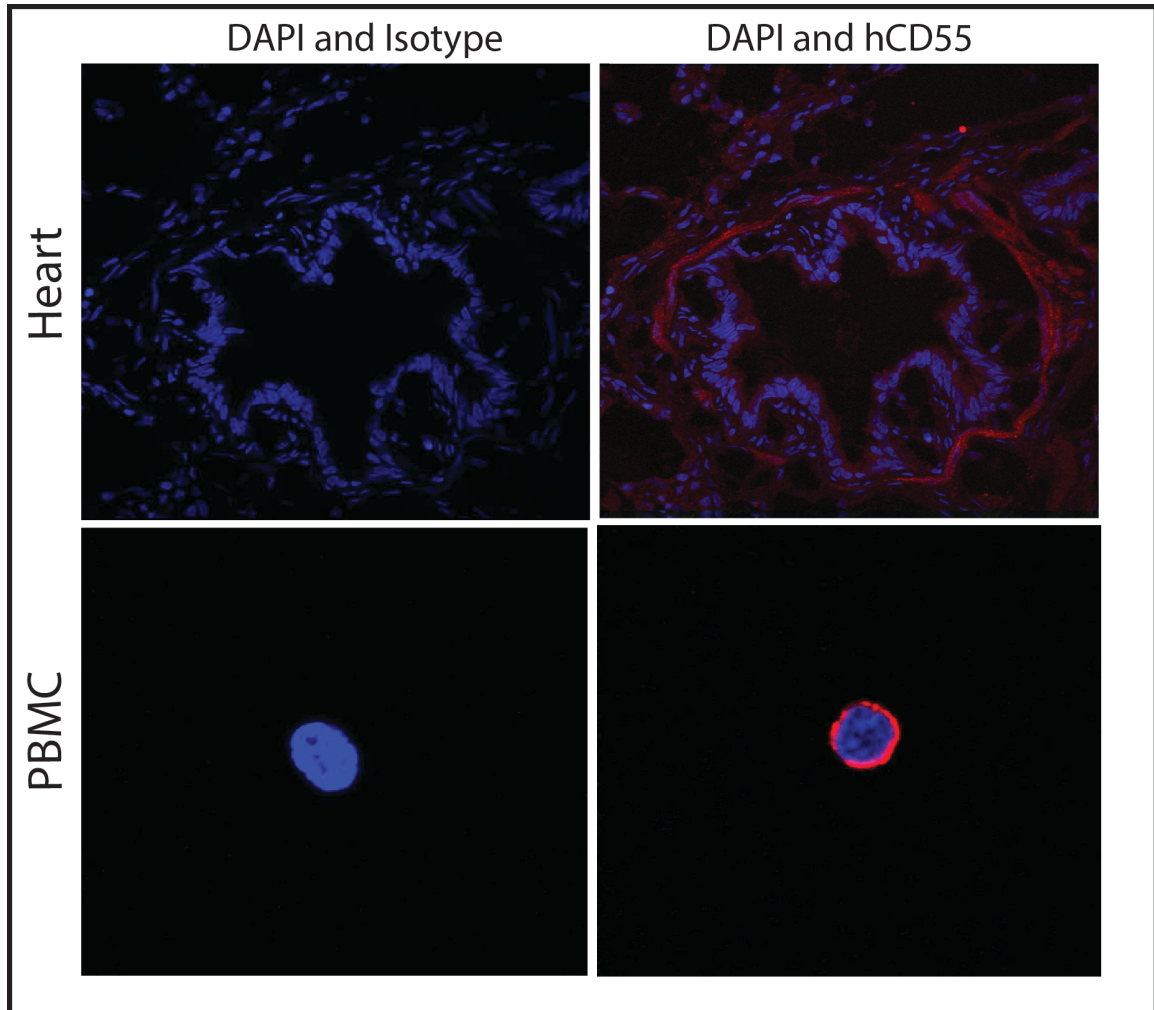


Figure 4.2: Transgenic expression of hCD55 on porcine tissue and cells.

Sections of tissue was obtained from a hDAF+ CMAH^{-/-} GGTA1^{-/-} (DKO CD55+) pig after euthanasia. Tissues were stained with anti-hCD55 [101] and a DAPI nuclear stain [75]. Top panels show tissue-level expression in heart. Bottom panels show cellular expression in PBMCs. Confocal settings were set to isotype control levels (left).

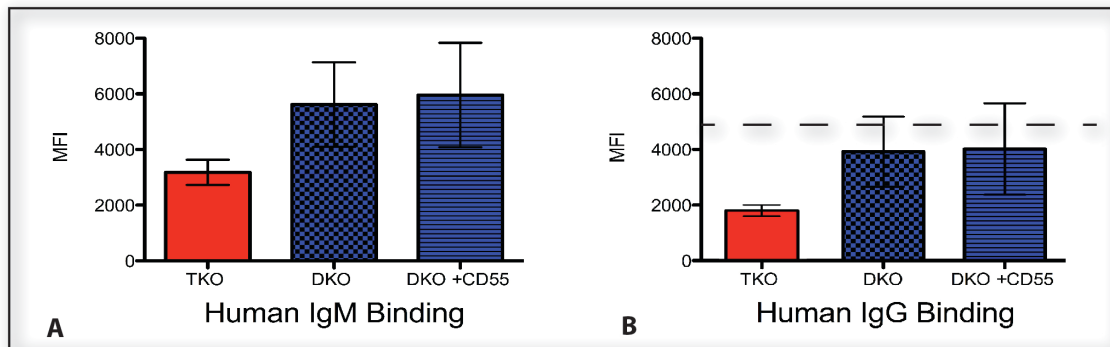


Figure 4.3: Human antibody binding directed towards porcine cells.

PBMCs from $CMAH^{-/-} GGTA1^{-/-}$ (DKO), $hDAF^{+} CMAH^{-/-} GGTA1^{-/-}$ (DKO CD55+) or $CMAH^{-/-} GGTA1^{-/-} B4GalNT2^{-/-}$ [125] swine were incubated with 25% heat inactivated human sera from 10 healthy human donors for 1 hour at 4°C. Secondary fluorescent antibodies were used to detect IgG and IgM binding to the cells with median fluorescence intensity being evaluated (MFI). T-test statistical analysis was used to analyze the difference between genotype cohorts (n=10). Human IgG and IgM binding was not statistically affected by the presence of hCD55. Both IgG and IgM binding was statistically lower to the TKO animal. The level of antibody binding to TKO cells was reduced below the threshold at which we do not expect allograft antibody-mediated acute rejection to occur, as depicted by the horizontal line. **A** represents patterns of human IgM binding (n=10). IgM binding is not a relevant metric for allotransplantation, and its significance to xenotransplantation remains in question. **B** represents patterns of human IgG binding (n=10).

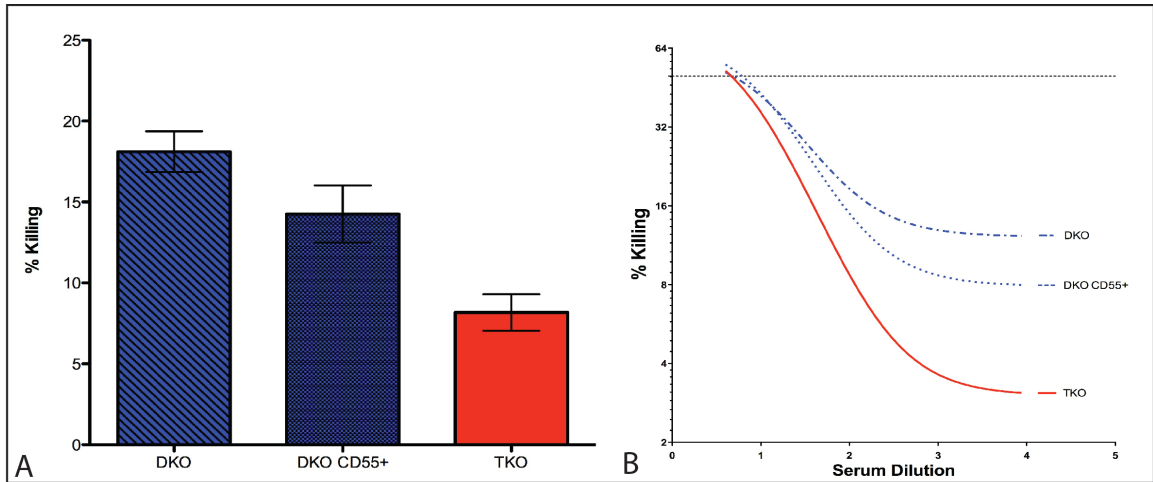


Figure 4.4: Human antibody-mediated complement-depended cytotoxicity to porcine cells.

Human sera was incubated in serial dilution with PBMCs from or $CMAH^{-/-}$ $GGTA1^{-/-}$ (DKO), DKO hCD55+ or $CMAH^{-/-}$ $GGTA1^{-/-}$ $B4GalNT2^{-/-}$ [125] swine. After wash, baby rabbit complement was added. Cell death was measured by live/dead co-labeling for analysis by flow cytometry. **A** represents the average percent cell death across animal cohorts at a 1/2 dilution. (n=10) **B** represents a nonlinear regression analysis of killing curves obtained from the seven-point dilution assay described. (n=10, R^2 score=0.98)

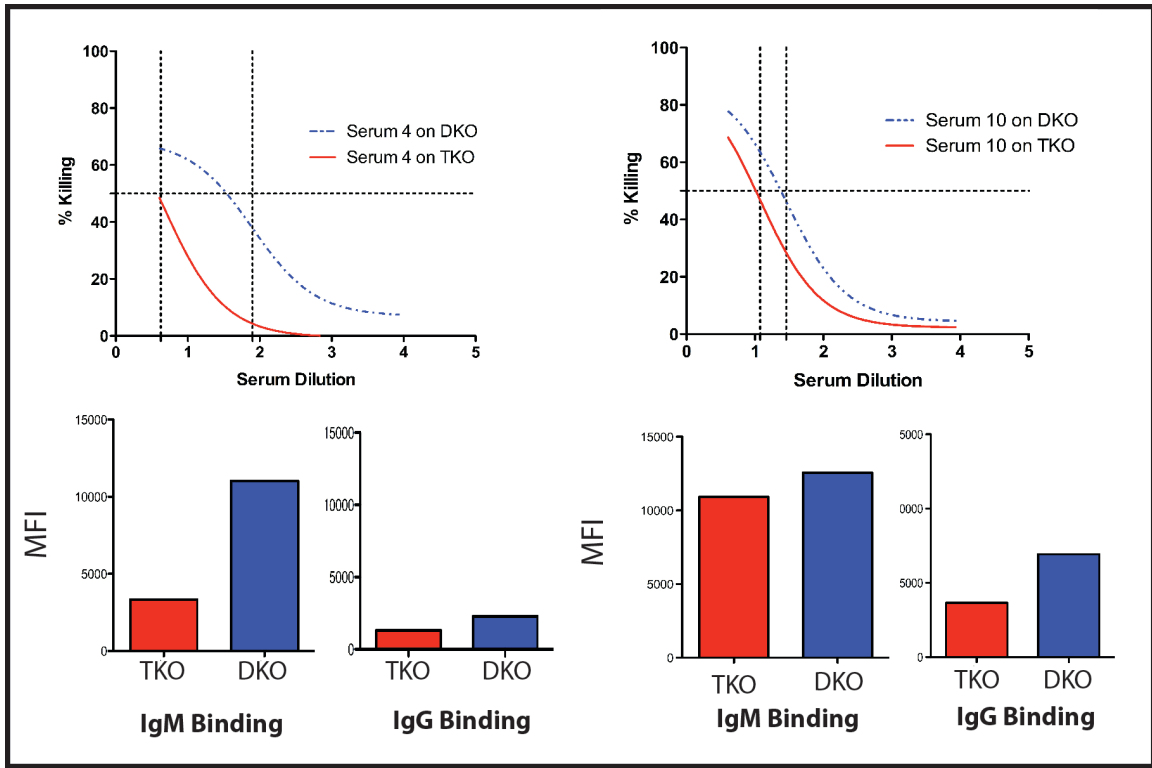


Figure 4.5: Antibody-mediated complement-dependent cytotoxicity is related to human IgM levels.

Within the lytic assay described, the magnitude of difference between $CMAH^{-/-} GGTA1^{-/-}$ (DKO) and $CMAH^{-/-} GGTA1^{-/-} B4GalNT2^{-/-}$ [125] cells varied for each human serum tested. The degree of separation between killing curves correlated to the degree of difference between human IgM binding across individual sera. **A** represents the cytotoxicity of human serum 4 (above) and median IgG and IgM binding from serum 4 (below). **B** represents the cytotoxicity of human serum 10 (above) and median IgG and IgM binding from serum 10 (below). Dashed lines indicate levels of 50% cell death as indicated by the linear regression model.

DISCUSSION

Antibody mediated rejection (AMR) has been *the* barrier to clinical application of xenotransplantation. In 2003 the first GGTA1^{-/-} pig was created, representing the first significant reduction to the AMR barrier and solidifying the importance of humanizing porcine carbohydrate profiles.[19, 32] The *in vivo* significance of this achievement was subsequently well described by work performed by Dr. David Cooper and colleagues; in 2005 his group achieved life-supporting xenograft survival in baboons up to 6 months using GGTA1^{-/-} porcine organs. [89, 126] Despite this great achievement in the pig-to-primate model, GGTA1^{-/-} organs eventually failed in the context of thrombotic microangiopathy raising the possibility of residual non-Gal antigen-driven AMR.

In the absence of other identifiable antigen targets, efforts to limit AMR of GGTA1^{-/-} organs relied on a direct complement regulation strategy. [127, 128] Within this climate, human CD55 and CD46 emerged as the central hCRPs for transgenesis. By disrupting the complement cascade pathway, these proteins enhance xenograft resistance to complement-mediated damage without affecting antibody binding. The protective effect of hCRP transgenes has been shown to be linearly proportional to expression level. [129] Subsequently, within a high antigen background, hCRP approaches have favored over-expression. [127] Alternatively, endogenous *porcine* complement regulatory proteins (pCRP) have also been shown to limit human C3b binding when overexpressed. [130, 131]

More recently, advances have been made on the *antigen-reduction* front, that significantly reduce human and primate antibody binding to porcine cells. [38, 47] It has

therefore become essential to examine the potential for complement regulatory proteins to limit cytotoxicity within this new context of lower xenoantibody binding.

The results of our study have several implications for the prospects of moving xenotransplantation to the clinic. First, the CMAH^{-/-} GGTA1^{-/-} B4GalNT2^{-/-} [125] pig exhibits very low levels of human IgG and IgM antibody binding and low levels of complement-mediated damage, even in the absence of a hCRP. The MFIs in the crossmatches of the TKO pigs suggest that the 10 subjects tested could receive a TKO pig organ transplant without the need for desensitization to avoid AMR. This finding is significant since it removes a barrier that has limited progress in xenotransplantation for the last 25 years. [132, 133] In allotransplantation the impact of IgM is not considered when evaluating the risk of AMR via crossmatching and donor IgM is removed from sera before analysis. [120] It is unclear whether IgM is important in xenotransplantation, although two of the three longest surviving pig-to-non-human primate renal xenografts (136 and 310 days) had high levels of xenoreactive IgM. [71, 134] The survival of those two primates suggests that similar to allotransplantation, xenoreactive IgG, and not IgM levels are the determinant of whether early AMR will occur.

This study shows that hCRPs can limit in vitro complement-induced cytotoxicity even when the antigen level is low. Our results also show that antigen deletion can reduce complement-mediated injury to a greater extent than direct complement regulation. These findings are not completely unexpected in the context of previously published data. In 2012 McGregor et al. noted that expression of hCD55 appeared to restrict local complement activation in a cardiac model of pig-to-primate transplant, but did not prolong graft survival. [135] Using a GGTA1^{-/-} background, they noted considerable

antibody deposition and concluded that identifying and eliminating non-Gal antigens was still important. Conversely, recent work by Azimzadeh et al. suggests that the addition of a hCRP into a GGTA1^{-/-} background can limit early graft failure in the pig-to-primate model. [136] Similarly, our findings support the assertion that hCRP expression limits antibody-mediated complement dependent cytotoxicity. Moreover, we show that complement-mediated damage can also be effectively minimized by silencing the GGTA1, CMAH and B4GalNT2 genes in concert. Ultimately the human complement regulatory strategy may be most effective when combined with significant antigen reduction. Taken together, our results show that the reduction of antigen on the surface of pig cells will facilitate movement of xenotransplantation to the clinic.

CHAPTER FIVE: Modified glycan models of pig-to-human xenotransplantation do not enhance the human-anti-pig T cell response.

INTRODUCTION

Historically humoral immunity has been *the* barrier to clinical application of pig-to-human xenotransplantation. The previous chapter describes a modified porcine glycan model that reduces human antibody binding to levels comparable with current allograft standards. The newly described genetic background provides an *answer* to the problem of acute humoral xenograft rejection (AHXR). From this unprecedented position of humoral acceptability, it is subsequently important to consider the impact these modifications may have on measures of *cell-mediated* rejection.

The previous chapters have described strategies that modify the porcine genome in ways that limit the xenogenic humoral response. As xenotransplantation moves closer to clinical application, cellular immunity remains an increasingly relevant consideration. Acute humoral rejection is avoided in allotransplantation by judicious selection of appropriately matched donor-recipient pairs; utilizing IgG and complement-dependent cross match assays similar to those described in chapters 3-5, favorable HLA antigen profiles are screened for across a diverse donor pool. However, *cellular* immunity still affects allotransplantation -largely through MHC-dependent pathways- and is conventionally controlled through pharmacologic maintenance of recipient immunosuppression. One ancillary advantage of the strategies for model animal creation described in chapters 2-5 is that they efficiently create *clonal* lineages; in this manner the

study of human-anti-porcine cellular immunity is arguably more *universally* translatable to clinical application than the study of allotransplant cellular rejection; in the pig-to-human models proposed, the donor antigen profile can be held as a controlled variable.

Unlike the process of matching *allografts* with recipients, porcine xenografts are affected by an inherent immunologic discordance that is associated with traversing the evolutionary divide across species; described in previous chapters, wild-type swine cells exhibit a carbohydrate profile to which humans have pre-formed antibodies. Unmodified, these antigens cause acute humoral xenograft rejection (AHXR) in a pig-to-primate model. The creation of GGTA1^{-/-} (GTKO) pigs in 2002 marked the first successful antigen reduction and legitimized the concept of pig-to-human xenotransplantation. [19] Over the past 15 years, many genetic modifications have been attempted to overcome AHXR. As described in chapter four, the creation of a triple-knockout animal successfully lowered human antibody binding to levels comparable with currently-accepted allograft standards. [27]

Since the development of the first GGTA1^{-/-} pig, there has been uncertainty about the severity of the human-anti-pig T cell response and whether it can be adequately controlled using approved immunosuppressive therapies. [137] In vivo, pig-to-primate solid organ transplant has been sustained using a wide range of pharmacologic strategies. [138] Unfortunately, the enduring efficacy of these regimens has been difficult to ascertain, as graft rejection often occurred early in the context of high xenoantigen level and thrombotic microangiopathy [139]. As such, discussions of cell-mediated rejection have not commanded the same attention afforded to problems of AHXR.

Advances in genetic engineering strategies have dramatically sped the process of identifying and eliminating xenoantigens.[115] Within the porcine genome, the GGTA1 locus drives α Gal glycan expression and the CMAH gene drives Neu5Gc glycan expression. Each of these gene products independently induces human antibody binding; when both genes are silenced, human IgG and IgM binding is dramatically lowered. [38] As these porcine cells now react similarly to human cells in crossmatch analysis, it is increasingly likely that xenograft AHXR can be effectively mediated by genetic donor modification; discussions of cell-mediated rejection pathways should now occupy a more prominent position within the study of xenotransplantation.

Though the dedicated study of glycoimmunology is relatively new, a growing body of evidence supports the ability of glycosylation variance to affect immune response;[140] modifications made to mammalian glycan profiles warrant careful consideration of the potential for immunogenic effects. Herein we describe the impact of successful glycan antigen-reduction models of pig-to-human xenotransplant in a cell-mediated proliferation assay. As these genetically modified cells have shown great promise by reducing antibody-mediated barriers of AHXR, their cell-mediated immunogenicity is of potential clinical importance.

MATERIALS AND METHODS

Modified Porcine Cell Construction

Genetically modified pigs were created utilizing a CRISPR/Cas9 approach and somatic cell nuclear transfer as previously described by Li et al. [24] Briefly, bicistronic CRISPR sgRNA expression vectors co-expressing the Cas9 gene were designed to bind and cleave the GGTA1 gene beginning at position 293654066 of NC_010443.4 (forward: CACCGCGAAAATAATGAATGTCAA) and CMAH gene beginning at position 210555038 of NCBI reference NC_010449.4 (forward: CACCGAGTAAGGTACGTGATCTGT). Porcine liver-derived cells were cultured, and transfected with targeted nuclease-expressing vectors using the Neon transfection system (Life Technologies, Grand Island NY, USA) as described by Lutz et al. [38] After negative selection by flow cytometry, knockout cells were identified and somatic cell nuclear transfer (SCNT) was used to create clonal animals from modified porcine cells. Genetically modified animals were grown to maturity and served as source of peripheral cells for analysis by blood draw. The Institutional Biosafety and Institutional Animal Care and Use Committee at Indiana University School of Medicine approved the use of animals in this research.

Preparation of Stimulator Populations

Porcine blood was obtained by venous sample from wild type (WT), GGTA1^{-/-} (GTKO) or CMAH^{-/-} GGTA1^{-/-} (DKO) animals. Human buffycoats were obtained from a local blood bank. PBMCs were isolated from these samples by Ficoll-Paque centrifugation (GE Health, Uppsala, Sweden) and assessed for viability using Trypan blue. These cells were then treated with mitomycin C at a concentration of 25ug/ml/4E6 cells for 30 minutes at 37 degrees C. 10 uL/ml of DNase added for the last 5 minutes of incubation. After mitomycin C treatment, the cells were washed three times with HBSS, counted by hemocytometer and brought to a final concentration of 2E6/mL in AIM V media (ThermoFischer, Grand Island, NY).

Preparation of Responder Populations

Human buffycoats were obtained from a local blood bank and PBMCs were isolated from these samples by Ficoll-Paque centrifugation. (GE Health, Uppsala, Sweden) Viability was assessed using Trypan blue. Isolated cells were washed three times with HBSS and brought to a final concentration of 2E6/mL in AMI V media. To control for inter-individual variability in human responders, three human samples were prepared and tested for each stimulator.

BrdU ELISA based Mixed lymphocyte reaction (MLR) assay

A 96 well micro-titer plate (MTP) was used for mixed lymphocyte reaction over a 5 day

period was set up and incubated for four days. All responder cells were added at a concentration of 200,000 PBMCs/well. All stimulator cells were added at a concentration of 200,000 PBMCs/well. Bromodeoxyuridine (BrdU) was then added for an overnight incubation and on day five a BrdU ELISA was performed utilizing a Roche ELISA proliferation kit following the manufacturers protocol (Roche Diagnostics, Indianapolis IN). Absorbance was read on a Dynex MRX plate reader at 450nm (MTX Lab Systems, Vienna, VA). Allogeneic reactions consisted of human PBMC responder cells with human mitomycin C treated PBMC stimulator cells. Xenogeneic reactions consisted of human responder cells with mitomycin C treated porcine PBMCs. Positive controls consisted of human or porcine PBMC responder cells with 2 ug/well of phytohemagglutinin [141]. Negative controls consisted of human or porcine mitomycin C treated PBMCs. Simulation index was calculated by absorbance of proliferation response of experimental treatment / absorbance of proliferation of PBMCs alone. As a proof of concept for pharmacologic intervention, DKO-stimulated xenogeneic reactions were performed in the presence of dexamethasone against an allogeneic control; in the absence of relevant clinical plasma levels for dexamethasone, concentration was chosen on the basis of previous in vitro study. [142-144] Each stimulator-responder pair was tested in triplicate; differences across groups were analyzed using a one-way analysis of variance.

Immunosuppressive treatment during MLR

A flow cytometric proliferative assay was performed to complement our DNA-synthesis measurements; by directly labeling responder cells, this approach directly examined

proliferative potential over a broad time course in the presence or absence of clinically relevant pharmacologic intervention. To better characterize the effect of immunosuppression on the *direct* xenogeneic human T cell response to GGTA1^{-/-} CMAH^{-/-} (DKO) cells, human CD4 T cells were isolated using human CD4 T isolation kit (Miltenyi Biotec Inc., San Diego, CA, USA), and labeled with CFSE using CellTrace™ CFSE Cell Proliferation Kit (Life Technologies, NY, USA). Splenocytes from human or GGTA1^{-/-} CMAH^{-/-} (DKO) pigs were used as stimulating populations; they were labeled using CellTrace™ Far Red DDAO-SE (Life Technologies, NY, USA), and irradiated by Gammacell-1000 Irradiator at 3000 Gy. Human CD4⁺ responders at 1x10⁵ cells/well in 96-well round-bottom plates (Corning, Lowell, MA, USA) were co-incubated with or without irradiated stimulators [145]. CFSE-labeled CD4 T cells were co-cultured with FarRed labeled splenocytes (R:S=1:8) in serum-free AIM V® Medium (Life Technologies, NY, USA) in the presence or absence of immunosuppressive agents dosed for clinical relevance: 10ng/ml FK-506 (FK, LC Laboratories); 10ng/ml Rapamycin (RAPA, InvivoGen); 200ng/ml Cyclosporin A (CsA, LC Laboraories). Analysis of proliferation was limited to live human T cells by light scatter gating and far-red exclusion of stimulator cells; an non-stimulated, non-suppressed human T cell control was included with each experiment. All tests were repeated in triplicate under identical conditions.

RESULTS

Creation of modified porcine cells

CRISPR/Cas9-directed mutagenesis created targeted disruptions at the GGTA1 and CMAH loci. (Figure 5.1) All disruptions produced a null phenotype at the loci of interest, and have been previously published by Li et al. [24] After phenotype selection and SCNT, these cells created healthy clonal animals. Animals used in this study were of a WT, GGTA1^{-/-} (GTKO), or CMAH^{-/-} GGTA1^{-/-} (DKO), background. The viability of all PBMCs obtained was above 97% by trypan blue staining.

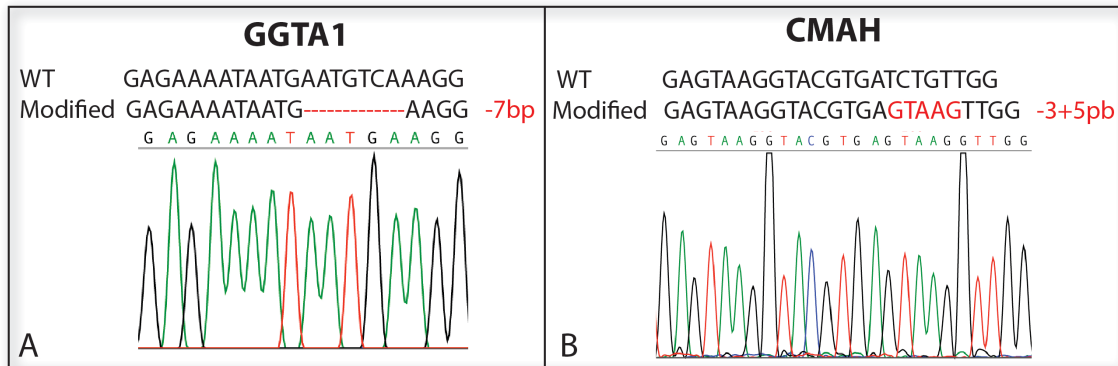


Figure 5.1: Targeted Genetic Disruptions

CRISPR/Cas9-directed mutagenesis created targeted disruptions at the GGTA1 and CMAH loci. A) Depicts a 7bp deletion within the GGTA1 locus B) Depicts a simultaneous 3bp deletion and 5bp insertion at the CMAH locus. All modifications produced a null phenotype.

BrdU ELISA based Mixed lymphocyte reaction (MLR) assay

Human and porcine PBMC cultures showed positive PHA proliferative responses whereas mitomycin C treated PBMCs had stimulation indexes (SI) less than baseline PBMC cultures (SI<1.0). Human responder PHA control groups exhibited a SI of 7.6, porcine PHA control groups exhibited SI ranging from 38.2 – 103.0. No evidence of overgrowth was noted throughout experimental wells. Allogeneic and xenogeneic responses to a one-way mixed lymphocyte reaction were comparable. The allogeneic response was positive with a stimulation index of 5.8. A xenogeneic response was seen for all tested cell stimulator populations with a stimulation index range of 5.5-7.1. Figure 5.2 depicts stimulation indices for the tested stimulator populations. Differences between porcine stimulator cells failed to reach statistical significance (p=.0529). Although the WT xenogeneic reaction was 16% stronger than the allogeneic reaction (p=.0023), the difference between an allogeneic reaction and *genetically modified* porcine cell-stimulated xenogeneic reactions failed to reach significance (p=0.15).

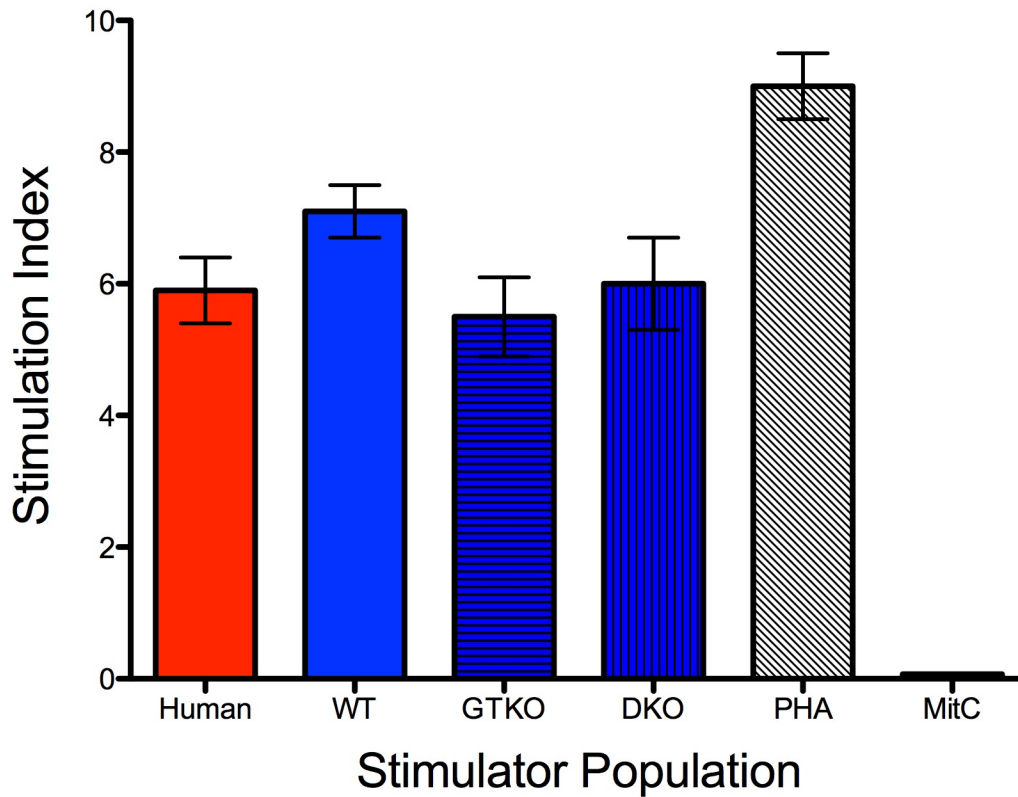


Figure 5.2: Stimulation Indices of allogeneic and xenogeneic mixed lymphocyte reactions

Represents the results of a one-way mixed lymphocyte reaction with a human responder population. Stimulator Populations varied and included human, wild-type porcine, or modified porcine cells of a $GGTA1^{-/-}$ (GTKO) or $GGTA1^{-/-}$ $CMAH^{-/-}$ (DKO) background. Positive controls consisted of human PBMC responder cells with 2 ug/well of phytohemagglutinin [141]. Negative controls consisted of human responder cells mitomycin C treated (MitC). Each stimulator-responder combination was repeated in triplicate under identical conditions.

As shown in Figure 5.3, both allogeneic and xenogeneic reactions were reduced to the level of background by the addition of 0.05uM of dexamethasone. Differences in dexamethasone-suppression between xenogeneic and allogeneic reactions were not significant ($p=0.078$).

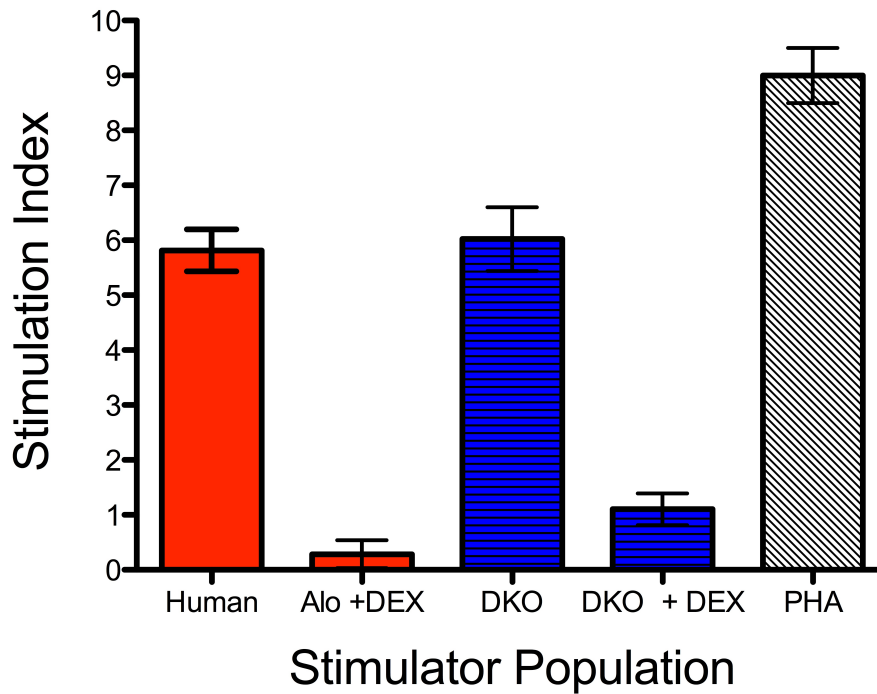


Figure 5.3: Stimulation Indices of allogeneic and xenogeneic mixed lymphocyte reactions in the presence of dexamethasone.

Represents the results of a one-way mixed lymphocyte reaction with a human responder population with and without dexamethasone (DEX) stimulation. Stimulator Populations varied and included human, or modified porcine cells of a $GGTA1^{-/-}$ $CMAH^{-/-}$ (DKO) background. Positive control consisted of human responder cells with 2 ug/well of phytohemagglutinin [141]. Each stimulator-responder combination was repeated in triplicate under identical conditions.

Effect of Immunosuppression on xenogenic human CD4 T cell proliferation in vitro.

Immunosuppressive drugs are used clinically to prevent immune rejection in allotransplantation. Given our ability to limit the human-anti-porcine cellular response in a CMAH^{-/-} GGTA1^{-/-} (DKO) model with dexamethasone, we sought to further characterize the clinical relevance of these findings. Plasma dexamethasone levels are not routinely followed clinically, post transplantation; this challenges the translation of information from in vitro assay. FK-506, RAPA, and CsA however, all have published plasma levels that can more easily correlate in vitro work to the clinic. [139, 146, 147] To assess the ability of these immunosuppressant agents to inhibit the direct xenogeneic human T cell response to glycan-modified porcine cells, a flow cytometry-based MLR assay was performed (Figure 5.4). Human CD4 T cell expansion was successfully induced by exposure to pig splenocytes; this xenogeneic reaction was significantly inhibited by independent addition of FK-506, RAPA and CsA.

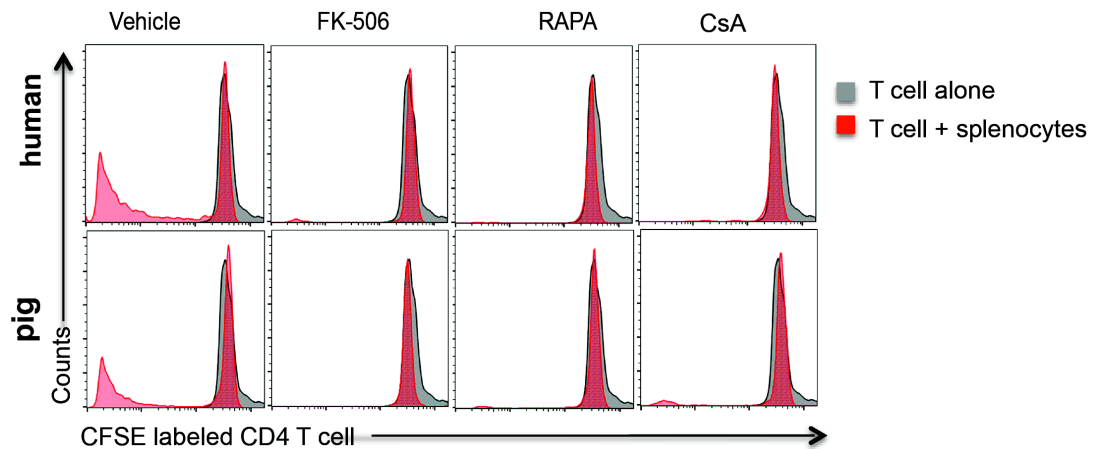


Figure 5.4. Effect of Immunosuppression agents on human T cell proliferation.

A flow cytometry-based MLR assay was performed using CFSE labeled human CD4 T cells as responders, and FarRed labeled human or GGTA1^{-/-} CMAH^{-/-} (DKO) pig splenocytes as stimulators. The culture medium was in the presence or absence of clinically relevant doses of immunosuppressant including 10ng/ml FK-506, 10ng/ml RAPA and 200ng/ml CsA. Proliferation of human CD4⁺T cells were quantified by CFSE dilution on day 7. Analysis of proliferation was limited to live human T cells by light scatter gating and far-red exclusion; an unstimulated human T cell control without immunosuppression was included with each experiment (Grey). Pharmacologic mediation of the xenogenic T-cell response was equivalent to the allogeneic T-cell response for all drugs tested. Representative histograms are shown. Experiments were repeated in triplicate under identical conditions.

DISCUSSION

As described in chapter one, the solid organ transplant community is gravely affected by a growing shortage of solid organs. Although considerable work has been done to make better use of available allografts, a recent study by Rana et al. notes that we have reached a plateau in the volume of all solid organ transplants. [148] From this position, answering the problem of a growing transplant list will require a supply-side addition to the donor pool. Utilizing the advanced techniques of genetic engineering described in chapter two, modification of pigs as surrogate organ donors represents the most immediate solution.

The porcine GGTA1 and CMAH genes are each independently responsible for driving human antibody binding to porcine cells. Recently, simultaneous knockouts of these genes have reduced human antibody binding towards porcine cells to the point at which acute humoral xenograft rejection (AHXR) would not be expected. [27, 38] Examining remaining barriers -beyond AHXR- to the clinical application of these models requires a consideration of the human-anti-porcine *cell-mediated* response to genetically modified pigs.

There has historically been some uncertainty about the severity of the xenogeneic T-cell response. Initially, xenogeneic cell-mediated responses were thought to be less proliferative than allogeneic reactions. [149-151] Due to differences between MHC molecules across species, xenogeneic cell-mediated rejection was not considered to be a significant barrier to clinical application. Although this theory was supported by early mouse-anti-human models, [152] more recent work has demonstrated xenogeneic cell-mediated responses to be comparable to allogeneic reactions. [153-155] The present

results support the previous conclusions of Yamada et al. [156] who demonstrated that the human-anti-porcine xenogeneic cell-mediated response was similar in strength to an allogeneic response.

Although the role of carbohydrates in cell-mediated immune response pathways are incompletely understood, any alteration in donor glycan profiles has the capacity to alter recipient T-cell response through both direct and indirect pathways. [157, 158] The genetic modifications in question within this study were of particular theoretical relevance to the human-anti-porcine cell-mediated response, as they alter sialic acid profiles. Of the various roles sialic acids play, their role as ligands of inhibitory sialic acid-binding Ig superfamily lectins (siglecs) provides a unique potential to affect the human immune system. [159] Siglecs drive negative feedback signals to dampen cell-mediated immune responses. [160] Recently, humanizing sialic acid profiles of animals has demonstrated unexpected effects on the T cell response. With particular relevance to our model, it has been shown that ‘humanized’ CMAH^{-/-} mice mount a *hyperactive* T cell response compared to WT mice. [161] Because imposing a human glycosylation mutation pattern onto porcine cells is imperative to avoid AHXR, it is important to directly study the effect that these mutations may have on cell-mediated human response. The present study is the first to show that silencing the porcine GGTA1 and CMAH genes does not negatively impact the human-anti-porcine cellular response. One reason that these genetic modifications do not raise the barrier of cellular immunity, may be that -under genetic pressure- the corresponding human siglec receptor profile has also been altered. [162, 163] In the absence of the appropriate receptors, the presence or absence of these unique sialic acid glycan caps are irrelevant to the human responder. Moreover, this

implies that there is likely no cross reactivity of GGTA1 or CMAH gene products to other receptors within the human siglec profile.

In vivo, pig-to primate xenotransplantation has been studied using a variety of immunosuppressive regimens. Unfortunately, clinical inferences from pig-to primate models are challenged by an inherent difference in proliferative potential between humans and non-human primate and the fact that many of these studies have utilized immunosuppression not suitable for human use. [164] As such, it is important to study the relevant genetic models of xenotransplantation –and their reaction to clinically available immunosuppression- within an in vitro pig-to-human model whenever possible. Given that human cellular responses to the porcine knockout models were not significantly different from the allogeneic response, it seems likely that standard pharmacologic regimens should provide effective immunomodulation.

At the most elemental level, this data further supports the clinical application of carbohydrate knockout models of pig-to-human xenotransplantation. We have previously published a significant reduction in human IgG and IgM binding directed towards GGTA1^{-/-} CMAH^{-/-} porcine cells. [27] As antibody-mediated immune injury is the principle driver of early graft injury and AHXR, these modifications overcome a pivotal barrier to pig-to-human xenotransplantation. In the present study, we show that silencing the GGTA1 and CMAH genes have no deleterious effect on the cell-mediated pathway of rejection. Furthermore, we show that the human T cell response to these knockout pigs is capable of being mediated by conventional immunosuppression. Although more work must be done to solidify an appropriate combination of immunomodifiers, this

information represents a promising start for the study of human cellular immunity to genetically modified pigs.

**CHAPTER SIX: The fate of human platelets exposed to porcine renal endothelium:
a single-pass model of platelet uptake in domestic and genetically modified porcine
organs.**

INTRODUCTION

The genetic modification strategies described in chapters 2-5 offer great promise to the clinical application of pig-to-human xenotransplantation; with new strategies to overcome both humoral and cellular xenograft rejection, it has now become relevant to consider potential *physiologic* organ-specific barriers to clinical application.

Thrombocytopenia may represent a significant challenge to the clinical application of solid-organ xenotransplantation. When studied in a pig-to-primate model, consumptive coagulopathy has challenged renal xenografts. Described in chapters 3-5, new strategies of genetic manipulation have altered porcine carbohydrate profiles to significantly reduce human antibody binding to pig cells. As this process continues to eliminate immunologic barriers to clinical xenotransplantation, the relationship between human platelets and pig organs must be considered.

If xenotransplantation using genetically modified porcine organs is to eliminate the shortage of donor organs for transplantation, both immunologic *and* physiologic barriers to clinical application must be understood. As previously discussed, antibody mediated rejection (AMR) has made it impossible to move to the clinic with xenotransplantation. Chapters 3-4 examine the importance of two important xenoantigens to which humans have xenoreactive antibodies, gal- α -(1,3)-gal, and N-

glycolylneuraminic acid (Neu5Gc). These xenoantigens are produced by enzymes that are present in humans and pigs, but in humans, gene activity has been silenced during the course of evolution. α -1,3-galactosyltransferase (GGTA1) produces the Gal α (1,3) Gal epitope, and the development of GGTA1^{-/-} pigs eliminated 70-85% of the xenoreactive antibodies that humans have as a barrier to xenotransplantation. The cytidine monophosphate-N-acetylneuraminic acid hydroxylase (CMAH) gene produces Neu5Gc. The creation of GGTA1^{-/-} CMAH^{-/-} pigs has reduced human antibody binding to the point where the crossmatch of pigs with humans is more favorable than a primate-to-human crossmatch. [29] More recently, as described in chapter four, the creation of GGTA1^{-/-} CMAH^{-/-} B4GalT2^{-/-} pigs have reduced levels of antibody binding to the point that 80% of patients on transplant lists would not be expected to have early AMR. As current models of pig-to-human xenotransplantation have reached immunologic equivalence to allografts, it is now important to carefully consider potential organ-specific barriers to xenotransplantation.

The most well characterized organ-specific challenge to xenotransplantation is thrombotic microangiopathy (TMA). This phenomenon is organ-dependent as it ranges from graft-limiting thrombotic microangiopathy in kidney models to consumptive coagulopathy in a liver model of pig-to-primate xenotransplantation. Porcine GGTA1^{-/-} kidneys transplanted into non-human primates (NHP) are not hyperacutely rejected, but they do still fail because of AMR. The AMR seen in GGTA1^{-/-} -to-primate transplantation is most notably characterized by thrombotic microangiopathy. [165] However, it remains unclear whether the TMA seen in GGTA1^{-/-} -to-primate xenotransplantation occurs because of AMR, or is due to coagulation dysregulation based

on species incompatibilities in thromboregulatory pathways. As previously described by Burlak et al., an unmodified porcine liver retains the capacity to consume human platelets in the absence of immunologic injury; this raises the possibility of an aberrant relationship between the human platelet and porcine endothelial surface. Although the mechanism of this interaction remains unclear, there is significant data that suggests pig VonWillebrand factor (vWf) may aggregate human platelets in the absence of immune mediated injury or shear force. [166] As shown in figure 6.1, differing glycosylation patterns between pig and human vWF A1 domain may affect the affinity of human platelet GpIba receptor.

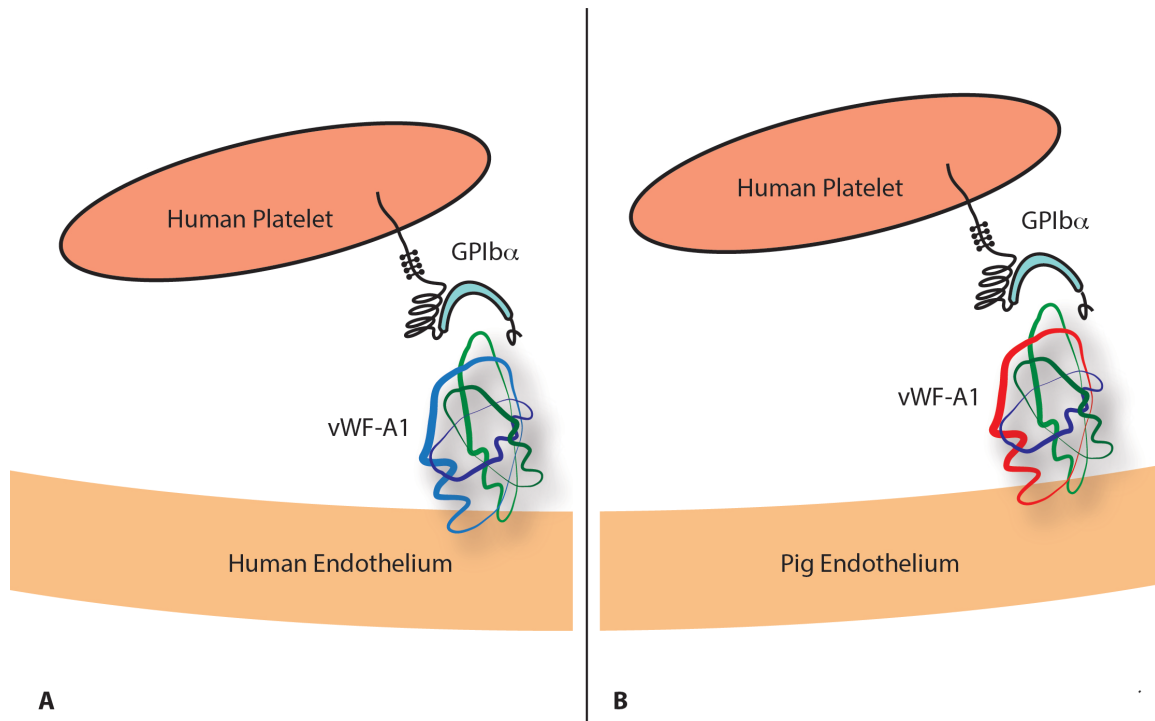


Figure 6.1: Porcine Von Willebrands Factor A1 Domain.

The porcine Von Willebrands factor (vWF) differs from the human protein in the glycosylation patterns of the A1-domain. **A)** Human vWf incorporates a N-linked pattern [75] **B)** Porcine vWF incorporates an O-linked glycosylation pattern [101]. As this region is responsible for interaction with the GpIb receptor on human platelets, it has been suggested that this difference may lead to aberrant interactions.

Although it is clear that graft modifications will be necessary to circumvent the hypercoagulable interaction between porcine *liver* endothelium and human platelets, no information has existed regarding the porcine *renal* endothelium and human platelets. The recent success of pig-to-primate renal transplants for several months without coagulopathy has suggested that unlike the porcine liver, the porcine renal endothelium is relatively inert in the absence of immune injury. [71, 167] As xenotransplantation continues to move towards clinical application, it is important move beyond primate models whenever possible, and to specifically consider pig-to-human interaction; this represents the first study to characterize the interaction between human platelets and the porcine kidney. The experiments in this report evaluated whether human platelets perfused through pig kidneys are retained in the absence of an immunologic injury. The results have important implications for the direction of further genetic modification of donor pigs.

MATERIALS AND METHODS

Creation of genetically modified pigs

Cas9 nuclease mediated gene editing with multiple guide RNAs was employed for the efficient production of genetically modified pigs. As previously described, CRISPR Guide RNAs were designed to target the CMAH and GGTA1 genes, responsible for the production of known xenoantigens, Neu5Gc and α Gal. [78] Porcine liver-derived cells were co-transfected with these CRISPR/Cas9 constructs using the Neon transfection system (Life Technologies, Grand Island NY). After the IB4 counter selection, cells bearing CMAH and GGTA1 mutations were enriched and further confirmed by DNA sequencing analysis. These cells were used as nuclear donors for somatic cell nuclear transfer (SCNT) to achieve pregnancy in a surrogate mother. [38] All the animals used in this study were approved by the Institutional Biosafety and Institutional Animal Care and Use Committee of IUPUI.

Isolation and staining of autologous (donor animal) platelets for perfusion

500ml of porcine blood was collected into tubes containing acid-citrate-dextrose at the time of surgery. After centrifugation (5 minutes at 2,000g) the top two thirds of platelet-rich plasma was removed and centrifuged (5 minutes at 5,000g). The pellet was resuspended in PBS/ACD 50:1 and washed twice. 10^{10} platelets were obtained by count on hemocytometer, of which 2.5^{10} were labeled with carboxyfluorescein succinimidyl

ester (CFSE) (Invitrogen, Grand Island, NY). All platelets were brought up to a final concentration of $10^{10}/L$ in Krebs solution.

Isolation and staining of human platelets

One unit of human platelets was purchased from a local blood bank. Platelet isolation was performed to remove human antibody. The platelets were transferred to 50ml conical tubes and centrifuged (5 minutes at 5,000g). The pellet was resuspended in PBS/ACD 50:1 and washed twice. 10^{10} platelets were obtained by count on hemocytometer, of which 2.5^{10} were CFSE-labeled (Invitrogen, Grand Island, NY) as described by Paris and Chihara. [168] All platelets were brought up to a final concentration of $10^{10}/L$ in Kreb's solution.

Procurement and preparation of porcine organs

Kidneys were obtained from healthy domestic, GGTA1^{-/-}, and GGTA1^{-/-} CMAH^{-/-} pigs. Livers were obtained from healthy domestic animals as a positive control. After euthanization, the abdomen was entered; the abdominal aorta was identified and cannulated below the renal arteries. The aorta was clamped above the renal arteries and an intracorporeal flush was performed with HTK solution (Essential Pharmaceuticals, Ewing, NJ, USA). Both kidneys were removed enbloc and divided on the backbench to accommodate an additional flush of 500ml HTK into each renal artery. Each renal artery and vein was cannulated and ureters were fenestrated. Livers were procured in a similar

fashion, with 4L of intracorporeal flush and 1-2L of backbench HTK flush. Organs remained on ice after procurement. Cold ischemic time between procurement and platelet perfusion did not exceed 3 hours.

Perfusion of organs

Procured kidneys were cannulated to achieve definitive control of the ureter, renal artery and vein. Kidneys were weighed and warmed to a controlled temperature range of 35-37 °C by perfusion with warmed Kreb's solution with 1ml/L heparin. This step also removed any remaining autologous platelets. Directly after warm flush, temperature was verified by IR thermometer (Fluke Corp, Everett WA). 1L of CFSE-labeled platelets was perfused through the renal artery. The right and left kidney was randomly assigned to receive either human or autologous platelets. A pre-perfusion sample was obtained proximal to the renal artery at time zero. Thereafter samples were collected into a polypropylene flow tube from renal vein outflow every 50 mL. Urine output was measured by direct cannulation of the ureter. All renal perfusions were repeated in biological triplicate for each data point collected. A single pass model of liver perfusion was performed on WT porcine livers as previously described by Paris et al. [67] to confirm the ability of fluorescence sampling to appropriately measure platelet disappearance in a model known to consume platelets. Owing to the higher flow rates achieved through liver, hepatic perfusion was time-limited rather than volume limited, and served to demonstrate the capacity of CFSE-labeling and fluorescence monitoring to detect human platelet uptake within a single-pass model. Hepatic perfusions were

repeated in biological triplicate for each data point collected. Tissue biopsy was obtained directly after platelet perfusion of livers and kidneys for confocal microscopic analysis.

Measuring of Fluorescence

Samples obtained from venous outflow were read on a Spetramax M2 fluoresce plate reader (Molecular Devices Corp., Sunnyvale, CA, USA). A control lane for each perfusion was established by creating a serial dilution by halves from each organ's pre-perfusion sample. 100ul from each venous sample obtained was sequentially plated to create experimental lanes. Nine consecutive readings were obtained from each sample collected and relative fluorescence values [121] were recorded as median 488 emission. Data output was analyzed on Prism software (Graphpad Software Inc., La Jolla, CA). Output was reported as % maximal fluorescence using the equation: $y = (\text{venous output fluorescence} / \text{arterial input fluorescence}) * 100$. Differences between human and autologous cohorts were analyzed across cohorts for statistical significance using a two-way ANOVA. Urine output from renal perfusions was recorded and calculated as a percentage of flow for each sample point using the equation: $[(\text{total urine output (L)} / 1) / \text{number of volume measurements obtained}] * 100$.

Confocal for Biopsy

Mounted tissues from post-perfusion biopsies were blocked in Odyssey blocking buffer (LI-Cor Biosciences, Lincoln, NE, USA) in HBSS for 1 h. The slides were then fixed in 4% paraformaldehyde for 10 min. Tissues were stained with CD31 (Invitrogen, Grand

Island, NY) to visualize the endothelial surface, followed by three HBSS washes and Donkey anti-Chicken DyLight 649 (Jackson Immuno Research Laboratories Inc., West Grove, PA). Tissues were incubated with secondary antibody for approximately 1 hour and then washed three times with 0.1% HBSS Tween. DAPI (Invitrogen, Grand Island, NY) was added to all slides for 1 min. as a nuclear stain followed by two 0.1% HBSS Tween washes. Tissues were mounted in ProLong Gold (Invitrogen, Grand Island, NY). Confocal microscopy was performed using an Olympus FV1000 (Olympus America Inc., Center Valley, PA, USA). All obtained samples were viewed (n=3 for each experimental group), captured images were representative of all samples viewed.

In Vitro Platelet Up-Take

Primary LSEC and REC isolation

A porcine liver and kidney were procured from a single domestic animal as previously described.[168] Briefly, each organ was placed in a chilled dish (4 °C) and then flushed with 0.025% of collagenase type IV from *Clostridium histolyticum* (Sigma, St. Louis, MO) at 37 °C followed by continued perfusion with collagenase at 37 °C for 20 min. Perfusion was paused for 30 min and collagenase was carefully removed from around organ and vessel sites. Perfusion was resumed at 10 ml/min for 45 min with gentle manipulation of the organ to assure even digestion. Enzyme activity in the perfusate was immediately quenched by the addition of 1/10 volume new born calf serum. The perfusate was centrifuged at 400 *g* for 10 min at room temperature. The cell pellet containing the LSEC or REC was saved and resuspended in RPMI medium supplemented

with 0.02% (w/v) EDTA. The cell suspension was centrifuged again at 400 *g* for 10 min at 4 °C. The pellet was resuspended in EC culture medium (RPMI medium supplemented with 10% fetal bovine serum (v/v), 100 µg/ml endothelial cell-specific growth factor, penicillin, streptomycin, and amphotericin B) and plated onto clear-bottomed cell culture-treated microscopy slide wells (100, 000 cells/well initial concentration). Medium was changed each day for 2 days, and all cells were utilized on day 4 after isolation.

Confocal analysis of endothelial lines

Primary LSEC and REC lines from a healthy domestic animal were cultured for 4 days at 37 °C and 5% CO₂ in clear-bottomed cell culture-treated microscopy slide wells (100, 000 cells/well initial concentration). Fresh human platelets were isolated from a healthy donor and labeled (CFSE) as described above. Four million CFSE-labeled platelets were added to experimental wells containing primary endothelial cells and media. Slides were incubated with platelets for 15, 30, 60 minutes. Duplicate wells for each time point were washed with 150 µl of PBS three times then fixed with 50 µl of 4% paraformaldehyde–PBS solution for 20 min. Cells were stained with Chicken anti-Pig CD31 (Invitrogen, Grand Island, NY) to visualize the endothelial surface, followed by three HBSS washes and Donkey anti-Chicken DyLight 649 (Jackson Immuno Research Laboratories Inc.). Tissues were incubated with secondary antibody for approximately 1 h and then washed three times with 0.1% HBSS Tween. DAPI (Invitrogen, Grand Island, NY) was added to all slides for 1 min as a nuclear stain followed by two 0.1% HBSS washes. Tissues were mounted in ProLong Gold (Invitrogen, Grand Island, NY).

Confocal microscopy was performed using an Olympus FV1000 (Olympus America Inc., Center Valley, PA, USA). Experiments were performed in triplicate for each cohort and images reported were representative of all images viewed (n= 16 for each cohort).

RESULTS

DNA sequencing analysis of the cloned pigs

Pig liver-derived cells transfected with nuclease-targeting knockout vectors for GGTA1 and CMAH genes exhibited gene-silencing mutational events; IB4 lectin-conjugated beads and sequence analysis facilitated the isolation of successfully mutated cells. These cells were used to create healthy clonal animals by SCNT. As shown in figure 6.2, the animals used in this analysis exhibited a GGTA1^{-/-} or GGTA1^{-/-} CMAH^{-/-} genotype. The phenotypes of these animals have been previously published by Li et al. [78]

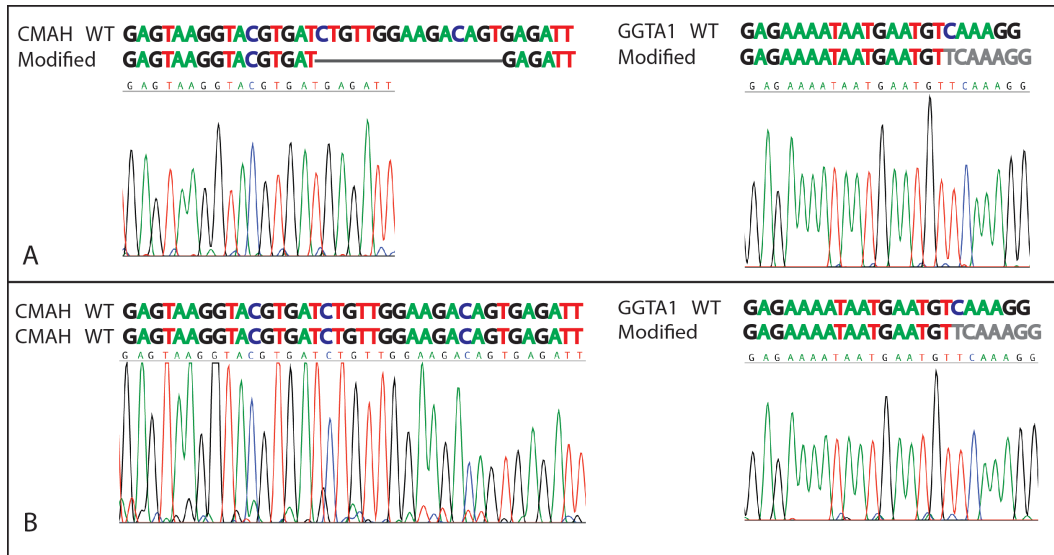


Figure 6.2: Genotype of Genetically Modified Pigs.

A) depicts an animal carrying a 15bp deletion interrupting the CMAH gene and a single bp insertion disrupting the GGTA1 gene. **B)** depicts an animal carrying an unmodified CMAH gene and a single base insertion in the GGTA1 gene. All depicted mutations created a frame shift mutation and a null phenotype with respect to the locus of interest.

Analysis of human platelet uptake

Human platelets were not removed by the porcine kidney in a single-pass model of perfusion under normothermic conditions. As displayed in figure 6.3, the % maximal fluorescence of human platelet samples measured from renal venous sampling did not significantly deviate from the platelet control values (autologous cohort n=3, human platelet cohort n=3 for each genetic background). Differences between human and porcine platelet loss through the system failed to reach statistical significance in each

cohort (WT $p=0.15$, GGTA1^{-/-} $p=0.12$, GGTA1^{-/-} CMAH^{-/-} $p=0.25$). Median renal perfusion time was 28 minutes (range 26-34) and was not statistically different between cohorts. Similarly, median urine output per sample point did not vary significantly between cohorts and accounted for 0.4% of filtered volume (range 0.31- 0.52%). When compared to a single-pass model of hepatic platelet uptake as shown in figure 6.3D, the absence of renal platelet consumption is underscored. Within this study, the unmodified porcine liver consumed human platelets in a single-pass model of platelet perfusion in fewer than 10 minutes. WT suprahepatic inferior vena cava fluoresce reached a maximum of just 76% of input fluoresce within the human platelet cohort and was significantly lower than the autologous platelet control cohort ($p=0.001$). Autologous platelet control groups failed to significantly differ between renal and liver perfusions ($p=0.92$), suggesting appropriate continuity between systems.

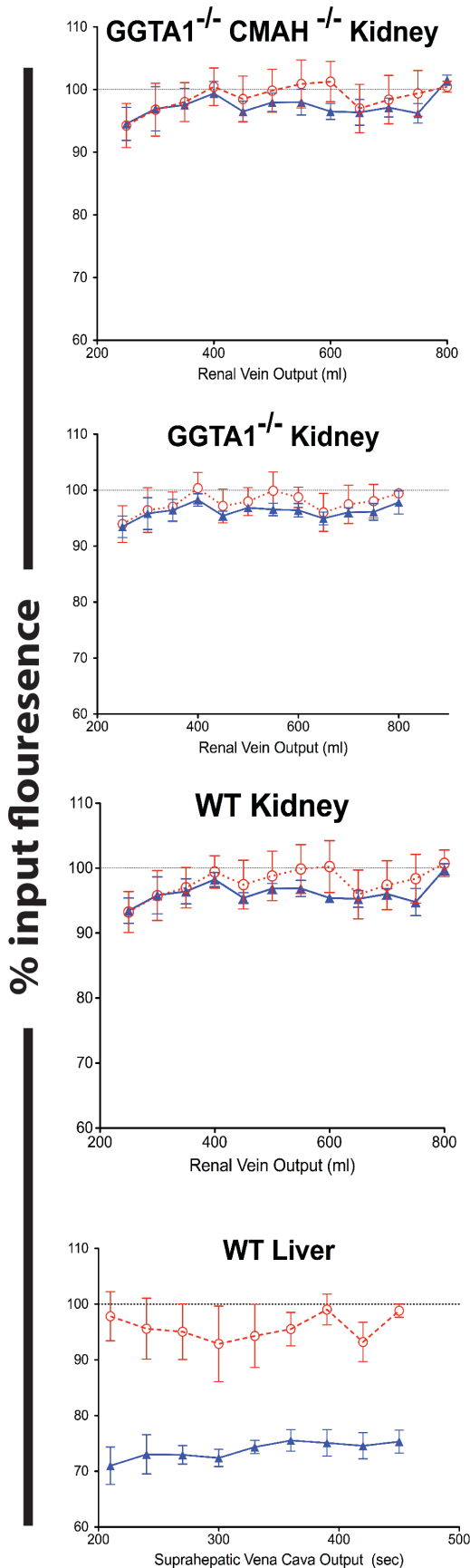


Figure 6.3: A single pass model of platelet uptake.

Depicts % input fluorescence (y axis) of samples drawn from venous output obtained at regular intervals (x axis).

All values depicted are normalized to the experiment's pre-infusion sample and were obtained using the equation $y = \frac{\text{input fluorescence}}{\text{output fluorescence}} * 100$. All experiments

were repeated in biological triplicate, mean data points and standard error are displayed. **A)** Human and autologous platelets passed through domestic porcine kidneys. **B)** Human and autologous platelets passed through GGTA1^{-/-} porcine kidneys. **C)** Human and autologous platelets passed through GGTA1^{-/-} CMAH^{-/-} porcine kidneys. **D)** Human and autologous platelets passed through domestic porcine livers.

Autologous Platelets
Human Platelets

Confocal analysis of tissue biopsies obtained after single-pass perfusions with CFSE-labeled plates confirm the relationships presented by the single-pass results (Figure 6.4). These images depict an absence of human platelets associating with porcine *renal* endothelium, compared to a strong association noted between human platelets and porcine *liver* endothelium.

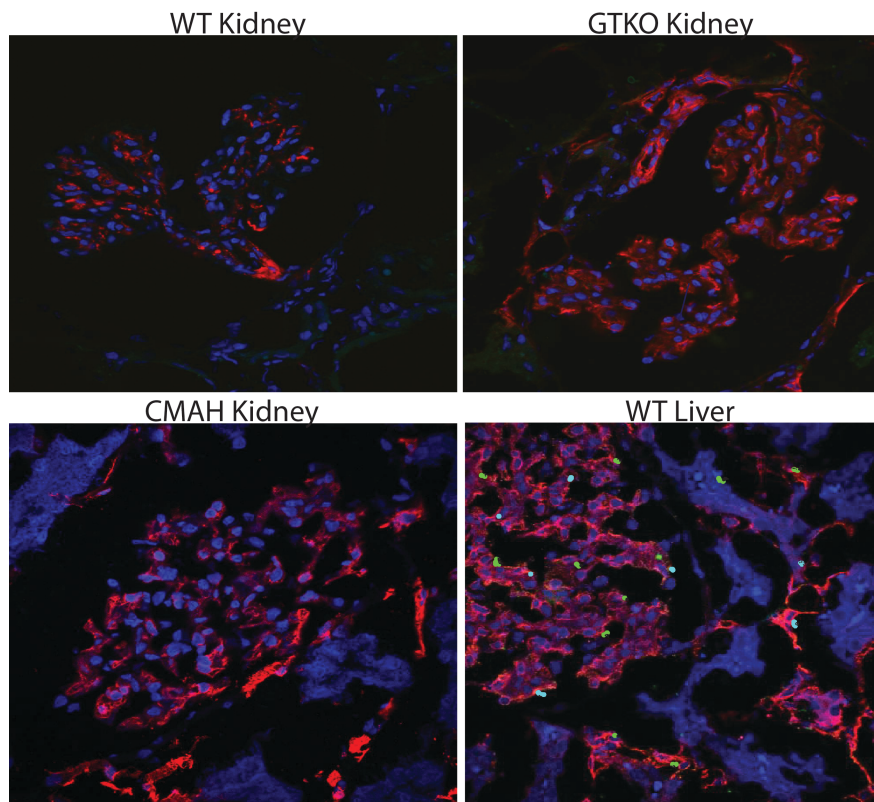


Figure 6.4: Biopsy Samples from human platelet perfusion.

Biopsy samples were obtained from kidneys post-perfusion with CFSE-labeled human platelets. In all three types of kidneys perfused (wild type, $GGTA1^{-/-}$ and $GGTA1^{-/-}$ $CMAH^{-/-}$), human platelets were not visible after post-perfusion flush. A wild-type liver was used as a positive control; here platelets are visible after post-perfusion flush. Images are representative of all samples viewed (n=3 for each perfusion).

The results of the in vitro platelet uptake assay performed also confirm the relationships presented by single-pass results. When studied in vitro, CFSE-labeled human platelets failed to associate with porcine renal endothelial cells. As displayed in figure 6.5, the presence of labeled platelets within renal cell populations is confined to the CD31-negative cells, suggesting that human platelets do not bind renal endothelial cells but do retain the capacity to recognize exposed sub endothelial surface. In contrast, the liver endothelial cells (CD31 –positive) demonstrate a strong association with human platelets.

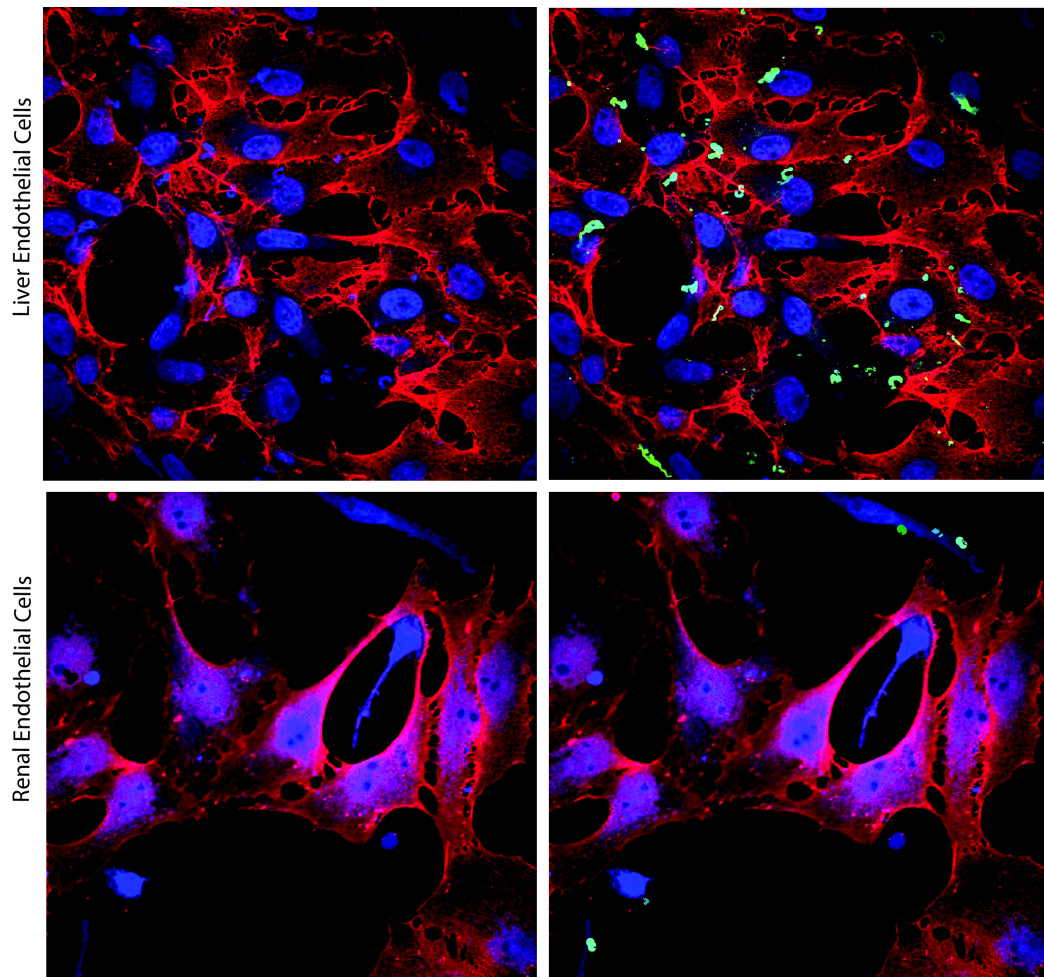


Figure 6.5: Confocal Imaging of In vitro Uptake.

A WT Liver Endothelial cell line (top) is compared to a WT renal endothelial cell line (bottom) procured from the same animal. Right panels include the 488 channel to expose human platelet binding. Both primary cell lines were isolated from the same animal and subjected to CFSE-labeled human platelets on day 4. Cells were labeled with CD31 [101] as to indicate endothelial origin. The results indicate that human platelets associate LSECs but not RECs. Platelet binding in the renal cell fields appears to be contained to CD31- sub-endothelial cells. Images are representative of all samples viewed (n= 16 per cohort).

DISCUSSION

Previous chapters describe new xenoantigen knockout pigs that have reduced the antibody barrier for xenotransplantation to the point where the pig-to-human species combination has a better crossmatch than the primate-to-human combination. Data from GGTA1^{-/-}-to-primate kidney xenotransplants show that renal xenografts are rejected by a mechanism that is characterized by both glomerular IgM and IgG and thrombotic microangiopathy (TMA). [165, 166, 169-171] As such, the essential question is whether this process of rejection is driven primarily by immune-mediated injury -with exposure of pro-coagulant subendothelial surfaces- or is the result of species incompatibility of coagulation regulation pathways. [172]

Incompatibilities of species-specific coagulation regulatory mechanisms have frequently been credited with the intravascular thrombosis that produces graft-limiting TMA. As previously described by Burlak et al., unmodified porcine livers retain the capacity to phagocytose human platelets. [173] The results of the present study confirm that this process is measurable within a single-pass model of isolated human platelet perfusion. Although the mechanism of this interaction is not yet fully characterized, recent work by Paris et al. has implicated the importance of the asialoglycoprotein receptor, produced by the porcine ASGR1 gene. [67, 168] When the ASGR1 gene was silenced, porcine livers consumed significantly less human platelets than the WT controls. That kidneys do not express the asialoglycoprotein receptor may contribute to the differences noted within the present study.

Porcine VonWillebrands factor (vWF) has also been implicated as a possible contributor to species-specific coagulation dysfunction as it is able to aggregate human platelets in the absence of shear stress. [174] As displayed in figure 6.1, Robson has shown that the porcine O-linked pattern glycosylation differs from human N-linking within the vWF-A1 domain, and may affect the interaction of pig vWF with human platelet receptor GPIIb/IIIa. [166, 175] Unlike the asialoglycoprotein receptor, vWF is expressed in the kidney, albeit at lower levels compared to other porcine tissue such as lung. [176] Our experiments were performed to specifically address the issue of whether in the absence of an immunologic injury, human platelets would be aggregated by species-incompatibility of coagulation regulatory mechanisms, such as vWF.

Our results suggest that human platelets respond in a variable fashion to organ-specific porcine endothelial surfaces. Although the present results display a consistent trend towards lower platelet uptake in autologous controls, these differences failed to reach statistical significance within renal cohorts. Moreover, it is unlikely that this trend represents any *biologic* relevance given the success of pig-to-primate renal transplantation; recently, two pig-to-primate renal transplants have achieved graft survival greater than four months without thrombocytopenia. [71, 167]. Unlike the kidney, the unmodified porcine liver exhibited a significant ability to consume human platelets within this study. Likely owed to its inherently phagocytic nature, the porcine liver will require further modification to avoid thrombocytopenia and facilitate successful hepatic xenotransplantation. A number of genetic engineering strategies have been employed to limit incompatibilities of species-specific coagulation regulatory mechanisms. The insertion of human transgenes for ecto-ADPase CD39,

thrombomodulin, tissue factor pathway inhibitor, and endothelial protein C receptor, have all been shown to reduce coagulation of pig organs in primates. [65, 177]

In light of our data, it seems likely that the graft-limiting intravascular thrombosis witnessed in pig-to-primate *renal* xenotransplantation is more closely the result of immunologic injury and not a primary platelet dysregulation. These findings are not unexpected. Foremost, TMA witnessed in renal allograft rejection has long been understood as a product of antibody-mediated rejection. [178] TMA is also present in other human diseases, such as paroxysmal nocturnal hemoglobinuria, where complement activation –the effector of immune-injury- is prevalent. [125] Within the field of xenotransplantation, Cooper et al. have recently shown a link between xenograft inflammation and coagulation. [179] In his new paradigm, inflammation precedes coagulation, implying that inflammation down-regulation may be independently beneficial for xenograft survival. Similarly, Byrne et al. showed in cardiac xenografts that increased immunosuppression, and not increased anticoagulation, was associated with improved graft survival. [180]

The number of circulating xenoreactive antibodies in human serum has been greatly reduced with the GGTA1^{-/-} CMAH^{-/-} pig, but there is still room for improvement with regards to eliminating xenoantigens. Byrne et al. recently described porcine B4GalNT2 as a gene producing an important xenoantigen in pig-to-primate cardiac xenografts. [181] Estrada et al. then demonstrated the benefit of silencing the B4GalNT2 gene in both a pig-to-human and pig-to-primate model. [47] The present data supports the notion that these xenoantigen reductions alone may be sufficient to avoid graft-limiting TMA in a renal xenograft. While the addition of human coagulation regulatory

transgenes to donor pigs improves xenograft survival in pig-to-primate model, if the xenoreactive titer is low enough these transgenes may be unnecessary for prolongation of renal xenograft survival.

In conclusion, the present study suggests that human platelets respond in a variable fashion to organ-specific porcine endothelial surfaces. Under normothermic conditions, human platelets alone are not removed from circulation by exposure to porcine *renal* endothelium, while they are removed by the *hepatic* endothelium. Kidneys possessing genetic modifications currently-relevant to clinical xenotransplantation failed to consume human platelets in an isolated single-pass model. In the absence of immune-mediated endothelial injury, the interaction between human platelets and porcine renal endothelium should not represent a barrier to clinical xenotransplantation.

CHAPTER SEVEN: Silencing porcine CMAH and GGTA1 genes significantly reduces xenogeneic consumption of human platelets by porcine livers.

INTRODUCTION

A profound thrombocytopenia limits hepatic xenotransplantation in the pig-to-primate model. As exposed by the hepatic control utilized in chapter six, porcine livers also have shown the ability to phagocytose human platelets in the absence of immune-mediated injury. Recently, inactivation of the porcine ASGR1 gene has been shown to decrease this phenomenon. Chapter four and five indicate that inactivating GGTA1 and CMAH genes has reduced the antibody-mediated barrier to xenotransplantation; herein I describe the effect that these modifications have on xenogeneic consumption of human platelets in the absence of immune-mediated graft injury.

As discussed in the first chapter, the most pressing issue affecting patients awaiting transplant is a growing dearth of available allografts. While peak transplanted volumes for all solid organs has plateaued, each year the number of patients added to solid-organ wait lists increases.[148] As recently stated by Salomon et al., from the AST/ASTS workshop on increasing liver donation: “our current system of organ donation is not meeting the growing demand”. [182] Xenotransplantation of genetically modified porcine organs is now positioned to be a clinically-viable answer to this growing problem. The advances in genetic engineering presented in chapter two have rapidly increased the pace at which model organs may be created and tested. [115] Recently, as described in chapter four, a triple knockout model has reduced human

antibody-dependent cytotoxicity below the threshold at which acute antibody-mediated rejection (AMR) would not be expected. [27] It is from this position of immunologic equivalence, that it is now important to examine organ-specific barriers to clinical xenotransplantation. While the previous chapter suggests that porcine *renal* endothelium will be inert to human platelets in the absence of concurrent immunologic insult, the consumption of human platelets by the wild-type livers included within that analysis suggests that human platelets respond in a variable fashion to organ-specific porcine endothelial surfaces.

The xenogenic consumption of platelets by porcine livers is well-precedented phenomenon; the use of porcine livers for xenotransplantation is limited by a dramatic thrombocytopenia when studied in a pig-to-primate model. [183] As described by Burlak et al., [173] porcine sinusoidal endothelial cells (LSEC) and Kupffer cells (KC) also remove *human* platelets from circulation in the absence of immunologic injury or shear-stress activation. Recently, gene silencing has been used to limit this thrombocytopenia. As described by Paris et al., [67] removing the asialoglycoprotein receptor 1 protein from the porcine livers significantly reduces the amount of human platelet uptake. Although carbohydrate reductions have proved essential to limiting AMR in a pig-to-human model, little attention has been afforded to the effect that these modifications may have on hepatic platelet consumption. Silencing of the GGTA1 gene, which facilitates cell surface expression of the Gal α (1,3)Gal (α Gal) xenoantigen, and the CMAH gene which allows expression of the N-Glycolylneuraminic acid (Neu5Gc) xenoantigen may help avoid early xenogeneic AMR; [38] it is therefore important to understand the effect that these modifications have on the human thromboregulatory system. Herein we describe the

effect that silencing the porcine GGTA1 and CMAH genes has on the consumption of human platelets by a porcine liver.

MATERIALS AND METHODS

Genetically modified pigs

The GGTA1^{-/-}, GGTA1^{-/-}CMAH^{-/-} and ASGR1^{-/-} pigs used in this study have been described previously.[24, 67] Briefly, the same parental background was used across all animals to limit variability from external loci. GGTA1 and CMAH gene silencing was accomplished by CRISPR/Cas9-directed mutagenesis as described by Li et al. [24] ASGR1 silencing was effected by TALEN- directed mutagenesis as described by Paris et al. [67] [100] The Institutional Biosafety and Institutional Animal Care and Use Committee at Indiana University School of Medicine approved the use of animals in this research.

Platelet Isolation and Staining

One unit of expired human platelets was purchased from a local blood bank. The platelets were centrifuged (5 minutes at 5,000xg). The pellet was resuspended in PBS/ACD 50:1 and washed twice. 2×10^{11} platelets were obtained by count on hemocytometer, of which 25 percent were labeled with carboxyfluorescein succinimidyl ester (CFSE) (Invitrogen, Grand Island, NY) as described. [173] Both labeled and unlabeled platelets were added to a total of 1L modified Krebs solution 2.0g/L D-glucose, 0.141 g/L MgSO₄, 0.16 g/L KH₂PO₄, 0.35 g/L KCl, 6.9 g/L NaCl, 2.10 g/L NaHCO₃, 0.37g/L CaCl₂, 2.38 g/L HEPES, 1U/mL Heparin (Sagent Pharmaceuticals, Schaumburg, IL) pH 7.2-7.4 and then

perfused through a Capiiox BT05 bubble trap (Terumo Medical, Tokyo, Japan) to remove aggregated platelets prior to perfusion. Platelets were again counted to account for platelet loss and resuspended at a concentration of $1 \times 10^{10}/L$ in modified Krebs solution. A total of 10L of platelet suspension was prepared and was warmed to 37 °C until perfusion.

Perfusion of Livers

Livers were procured from genetically modified animals and flushed at time of procurement with HTK solution (Essential Pharmaceuticals, Ewing, NJ, USA). Organs were removed from cold preservation within 2 hours and cannulated to achieve definitive control of the portal vein, hepatic artery and suprahepatic inferior vena cava and were warmed to a controlled temperature range of 35-37 °C by perfusion with warmed Krebs solution. Livers were perfused in an oxygenated and pulsatile circuit as previously described. [67] For the single-pass model, sampling occurred simultaneously from the hepatic artery, portal vein and suprahepatic inferior vena cava; samples were collected every 30 seconds for 10 minutes. A sample from the vena cava port was collected at time 0 to calculate a background fluorescence which was subtracted from all samples. For the continuous-pass model, a time zero sample of platelets was obtained prior to the introduction of platelets, and samples were taken from a central reservoir at reported time points and immediately fixed 1:1 in 10 percent formalin solution prior to counting.

Measuring Xenogeneic Human Platelet Consumption

For the continuous-pass model, each of the time point samples were counted using a hemocytometer and total available platelets in the perfusion system were calculated. These values were compared to input platelet amounts and percent remaining available platelets were calculated. Results were subjected to analysis by ANOVA with repeated measures and Tukey's post test to determine significance. Samples obtained from single-pass hepatic perfusions were analyzed by measuring the fluorescence (Ex: 485, Em: 525) of 200uL perfusate loaded into 96 well micro clear plates (Greiner Bio One, Monroe, NC, USA) on a Spectramax M2 plate reader (Molecular Devices Corp., Sunnyvale, CA, USA). Percent maximum fluorescence was calculated by comparing individual time points to input fluorescence. Percent maximum values were analyzed on Prism software (Graphpad Software Inc., La Jolla, CA). Inclusion criteria for statistical analysis required that arterial and portal vein fluorescence reached at least 90% of input fluorescence to suggest adequate circulation of labeled platelets through the system. Comparison of platelet quantities in the perfusate were made once the platelet levels had plateaued indicating that the system had reached a steady state. Statistical significance was determined by unpaired t-test of percent fluorescence values obtained after inclusion criteria were met.

Staining and Confocal Microscopy

For histologic analysis by in vitro assay, primary WT, GGTA1^{-/-}, ASGR1^{-/-} and CMAH^{-/-} GGTA1^{-/-} LSEC lines were isolated as previously described. [173] Cells were cultured

for 4 days post isolation at 37 °C and 5% CO₂ in clear-bottomed cell culture-treated microscopy slide wells (100, 000 cells/well initial concentration). Fresh human platelets were isolated from a healthy donor and labeled with carboxyfluorescein succinimidyl ester (CFSE) as described above. Four million CFSE-labeled platelets were added to experimental wells containing primary endothelial cells and media. Slides were incubated with platelets for 60 minutes. Duplicate wells for each group were washed with 150 µL of PBS three times then fixed with 50 µL of 4% paraformaldehyde–PBS solution for 20 min. To facilitate immunohistochemical visualization, and confirmation of platelet deposition within ex vivo platelet-perfused livers, punch biopsies were obtained at the conclusion of perfusions, sectioned at 4µm and then fixed with 50 µL of 4% paraformaldehyde–PBS solution for 20 min. Cells and tissues were stained with goat anti-Pig CD31 1:100 (R and D systems, Minneapolis, MN) to visualize the endothelial surface, followed by three PBS washes and bovine anti-goat IgG DyLight 649 (Jackson Immuno Research Laboratories Inc., West Grove, PA). Slides were incubated with secondary antibody for approximately 1 h and then washed three times with PBS. DAPI (Invitrogen, Grand Island, NY) was added to all slides for 1 min as a nuclear stain followed by two PBS washes. Slides were mounted in ProLong Gold (Invitrogen, Grand Island, NY). Confocal microscopy was performed using an Olympus FV1000 (Olympus America Inc., Center Valley, PA, USA).

RESULTS

Analysis of in Vitro Human Platelet Uptake

CFSE-labeled human platelets associate less with isolated porcine liver endothelial cells from the GGTA1^{-/-}CMAH^{-/-} background compared to GGTA1^{-/-} and WT cells. The ratio of human platelets [19] bound by liver endothelial cells [101] was measured by colocalization of platelet per CD31+ cell for all 16 fields viewed per cohort. The median LSECs per field was 58 and was not significantly different across cohorts (p=0.32).

When subjected to statistical analysis by ANOVA with Tukey's multiple comparison test, GGTA1^{-/-}CMAH^{-/-} LSECs bound significantly fewer human platelets when compared to GGTA1^{-/-} (0.13 vs 0.34 platelets per LSEC p=0.002, n=16) and WT (0.13 vs 0.37 platelets per LSEC p=0.002 n=16) cells; ASGR1^{-/-} LSECs exhibited significantly less platelet binding than GGTA1^{-/-} (0.17 vs 0.34 platelets per LSEC p=0.013, n=16) and WT (0.17 vs 0.37 platelets per LSEC p=0.009, n=16) cells. Although GGTA1^{-/-}CMAH^{-/-} LSECs appeared to be associated with fewer human platelets than ASGR1^{-/-} LSECs, the difference failed to reach statistical significance (0.13 vs 0.17 platelets per LSEC p= 0.8, n=16). Cells from GGTA1^{-/-} and wild type livers exhibited similar levels of platelet retention (0.34 vs 0.37 platelets per LSEC p=0.99, n=16). The images in figure 7.1 are representative of all images captured (n= 16 for each cohort).

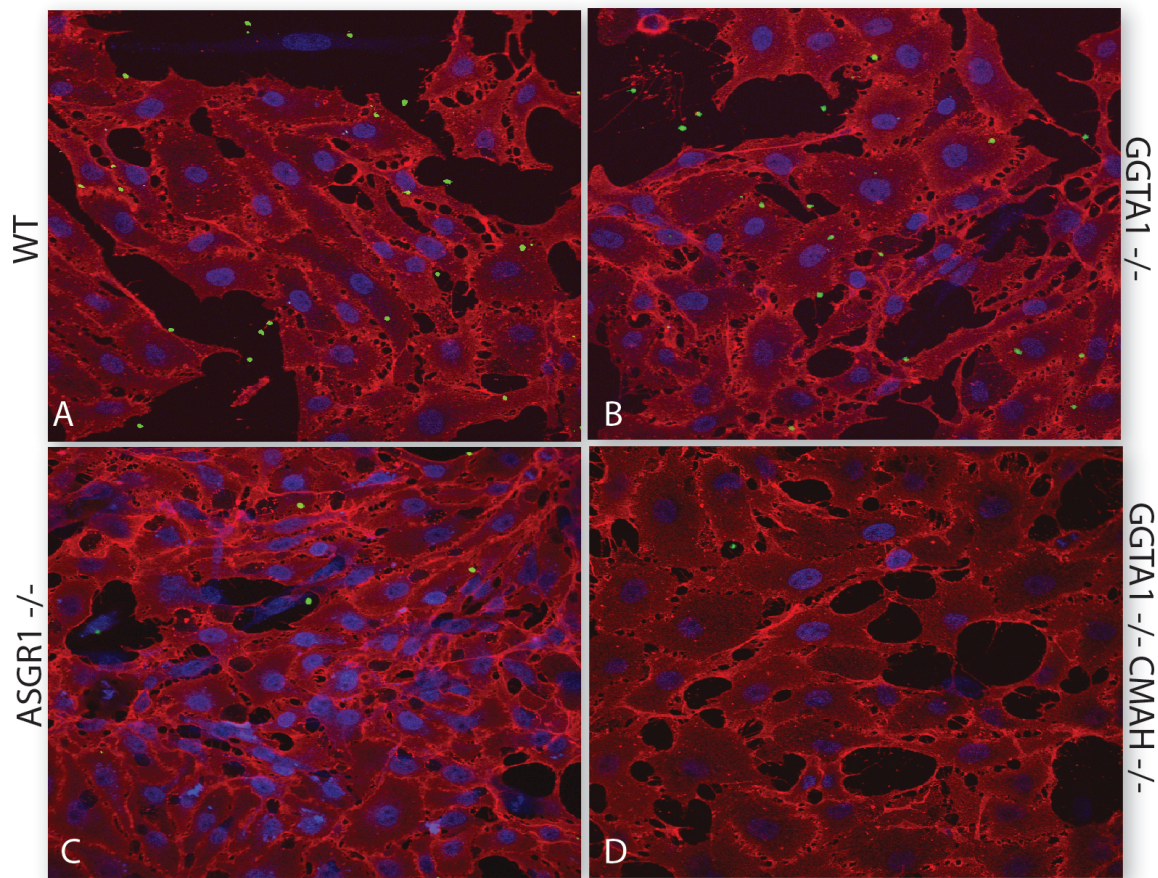


Figure 7.1: Human platelet accumulation by GGTA1^{-/-}CMAH^{-/-}, GGTA1^{-/-}, ASGR1^{-/-} and WT liver sinusoidal endothelial cells in vitro.

Primary WT, GGTA1^{-/-}, ASGR1^{-/-} and CMAH^{-/-}GGTA1^{-/-} LSEC lines were isolated and cultured for 4 days. Human platelets were isolated from a healthy donor and labeled with carboxyfluorescein succinimidyl ester (CFSE). Labeled Platelets [19] were added to experimental wells containing primary endothelial cells. Cells were stained with anti-Pig CD31 [101] to visualize the endothelial surface; and DAPI [75] was added to all slides as a nuclear stain. Confocal microscopy was performed using an Olympus FV1000. The relationships between human platelets and GGTA1^{-/-}CMAH^{-/-} or GGTA1^{-/-} livers seen in

the ex vivo perfusion model was upheld by in vitro analysis. Based on colocalization analysis, CFSE-labeled human platelets associated less with porcine liver endothelial cells from the GGTA1^{-/-}CMAH^{-/-} background compared to WT (p=0.002) and GGTA1^{-/-} (p=0.002) cells; ASGR1^{-/-} LSECs exhibited significantly less platelet binding than GGTA1^{-/-} (p=0.013) and WT (p=0.009) cells. Although GGTA1^{-/-}CMAH^{-/-} LSECs appeared to associate fewer human platelets than ASGR1^{-/-} LSECs, the difference failed to reach statistical significance (p= 0.8). Figure is representative of all images captured (n= 16 for each cohort).

Analysis of Ex Vivo Perfusion with Human Platelets

Because of the reduced interaction of human platelets with GGTA1^{-/-}CMAH^{-/-} porcine liver sinusoidal endothelial cells, perfusion studies were performed to determine if the removal of human platelets from a perfusion circuit was also minimized. In a continuous-pass model of platelet uptake, GGTA1^{-/-}CMAH^{-/-} livers consumed fewer platelets than GGTA1^{-/-} (p<0.0001) and WT (p<0.0001) livers at every time point (Figure 7.2). We have previously demonstrated that eliminating the asialoglycoprotein receptor from pig livers reduced human platelet consumption when compared to WT; [67] when compared within this analysis, these findings were confirmed (p<0.0001). Although a trend towards lower platelet uptake was noticed when comparing GGTA1^{-/-}CMAH^{-/-} to ASGR1^{-/-} livers, the difference failed to reach statistical significance at two of the time points within this model (p<0.161). Representative immunochemical histology obtained post continuous pass perfusion is shown in figure 7.2B and confirms that the loss of platelets through the system is a function of hepatic deposition.

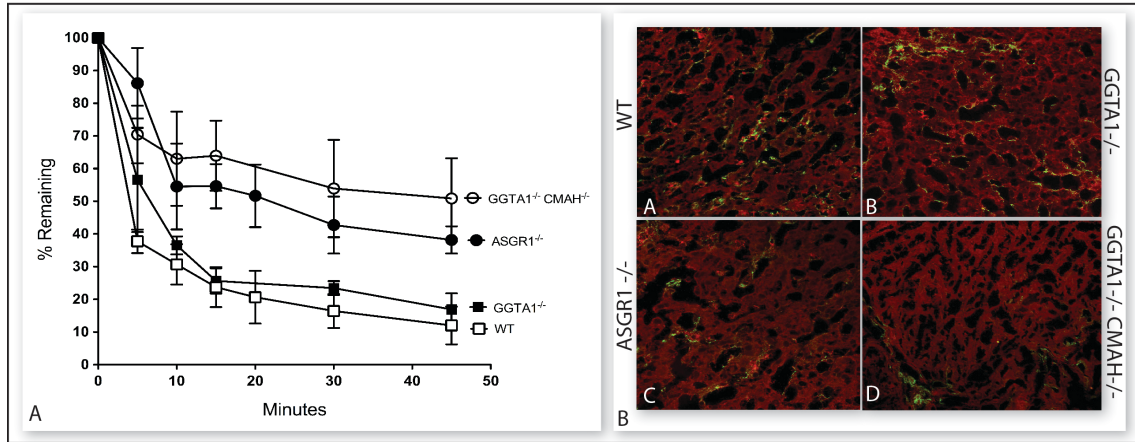


Figure 7.2: A Continuous-pass model for the xenogenic consumption of human platelets by modified porcine livers.

(A) In a continuous-pass model of platelet uptake, both GGTA1^{-/-} CMAH^{-/-} and ASGR1^{-/-} livers consumed fewer platelets than GGTA1^{-/-} or WT livers ($p < 0.0001$ for all comparisons). Platelet disappearance from the system was less at each measured time point after time zero. Although a trend towards lower platelet uptake was noticed when comparing GGTA1^{-/-} CMAH^{-/-} to ASGR1^{-/-} livers, the difference failed to reach statistical significance at two of the time points within this model ($p < 0.161$). (GGTA1^{-/-} $n=2$, GGTA1^{-/-} CMAH^{-/-} $n=3$, WT $n=3$ and ASGR1^{-/-} $n=3$). The ASGR1^{-/-} data was published previously and used here with permission. [67] (B) Representative immunochemical histology obtained from post continuous pass perfusion hepatic tissue sectioning is shown and confirms that the loss of platelets through the system is a function of hepatic deposition. Labeled Platelets [19] were added to experimental wells containing primary endothelial cells. Cells were stained with anti-Pig CD31 [101] to visualize the endothelial surface. Confocal microscopy was performed using an Olympus FV1000. Images are representative of all samples viewed ($n=6$ for each perfusion).

To better characterize the difference between GGTA1^{-/-}CMAH^{-/-} livers and ASGR1^{-/-} livers, we sought to increase the sensitivity of our perfusion model. Though continuous pass circuits are sufficient for demonstrating large differences in platelet uptake, it was insufficient to reliably measure more subtle differences. Consequently, we developed a “single pass” perfusion circuit to examine the loss of platelets following transit through the organ a single time. Serial samples were collected until the input (artery and portal vein,) and the output (vena cava) reached a plateau, indicating steady state had been reached (Figure 7.3). After plateau phase was achieved, data from time points 390, 420 and 450 seconds were averaged (Figure 7.3D); suprahepatic inferior vena cava fluorescence reached 95.4% (SEM=0.590) of initial sample fluorescence for GGTA1^{-/-} CMAH^{-/-} livers compared to 83.9% (SEM=0.513) in ASGR1^{-/-} livers during steady-state. (P= 0.001, GGTA1^{-/-} CMAH^{-/-} n=3, ASGR1^{-/-} n= 4)

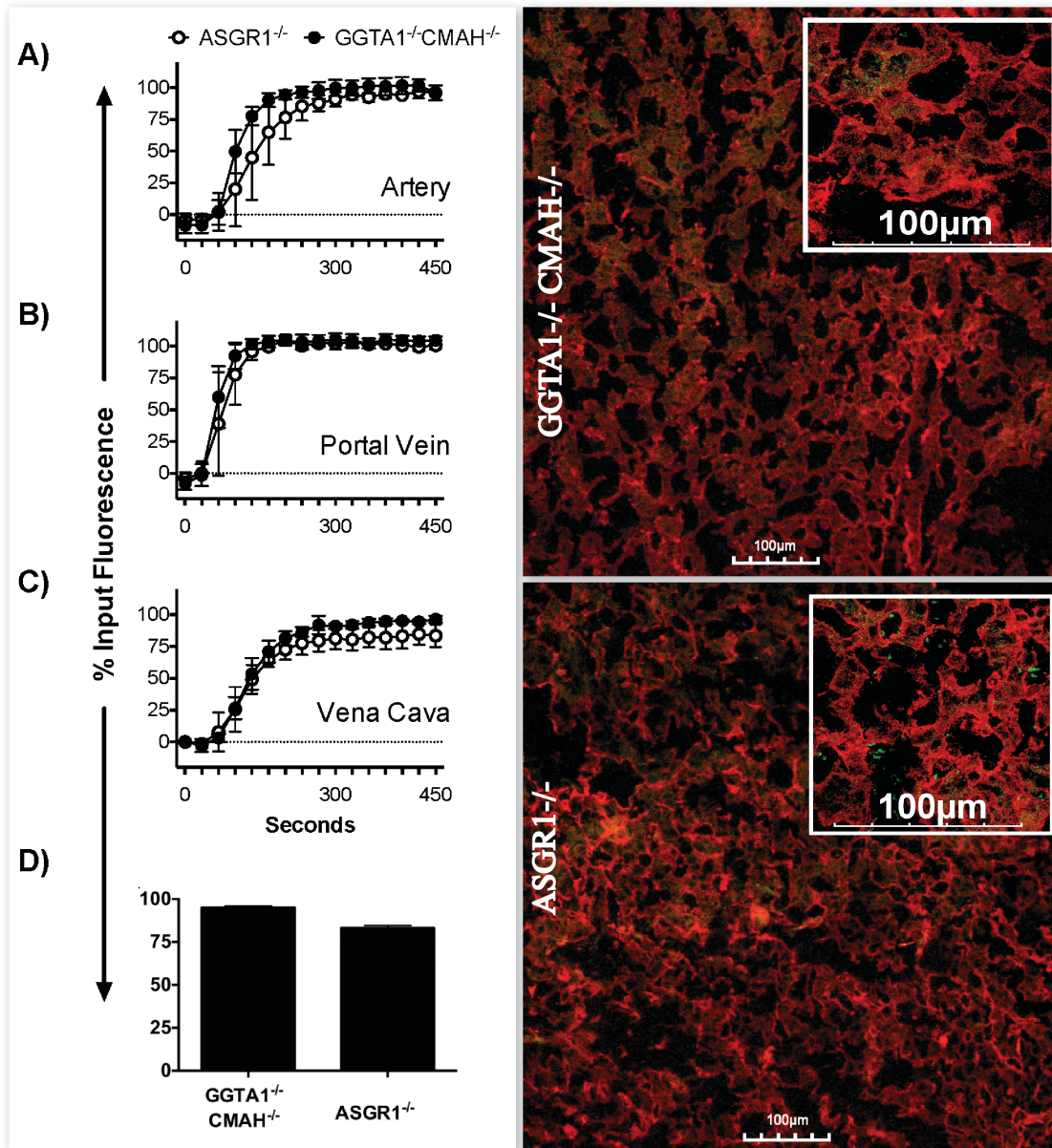


Figure 7.3: A single-pass model of human platelet uptake for GGTA1^{-/-} CMAH^{-/-} and ASGR1^{-/-} livers.

To further characterize a trend noted within a continuous pass model, livers of a GGTA1^{-/-} CMAH^{-/-} background were compared to ASGR1^{-/-} livers in a more sensitive single pass model. Livers of a GGTA1^{-/-} CMAH^{-/-} background consumed significantly fewer platelets than ASGR1^{-/-} livers in a single-pass model of human platelet uptake. After the addition

of CFSE-labeled human platelets into the circuit, samples were obtained simultaneously from the hepatic artery (A), portal vein (B), and suprahepatic inferior vena cava (C), over time and measured for fluorescence. Each sample was measured against the pre-perfusion fluorescence measurement to achieve a percent input fluorescence value. (D) After plateau phase was achieved, data from time points 390, 420 and 450 seconds were averaged; suprahepatic inferior vena cava fluorescence reached 95.4% (SEM=0.590) of initial sample fluorescence for GGTA1^{-/-} CMAH^{-/-} livers compared to 83.9% (SEM=0.513) in ASGR1^{-/-} livers during steady-state. (P= 0.001, GGTA1^{-/-} CMAH^{-/-} n=3, ASGR1^{-/-} n= 4) Representative immunochemical histology obtained post single pass perfusion is shown at figure-right and confirms that the loss of platelets through the system is a function of hepatic deposition.

DISCUSSION

With the recent success of new knockout models described in previous chapters, the antibody barrier to clinical application has effectively been crossed. [27] Prior to human trials, it is important to understand the physiologic compatibility of these organs with the human thromboregulatory system. Unlike *renal* xenotransplantation, Pig-to-primate and pig-to-human models of hepatic xenotransplantation are challenged by early thrombocytopenia. Although activated human platelets will interact with all porcine endothelial cells, the porcine liver is uniquely capable of removing *unactivated* platelets from circulation. [173, 184] Though the mechanism remains poorly understood, it appears that porcine asialoglycoprotein receptor and Von Willebrand factor may contribute to this interaction. [166, 168, 175, 185] Recent efforts to reduce xenogeneic thrombocytopenia in a pig-to-primate model have also exposed the importance of limiting immune-mediated graft injury. [186, 187] Judicious immunosuppression has prevented thrombocytopenia following pig-to-primate xenotransplantation of the porcine heart and kidney. [15, 188] Given this information, it is possible that a combination of immunosuppression and the reduced antigenicity of newer knockout porcine donors alone may facilitate success for renal or cardiac xenografts. Owing to the inherently phagocytic tendency of the liver, further modifications will be necessary to avoid thrombocytopenia with hepatic xenografts.

The porcine ASGR1 gene produces the asialoglycoprotein receptor, which is known to bind and clear human platelets. Paris et al. previously demonstrated that ASGR1^{-/-} livers consume fewer human platelets than WT livers, making them a more

appropriate comparison for the present study. [67] GGTA1 and CMAH genes produce carbohydrates on the porcine cell surface; humans and primates have inactivated these genes over the course of evolution and therefore carry pre-formed antibodies against the products. Silencing these carbohydrate genes results in a favorable crossmatch against human sera, and therefore will be necessary for clinical application of pig-to-human xenotransplantation. [38] Surprisingly, these same modifications that have reduced the xenoantigen barrier also reduce the consumption of human platelets by the porcine liver, even in the absence of immune-mediated injury. Elimination of the CMAH gene appears to provide the majority of protection from platelet consumption.

Though the relationship between carbohydrate profiles and hepatic platelet uptake is still being defined, the ability of carbohydrates to affect hepatic recognition and transport has been recognized for over 30 years. [189] More recently, hepatic lectins and surface carbohydrates have been implicated in the process of hepatic platelet consumption. [190-192] Although the specific role of Neu5Gc (CMAH gene product) remains unknown, its induced expression on human atherosclerotic plaques [141] and cancer cells [193] *in vivo* suggests a link between altered N-glycan structure and human platelet adhesion. It is plausible that the induced expression of Neu5Gc in human solid-organ malignancies is partially responsible for the tumor-induced prothrombotic state, and that Neu5Gc-mediated aggregation is responsible for the human platelet's supportive role in tumor metastasis. [194]

Humanizing the porcine carbohydrate profile significantly reduces xenogeneic consumption of human platelets by the porcine liver. Simultaneous silencing of the GGTA1 and CMAH genes outperformed both GGTA1^{-/-} and ASGR1^{-/-} livers with respect

to reduction in human platelet uptake. It is likely that a combination of carbohydrate and receptor protein knockout strategies will limit the xenogeneic thrombocytopenia associated with pig-to-human hepatic transplantation and facilitate clinical application.

**CHAPTER EIGHT: Conserved FcRN-albumin interactions across species:
implications for porcine-to-human renal xenotransplantation.**

INTRODUCTION

The previous two chapters have described significant improvements in our understanding of thromboregulatory barrier to porcine-to-human xenotransplantation. The pivotal gene-modifications described in chapter four have now made clinical application an *immunologic* possibility; they also appear to limit *physiologic* barriers at the endothelial level. One of the salient findings described within chapters 6-7, is that human platelets react to porcine endothelium in an *organ-specific* manner. Although it is likely that more genome modifications will be needed to avoid xenogenic consumption of human platelets by porcine *livers*, porcine-to-human *renal* transplantation appears unaffected by this problem. For this reason, it is appropriate to appraise porcine kidneys as the first suitable xenograft for human trials.

Renal transplant currently represents the best available treatment for end-stage renal diseases. Unfortunately, the application of this life-saving treatment is severely limited by a growing shortage of available allografts for transplant. Despite considerable effort to increase availability of allografts for transplant, increases in organ supply continue to be outpaced by a growing number of patients awaiting renal transplant. Although xenotransplantation has been studied for multiple decades as a potential answer to this problem, only recently has it reached potential clinical relevance. Specifically, the carbohydrate-modified model of porcine-to-human xenotransplantation described in

chapter four now exhibits very low levels of human antibody binding.[195] Because the human antibody response to genetically modified porcine cells is now at standards established by matched allograft allocation, clinical application is within reason.

With the salient barrier of hyperacute humoral xenogeneic response circumvented, it is now increasingly important to consider potential *physiologic* barriers to clinical application at an organ-specific level. Although a clinical trial is needed, considerable *in vivo* and *ex vivo* evidence indicates that porcine kidneys will perform appropriately when transplanted into humans. Despite the evidence to support physiologic compatibility, the potential for graft-induced proteinuria has remained contentious.

Renal pathologies defined by macromolecule loss, such as serum albumin, have traditionally been associated with damage at the glomerular filtration barrier. This paradigm explains the flagrant proteinuria encountered during complement-mediated damage to the vascular endothelium that defines immune-mediated allograft rejection. Because historic models of porcine-to-primate renal xenotransplantation were afflicted by immunologic incompatibility and early graft loss, it remained unclear whether observed proteinuria was indicative of a primary molecular incompatibility or was simply derivative to immune-mediated damage.

Recently, it has been discovered that serum albumin is a renal *filtrate*; serum proteostasis is dependent on post-glomerulus albumin absorption.[196] In particular, the neonatal Fc receptor (FcRn) has been identified as a primary driver of renal proximal tubule albumin absorption. (Figure 8.1)

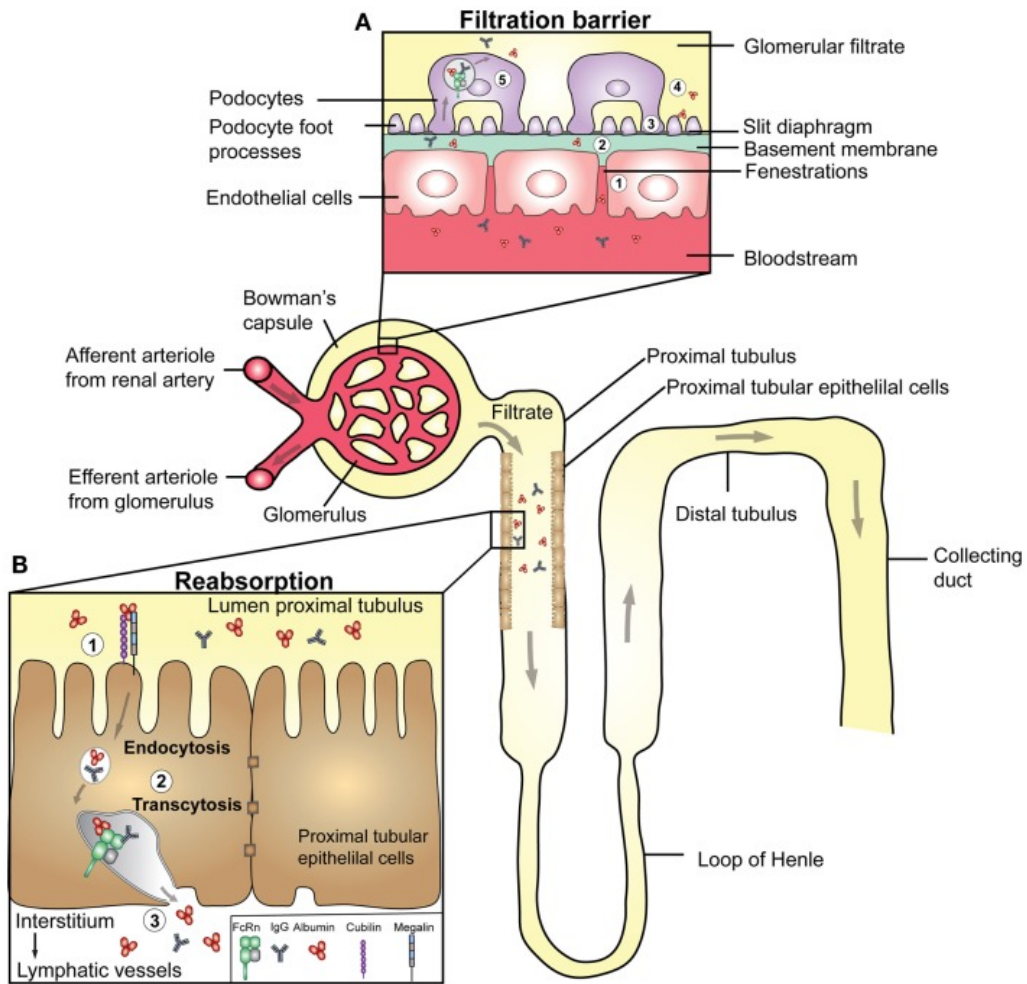


Figure 8.1: FcRN mediated albumin absorption at the proximal tubule.

Recent evidence supports the fact that albumin is freely filtered across Bowman's capsule. To maintain homeostatic serum concentrations, albumin is absorbed by the proximal tubule cell. The FcRN-albumin interaction is essential to this process.

FcRn sequence is highly conserved across species, making physiologic compatibility across species very likely (Figure 8.2), despite this level of homology the interaction warrants dedicated investigation prior to human clinical trials. The object of the present work is to examine the porcine kidney's potential to process human protein in the absence of immunologic injury. We describe the interaction between human albumin and the porcine kidney at a molecular, cellular and organ level, finally we examine proteinuria in a modern *in vivo* model of renal xenotransplantation.

	(1)	1	10	20	30	40	50	60	77	Section 1		
CynoFCGRT Q8SPV9	(1)	MRVPRQPWALG	LLFL	LPGL	GAESHLS	LLYH	LTA	VSS	PAPGT	PAFWVSGWLG	PQQYLSYDS	LRGQAEPCGAWVWE
Rhesus FCGRT F7DS92	(1)	MRVPRQPWALG	LLFL	LPGL	GAESHLS	LLYH	LTA	VSS	PAPGT	PAFWVSGWLG	PQQYLSYDS	LRGQAEPCGAWVWE
Rhesus FCGRT I0FJX2	(1)	MRVPRQPWALG	LLFL	LPGL	GAESHLS	LLYH	LTA	VSS	PAPGT	PAFWVSGWLG	PQQYLSYDS	LRGQAEPCGAWVWE
Consensus	(1)	MRVPRQPWALG	LLFL	LPGL	GAESHLS	LLYH	LTA	VSS	PAPGT	PAFWVSGWLG	PQQYLSYDS	LRGQAEPCGAWVWE
	(78)	78	90	100	110	120	130	140	154	Section 2		
CynoFCGRT Q8SPV9	(78)	NQVSWYWEKETT	DLRIKE	KLFL	EAFKAL	GGKGP	YTLQ	GLLGC	ELSPD	NTSVPTAK	FALNGEE	FMNFDLKQGTWGGDW
Rhesus FCGRT F7DS92	(78)	NQVSWYWEKETT	DLRIKE	KLFL	EAFKAL	GGKGP	YTLQ	GLLGC	ELSPD	NTSVPTAK	FALNGEE	FMNFDLKQGTWGGDW
Rhesus FCGRT I0FJX2	(78)	NQVSWYWEKETT	DLRIKE	KLFL	EAFKAL	GGKGP	YTLQ	GLLGC	ELSPD	NTSVPTAK	FALNGEE	FMNFDLKQGTWGGDW
Consensus	(78)	NQVSWYWEKETT	DLRIKE	KLFL	EAFKAL	GGKGP	YTLQ	GLLGC	ELSPD	NTSVPTAK	FALNGEE	FMNFDLKQGTWGGDW
	(155)	155	160	170	180	190	200	210	220	231	Section 3	
CynoFCGRT Q8SPV9	(155)	PEALAI	SQRW	QQDKA	ANKELT	FLLF	SCPH	RLRE	HLER	GRGN	LEWKE	PPSMRLKARPGNPGFSVLTCSAFSFPPEL
Rhesus FCGRT F7DS92	(155)	PEALAI	SQRW	QQDKA	ANKELT	FLLF	SCPH	RLRE	HLER	GRGN	LEWKE	PPSMRLKARPGNPGFSVLTCSAFSFPPEL
Rhesus FCGRT I0FJX2	(155)	PEALAI	SQRW	QQDKA	ANKELT	FLLF	SCPH	RLRE	HLER	GRGN	LEWKE	PPSMRLKARPGNPGFSVLTCSAFSFPPEL
Consensus	(155)	PEALAI	SQRW	QQDKA	ANKELT	FLLF	SCPH	RLRE	HLER	GRGN	LEWKE	PPSMRLKARPGNPGFSVLTCSAFSFPPEL
	(232)	232	240	250	260	270	280	290	308	Section 4		
CynoFCGRT Q8SPV9	(232)	QLRFLR	NGMA	AGTQ	QD	FGPNS	DG	SF	HASS	SLTV	KSGD	EHYCCIVQHAGLAQPLRVELETPAKSSVLVVGIVIGVL
Rhesus FCGRT F7DS92	(232)	QLRFLR	NGMA	AGTQ	QD	FGPNS	DG	SF	HASS	SLTV	KSGD	EHYCCIVQHAGLAQPLRVELETPAKSSVLVVGIVIGVL
Rhesus FCGRT I0FJX2	(232)	QLRFLR	NGMA	AGTQ	QD	FGPNS	DG	SF	HASS	SLTV	KSGD	EHYCCIVQHAGLAQPLRVELETPAKSSVLVVGIVIGVL
Consensus	(232)	QLRFLR	NGMA	AGTQ	QD	FGPNS	DG	SF	HASS	SLTV	KSGD	EHYCCIVQHAGLAQPLRVELETPAKSSVLVVGIVIGVL

Figure 8.2: FcRn receptor sequence is highly conserved across species.

The porcine FcRn cDNA is 1,577 bp in length (GenBank Accession Number: AY135635) and contains a 1,077 bp open reading frame [136] encoding a 356-amino acid polypeptide. The 3' end of the sequence contains a poly(A) stretch, preceded by a putative polyadenylation signal AATAAA (nucleotides 1523–1529). Blast analysis revealed that the mRNA sequence of the porcine FcRn gene has 79.4%, 66.3% and 83.9% nucleotide identity with the corresponding gene in human, and rhesus respectively. Comparison of predicted porcine FcRn amino acid sequence with that of human, mouse,

rat and cattle indicated an identity of 77.1%, 66.3%, 64.2% and 83.9%, respectively. The complete porcine FcRn genomic DNA sequence spans 8,900 bp (GenBank accession number: HQ026019) and it consists of 5 introns separating 6 exons. The intron/exon organization of porcine (5 introns and 6 exons) is identical with that of the human and rhesus FcRn gene. Although these sequences may predict conserved functional FcRn-albumin interactions across species, specific inquiry is warranted at a molecular and cellular level.

MATERIALS AND METHODS

Intravital 2-photon microscopy

Although urinary loss of serum macromolecules is traditionally associated with insult to cellular integrity at the glomerular level, recent evidence supports the fact that albumin is universally *filtered* in the normal physiologic state; resorption of filtered albumin by the proximal tubule epithelial cells is essential for maintaining serum levels albumin.

Intravital 2-photon microscopy has been instrumental in the elucidation of this phenomenon; by visualizing labeled serum albumin perfused through kidneys in real time, its presence in the glomerular filtrate may be appreciated under physiologic conditions.[197] Though this process has been identified across species including rat, mouse, and human, this is the first reported use of dual photon microscopy to assess the porcine kidney.

Fluorescent labeling of human albumin

100mg of human serum albumin (HSA) (Albumin Bioscience, Huntsville AL, USA) was solubilized in 6.667ml of 100 mM Sodium Bicarbonate pH 9.0; final concentration of 15mg/ml. 200ul of high quality anhydrous Dimethyl Formamide (DMF) was added to a 10 mg vial of Texas Red Sulfonyl Chloride (TRSC) (ThermoFisher Scientific, Waltham MA, USA) and this solution was incubated with 50ml of solubilized HSA at 4degrees for one hour. The solution of labeled HSA was then dialyzed to remove unconjugated TRSC.

Porcine kidney preparation and microcopy

Wild type porcine kidneys were obtained through surgical procurement as previously described.[198] All animals used were approved for use by the Institutional Animal Care and Use Committee at Indiana University. After procurement, kidneys were immediately pumped in a pulsatile perfusion circuit at 35 degrees as previously described. One Liter of autologous whole blood obtained from donor animal diluted 1:1 with Tyrode's solution (Sigma-Aldrich, St. Louis, MO, USA) was used for perfusate. TRSC-labeled human albumin was added to the circuit to achieve physiologic concentration of human albumin. A window through the fibrous renal capsule was removed to allow for better microcopy resolution. An Olympus FV1000 2-photon confocal microscope was fitted with an inverted microscope stage and was used to collect images. The gallium-arsenide phosphide non-descanned photodetectors were set to 750 to collect green emissions, and 625 to collect red emissions.

In vitro proximal tubule cell analysis

Because recent evidence supports both the filtration and resorption of serum albumin, we sought to obtain a more precise measurement of renal proximal tubule handling of filtered albumin in the porcine-to-human model of renal xenotransplantation. To this end we obtained porcine and human proximal tubule cell lines. The porcine 'LLCPK1' proximal tubule cell line as described by Nielsen et al.[199] was purchased from American Type Culture Collection (ATCC, Manassas VA, USA). The 'TH1' human renal proximal tubule cell line was purchased from Kerfast (Boston, MA USA). Cell

lines were maintained in modified endothelial cell line Medium 199+ 2mM Glutamine + 10% Fetal Bovine Serum (Sigma-Aldrich, St. Louis, MO, USA) at 37degrees in 5% CO₂. Cultures were seeded at 2e6cells/cm² and grown to confluence. Incubation with TRSC-labeled human albumin at confluence in a 96-well optical chamber at a concentration of 6.47uM for 30 mins at 37deg. All chambers were then washed in triplicate with phosphate buffered solution (PBS) to remove unabsorbed albumin. Albumin uptake was read on a Spetramax M2 fluoresce plate reader (Molecular Devices Corp., Sunnyvale, CA, USA). Nine consecutive readings were obtained for each sample and relative fluorescence values [121] were recorded as median 647 emissions. For duplicate analysis of uptake, cells were then trypsinized using 0.25 trypsin/EDTA, and read in median fluorescence intensity (MFI) by flow cytometry using an Accuri C6 flow cytometer (Accuri, Ann Arbor, MI, USA). All experiments were performed in triplicate.

Kinetics analysis of FcRN-Albumin interaction

With an established model to assess cross-species albumin-FcRN interaction at the cellular level, we sought to better understand the this relationship at the molecular level. The neonatal FcRn molecule is known to be responsible for binding albumin. The FcRN receptor is highly conserved across species, and although previously published data supports the fidelity of the albumin-FcRN interaction across several species, this is the first report to specifically query the interaction between human albumin and porcine FcRn. Human soluble FcRN Binding experiments were performed on Biacore 3000 at 25°C. The ligand pFcRn~his, huFcRn~GST and pFcRn~GST were directly immobilized

to 3 different flow cells of the CM5 chip by EDC/NHS amine coupling method as per GE instruction. The un-occupied sites were blocked with 1M ethanol amine. Flow cell1 was used as blank for reference subtraction. The analyte as indicated was flowed over the chip at variable concentrations. Binding of analyte to the ligand was monitored in real time. KD was determined from the observed on rate (k_a) and off rate (k_d). Scouting Analysis was performed at single analyte concentration (1000nM) to confirm yes / no binding. Full kinetic analysis was performed at a highest concentration as indicated, followed by 2-fold serial dilution. Chi square (χ^2) analysis was carried out between the actual Sensorgram (colored line) and the sensorgram generated from the BIAAnalysis software (black line) to determine the accuracy of the analysis. χ^2 value within 1- 2 is considered significant (accurate) and below 1 is highly significant (highly accurate).

In vivo evaluation of proteinuria

Genetically modified pigs were created by CRISPR/Cas9 mutagenesis and somatic cell nuclear transfer as previously described by Li et al.[24] Animals for the present analysis were of a GGTA1^{-/-} B4GalNt2^{-/-} background. Pigs were grown to physiologic maturity at which point kidneys were removed under general anesthetic. All use of animals was approved under the Emory University and Indiana University Institutional Animal Care and Use Committee. Kidneys were transplanted into rhesus macaque monkeys after bilateral recipient nephrectomy. Immunosuppression protocol described by Higginbotham et al. was used.[71] Proteinuria was measured by urine analysis over time after transplant.

RESULTS

Texas Red Sulfonyl Chloride-labeled human albumin marker established a visualizable marker of renal protein handling. Dual-photon intravital microcopy was able to penetrate decapsulated porcine kidneys to the level of the porcine glomerulus. This process was successful in illustrating the presence of human albumin as a renal filtrate in the absence of immune-mediated injury. (Figure 8.3A).

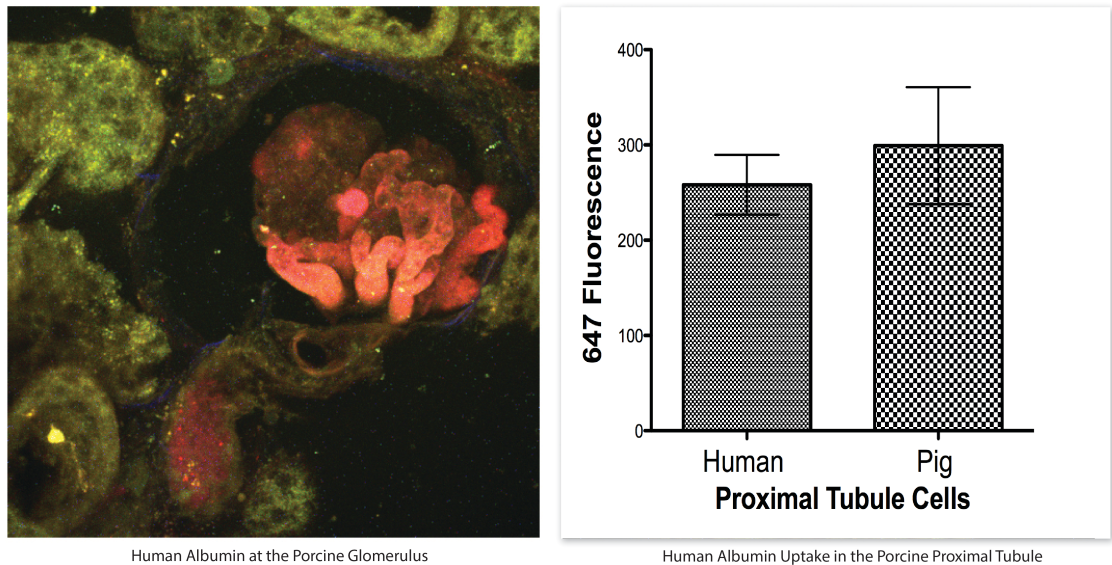


Figure 8.3: Human albumin in the porcine kidney: filtered and absorbed.

Recently it has been discovered in human, mouse and rat models that albumin passes the glomerular barrier in physiologic state. Here we utilized dual photon microscopy and fluorescent labeled human albumin to establish that human albumin is also a part of the porcine renal filtrate under physiologic conditions. Furthermore, when studied on a cellular level porcine proximal tubule cells absorb human albumin in equivalent amounts to human proximal tubule cells. This suggests a conserved physiology of renal albumin trafficking across the human and porcine species.

As has recently been described in mouse, rat and human models, albumin is filtered at the porcine glomerulus. The porcine renal proximal tubule cell is capable of absorbing human albumin at equivalent efficiency as the human renal proximal tubule cells. Once filtered, albumin enters the proximal tubule. Here we established that porcine proximal tubule cells absorb human albumin at levels equivalent to human proximal tubule cells. (Figure 8.3B) At the molecular level FcRn is known to mediate albumin trafficking. To assess the protein-protein interaction of albumin and FcRn across species, we established a surface plasmon resonance analysis. We found that the molecular interaction between FcRn and albumin is conserved across the porcine and human proteomes. FcRn binds human albumin with the same affinity it does autologous porcine albumin; KD values of $7.22e-7$ vs $3.92e-7$ respectively ($p= 0.21$). (Figure 8.4).

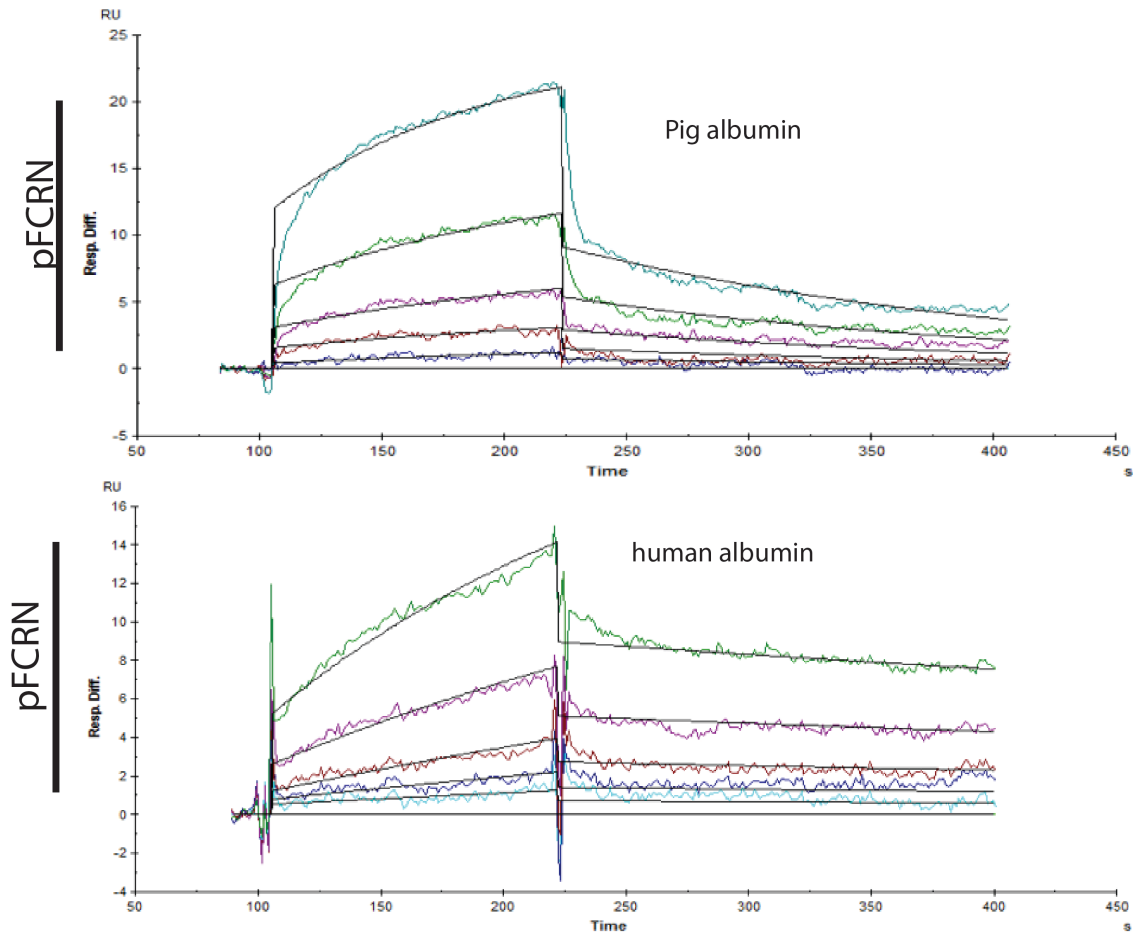


Figure 8.4: Surface plasmon resonance analysis of FcRn-albumin kinetics.

FcRn functions in the renal cortex as an albumin receptor, as such it is essential in maintain serum proteostasis. When the protein-protein interaction between albumin and FcRn across species we found that porcine FcRn binds human albumin with the same affinity as it does autologous porcine albumin, suggesting that that there is no inherent molecular incompatibility that would promote renal albumin loss in porcine-to-human renal transplantation.

Prior to human clinical trials of renal xenotransplantation, *in vivo* study has relied on porcine-to-primate models. Although older pig-to-primate models raised the concerns of post-transplant proteinuria, this problem is not appreciated in the absence of graft rejection. Because the CMAH gene product (Neu5Gc) discussed in chapters 2-4 is expressed in the rhesus monkey, its relevance as a xenoantigen is limited to the porcine-to-*human* model; GGTA1 and B4GalNt2 genes are the most significant glycan drivers of primate-anti-porcine humoral response. Using a GGTA1^{-/-} B4GalNt2^{-/-} porcine kidney for transplant after bilateral native renal ligation, coupled with conventional immune suppression, graft function has been sustained for greater than one year. Over this time period no proteinuria has been appreciated. (Figure 8.5).

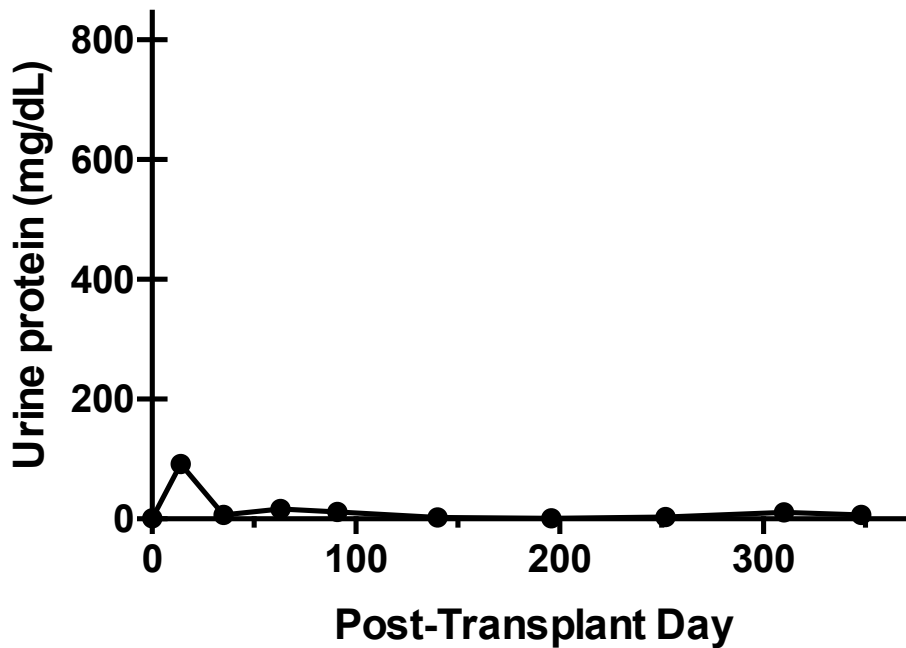


Figure 8.5: Urine protein over time in a pig-to-primate model of xenotransplantation.

A GGTA1^{-/-} B4GalNt2^{-/-} Pig was created by methods described within chapter three. This pig was grown to maturity, serving as renal xenograft donor for a life sustaining xeno-renal transplant into a rhesus macaque. Bilateral native renal vascular ligation was performed at the time of transplant. Immunosuppressive regime was used as described by Higginbotham et al. [71]. Urine protein was measured over time measure the porcine kidney's ability to facilitate primate proteostasis. The peak observed within the first two weeks after transplant is attributable to reperfusion injury, and is universally appreciated in human allotransplantation. Urine protein remained negligible in this model thereafter.

Although xenotransplantation of porcine kidneys will require a human clinical trial to definitively assess clinical relevance, information gained from non-human primate recipients remains helpful. To date, a considerable body of *in vivo* and *ex vivo* data suggests that porcine kidneys will function well in humans. Within these studies, proteinuria has arisen as the salient remaining physiologic question. Here we show that when the immunologic barrier of humoral xenograft rejection is removed, proteinuria is not encountered.

DISCUSSION

A hallmark of many renal disease states is the urinary loss of essential macromolecules like serum albumin. Traditionally this has been associated with insult to the filtration barrier. In renal transplantation, the vascular endothelium comprises the first site of complement-mediated humoral graft injury. The *in vivo* study of porcine renal xenografts has relied on non-human primate recipients. Unfortunately, previous models of porcine-to-primate xenotransplantation were affected by significant humoral rejection; in this context reliable study of long-term serum proteostasis has been challenging. Although hypoalbuminemia and proteinuria have been reported in baboon and cynomolgous monkey recipients of porcine kidneys, authors have avoided making definitive conclusion regarding the etiology of this phenomenon. Aware of the immunologic shortcomings to previous pig-to-primate models, they have only concluded that this witnessed proteinuria “may be indicative of renal injury after xenotransplantation or abnormal handling by the pig kidney of primate plasma proteins.” Herein we report the first series of experiments that specifically query the physiology of renal protein interactions across porcine-primate lines.

Serum albumin is the salient driver of clinically relevant proteinuria post-transplant; as the most abundant serum macromolecule, it is the primary driver of serum oncotic pressure. As such we felt that the relationship between human serum albumin and the porcine kidney deserved privileged attention. The results of the present study answer a lingering debate as to whether the hypoalbuminuria noted in some previous porcine-to-primate models represented anything more than immune-mediated graft injury. It appears

that in the absence of acute humoral xenograft rejection (AHXR), porcine kidneys will be capable of maintaining physiologic serum albumin levels.

Although xenotransplantation of porcine kidneys will require a human clinical trial to definitively assess clinical relevance, information gained from non-human primate recipients remains helpful. To date, a considerable body of *in vivo* and *ex vivo* data suggests that porcine kidneys will function well in humans. Within these studies, proteinuria has arisen as the salient remaining physiologic question. Proteinuria after renal allotransplantation is routine; it is associated with transient glomerular reperfusion injury. Importantly, extensive human data has shown that continuous but *not intermittent* proteinuria is associated with diminished graft survival. The results of the present study show that when the barrier of acute humoral xenograft rejection is removed, porcine kidneys are capable of maintaining serum proteostasis for greater than one-year post transplantation. Proteinuria should no longer be considered a physiologic barrier to clinical application porcine-to-human renal xenotransplantation.

CLOSING REMARKS

Dr. Thomas Starzl, who passed away in the month before this thesis was presented publically, pioneered the success of human allotransplantation through a meticulous study of both operative technique and immune-modification. Though allotransplantation has now become a critical component of modern medical care for patients with end-stage-organ dysfunction, the practice remains severely limited by a growing shortage of available allografts. As discussed in chapter one, approximately 14 patients die each day in the United States while waiting for a renal allograft. However the true burden of world-wide organ shortages likely escapes objective metrics. Faced with a growing dearth of available solid organs for transplant, indications for transplantation are limited. The current allocation process favors patients most-likely to receive durable benefit from transplantation. By including things like age, psychological assessment, concurrent malignancy and even financial ability to cover surveillance costs, current transplant wait-listing excludes many who need life-saving organs; this process of organ-rationing translates directly into death without transplant for an unquantifiable number. Finally, as is the case in many arenas of gross supply-demand inequality, a dark undercurrent of social injustice ebbs outside the borders of regulation. Although beyond the scope of the present discussion, the monetization of human organs by organ-trafficking is a world-wide problem, with an arguably underappreciated imprint on global human rights.

Dr. Starzl himself anticipated many of these problems, and even in the burgeoning era of transplantation when solid organ wait-times were minimal, he dreamed of xenotransplantation as a potential answer to today's problem. Dr Starzl was an early

mentor to Dr. A. Joseph Tector and today I am in great debt to the constant mentorship of Dr Tector, who has dedicated decades of meticulous work to making xenotransplantation a clinical reality. Today, the current climate of xenotransplantation is rich. Though it is my hope that the present work enhances the bright landscape of xenotransplantation research, it would not be possible without the preceding years of tedious progress.

Nuclease-editing in the porcine genome has facilitated our ability to create and study models of porcine-to-human xenotransplantation at an unprecedented pace. Chapter four describes combination of gene-deletions that creates a pig now within the immunologic standards of donor-recipient compatibility established by clinical allotransplantation. This animal has created a paradigm shift for the study of porcine-to-human xenotransplantation, solidifying the merits of pursuing antigen-reduction by glycome modification. Although devotion to antigen-reduction represents a divergence from the previously-popular strategy of transgene insertion, steadfast pursuit of gene-deletion provided the central foundation upon which the present body of work is built. The unpopularity of this approach has most likely indebted to its unique potential for failure; as outlined in chapter three, not all gene-deletion trials are successful in reducing human-anti-porcine immunogenicity. However, dedication to this strategy ultimately proved fruitful and -as described within this work- surpassed the clinical relevance of traditional transgenic approaches.

Similarly, the present body of work is indebted to the current climate of progress within the field of genetic engineering. As outlined within chapter one, the present research adds to a growing body of work that makes the manipulation of mammalian genomes increasingly accessible. Although positioned within our study of

xenotransplantation, glycobiology and immunology, it is my hope that the durability of this research will reach beyond the fields to which we aimed our inquiry. The ability to create and select for multiple mutational events simultaneously, as well as the ability to control these events at the base-pair or whole gene level should be universally applicable across genomes.

One of the greatest achievements in transplant medicine was the early adoption of calcineurin inhibitors; by controlling the early immunologic injury, Dr Starzl used tacrolimus to catalyze *allograft transplantation* into a reliable treatment. Now a benchmark in transplant immuno-suppression, these macrolide lactones were first isolated from the bacterium *Streptomyces tsukubanesis* in Japanese soil. Perhaps ironically, the present body of work is greatly indebted to products of a similar prokaryotic genus; as discussed in chapter one, CRISPR/Cas9 traces its origins to *Streptococcus thermophilus*. The central aim of the present body of work is that we may soon recognize nuclease-based genetic engineering as the catalyst that turns *xenotransplantation* into a clinical reality.

REFERENCES

1. Mali, P., K.M. Esvelt, and G.M. Church, *Cas9 as a versatile tool for engineering biology*. Nat Methods, 2013. **10**(10): p. 957-63.
2. Marraffini, L.A. and E.J. Sontheimer, *Self versus non-self discrimination during CRISPR RNA-directed immunity*. Nature, 2010. **463**(7280): p. 568-71.
3. Horvath, P., et al., *Diversity, activity, and evolution of CRISPR loci in Streptococcus thermophilus*. J Bacteriol, 2008. **190**(4): p. 1401-12.
4. Brouns, S.J., et al., *Small CRISPR RNAs guide antiviral defense in prokaryotes*. Science, 2008. **321**(5891): p. 960-4.
5. Deltcheva, E., et al., *CRISPR RNA maturation by trans-encoded small RNA and host factor RNase III*. Nature, 2011. **471**(7340): p. 602-7.
6. Garneau, J.E., et al., *The CRISPR/Cas bacterial immune system cleaves bacteriophage and plasmid DNA*. Nature, 2010. **468**(7320): p. 67-71.
7. Marraffini, L.A. and E.J. Sontheimer, *CRISPR interference limits horizontal gene transfer in staphylococci by targeting DNA*. Science, 2008. **322**(5909): p. 1843-5.
8. Sapranaukas, R., et al., *The Streptococcus thermophilus CRISPR/Cas system provides immunity in Escherichia coli*. Nucleic Acids Res, 2011. **39**(21): p. 9275-82.
9. Jinek, M., et al., *A programmable dual-RNA-guided DNA endonuclease in adaptive bacterial immunity*. Science, 2012. **337**(6096): p. 816-21.
10. Cong, L., et al., *Multiplex genome engineering using CRISPR/Cas systems*. Science, 2013. **339**(6121): p. 819-23.
11. Capecchi, M.R., *Gene targeting in mice: functional analysis of the mammalian genome for the twenty-first century*. Nat Rev Genet, 2005. **6**(6): p. 507-12.
12. Thomas, K.R., K.R. Folger, and M.R. Capecchi, *High frequency targeting of genes to specific sites in the mammalian genome*. Cell, 1986. **44**(3): p. 419-28.
13. Critser, J.K., et al., *Proceedings of the Conference on Swine in Biomedical Research*. ILAR J, 2009. **50**(1): p. 89-94.
14. Swindle, M.M., et al., *Swine as models in biomedical research and toxicology testing*. Vet Pathol, 2012. **49**(2): p. 344-56.

15. Ekser, B., et al., *Clinical xenotransplantation: the next medical revolution?* Lancet, 2012. **379**(9816): p. 672-83.
16. Brevini, T.A., G. Pennarossa, and F. Gandolfi, *No shortcuts to pig embryonic stem cells.* Theriogenology, 2010. **74**(4): p. 544-50.
17. Campbell, K.H., et al., *Sheep cloned by nuclear transfer from a cultured cell line.* Nature, 1996. **380**(6569): p. 64-6.
18. Polejaeva, I.A., et al., *Cloned pigs produced by nuclear transfer from adult somatic cells.* Nature, 2000. **407**(6800): p. 86-90.
19. Lai, L., et al., *Production of alpha-1,3-galactosyltransferase knockout pigs by nuclear transfer cloning.* Science, 2002. **295**(5557): p. 1089-92.
20. Bibikova, M., et al., *Targeted chromosomal cleavage and mutagenesis in Drosophila using zinc-finger nucleases.* Genetics, 2002. **161**(3): p. 1169-75.
21. Butler, J.R., et al., *Recent advances in genome editing and creation of genetically modified pigs.* Int J Surg, 2015. **23**(Pt B): p. 217-22.
22. Hauschild, J., et al., *Efficient generation of a biallelic knockout in pigs using zinc-finger nucleases.* Proc Natl Acad Sci U S A, 2011. **108**(29): p. 12013-7.
23. Carroll, K.J., et al., *A mouse model for adult cardiac-specific gene deletion with CRISPR/Cas9.* Proc Natl Acad Sci U S A, 2016. **113**(2): p. 338-43.
24. Li, P., et al., *Efficient generation of genetically distinct pigs in a single pregnancy using multiplexed single-guide RNA and carbohydrate selection.* Xenotransplantation, 2015. **22**(1): p. 20-31.
25. Reyes, L.M., et al., *Creating class I MHC-null pigs using guide RNA and the Cas9 endonuclease.* J Immunol, 2014. **193**(11): p. 5751-7.
26. Yang, L., et al., *Genome-wide inactivation of porcine endogenous retroviruses (PERVs).* Science, 2015. **350**(6264): p. 1101-4.
27. Estrada, J.L., et al., *Evaluation of human and non-human primate antibody binding to pig cells lacking GGTA1/CMAH/beta4GalNT2 genes.* Xenotransplantation, 2015. **22**(3): p. 194-202.
28. Butler, J.R., et al., *Silencing porcine genes significantly reduces human-anti-pig cytotoxicity profiles: an alternative to direct complement regulation.* Transgenic Res, 2016.

29. Burlak, C., et al., *Reduced binding of human antibodies to cells from GGTAI/CMAH KO pigs*. Am J Transplant, 2014. **14**(8): p. 1895-900.
30. Sandrin, M.S., N. Osman, and I.F. McKenzie, *Transgenic approaches for the reduction of Galalpha(1,3)Gal for xenotransplantation*. Front Biosci, 1997. **2**: p. e1-11.
31. Costa, C., et al., *Expression of the human alpha1,2-fucosyltransferase in transgenic pigs modifies the cell surface carbohydrate phenotype and confers resistance to human serum-mediated cytotoxicity*. FASEB J, 1999. **13**(13): p. 1762-73.
32. Phelps, C.J., et al., *Production of alpha 1,3-galactosyltransferase-deficient pigs*. Science, 2003. **299**(5605): p. 411-4.
33. Gaj, T., C.A. Gersbach, and C.F. Barbas, 3rd, *ZFN, TALEN, and CRISPR/Cas-based methods for genome engineering*. Trends Biotechnol, 2013. **31**(7): p. 397-405.
34. Orlando, S.J., et al., *Zinc-finger nuclease-driven targeted integration into mammalian genomes using donors with limited chromosomal homology*. Nucleic Acids Res, 2010. **38**(15): p. e152.
35. Szczepek, M., et al., *Structure-based redesign of the dimerization interface reduces the toxicity of zinc-finger nucleases*. Nat Biotechnol, 2007. **25**(7): p. 786-93.
36. Zhang, H., et al., *The CRISPR/Cas9 system produces specific and homozygous targeted gene editing in rice in one generation*. Plant Biotechnol J, 2014. **12**(6): p. 797-807.
37. Christian, M., et al., *Targeting DNA double-strand breaks with TAL effector nucleases*. Genetics, 2010. **186**(2): p. 757-61.
38. Lutz, A.J., et al., *Double knockout pigs deficient in N-glycolylneuraminic acid and galactose alpha-1,3-galactose reduce the humoral barrier to xenotransplantation*. Xenotransplantation, 2013. **20**(1): p. 27-35.
39. Carlson, D.F., et al., *Efficient TALEN-mediated gene knockout in livestock*. Proc Natl Acad Sci U S A, 2012. **109**(43): p. 17382-7.
40. Xin, J., et al., *Highly efficient generation of GGTAI biallelic knockout inbred mini-pigs with TALENs*. PLoS One, 2013. **8**(12): p. e84250.
41. Wood, A.J., et al., *Targeted genome editing across species using ZFNs and TALENs*. Science, 2011. **333**(6040): p. 307.

42. Fu, Y., et al., *Improving CRISPR-Cas nuclease specificity using truncated guide RNAs*. Nat Biotechnol, 2014. **32**(3): p. 279-84.
43. Ramirez, C.L., et al., *Engineered zinc finger nickases induce homology-directed repair with reduced mutagenic effects*. Nucleic Acids Res, 2012. **40**(12): p. 5560-8.
44. Shen, B., et al., *Generation of gene-modified mice via Cas9/RNA-mediated gene targeting*. Cell Res, 2013. **23**(5): p. 720-3.
45. Ran, F.A., et al., *Double nicking by RNA-guided CRISPR Cas9 for enhanced genome editing specificity*. Cell, 2013. **154**(6): p. 1380-9.
46. Veres, A., et al., *Low incidence of off-target mutations in individual CRISPR-Cas9 and TALEN targeted human stem cell clones detected by whole-genome sequencing*. Cell Stem Cell, 2014. **15**(1): p. 27-30.
47. Estrada, J.L., et al., *Evaluation of human and non-human primate antibody binding to pig cells lacking GGTA1/CMAH/beta4GalNT2 genes*. Xenotransplantation, 2015.
48. Fodor, W.L., et al., *Expression of a functional human complement inhibitor in a transgenic pig as a model for the prevention of xenogeneic hyperacute organ rejection*. Proc Natl Acad Sci U S A, 1994. **91**(23): p. 11153-7.
49. Cozzi, E. and D.J. White, *The generation of transgenic pigs as potential organ donors for humans*. Nat Med, 1995. **1**(9): p. 964-6.
50. Osman, N., et al., *Combined transgenic expression of alpha-galactosidase and alpha1,2-fucosyltransferase leads to optimal reduction in the major xenoepitope Galalpha(1,3)Gal*. Proc Natl Acad Sci U S A, 1997. **94**(26): p. 14677-82.
51. Diamond, L.E., et al., *A human CD46 transgenic pig model system for the study of discordant xenotransplantation*. Transplantation, 2001. **71**(1): p. 132-42.
52. Miyagawa, S., et al., *Remodeling of the major pig xenoantigen by N-acetylglucosaminyltransferase III in transgenic pig*. J Biol Chem, 2001. **276**(42): p. 39310-9.
53. Klose, R., et al., *Expression of biologically active human TRAIL in transgenic pigs*. Transplantation, 2005. **80**(2): p. 222-30.
54. Wu, G., et al., *Coagulation cascade activation triggers early failure of pig hearts expressing human complement regulatory genes*. Xenotransplantation, 2007. **14**(1): p. 34-47.

55. Dieckhoff, B., et al., *Knockdown of porcine endogenous retrovirus (PERV) expression by PERV-specific shRNA in transgenic pigs*. *Xenotransplantation*, 2008. **15**(1): p. 36-45.
56. Phelps, C.J., et al., *Production and characterization of transgenic pigs expressing porcine CTLA4-Ig*. *Xenotransplantation*, 2009. **16**(6): p. 477-85.
57. Petersen, B., et al., *Pigs transgenic for human thrombomodulin have elevated production of activated protein C*. *Xenotransplantation*, 2009. **16**(6): p. 486-95.
58. Weiss, E.H., et al., *HLA-E/human beta2-microglobulin transgenic pigs: protection against xenogeneic human anti-pig natural killer cell cytotoxicity*. *Transplantation*, 2009. **87**(1): p. 35-43.
59. Oropeza, M., et al., *Transgenic expression of the human A20 gene in cloned pigs provides protection against apoptotic and inflammatory stimuli*. *Xenotransplantation*, 2009. **16**(6): p. 522-34.
60. Yazaki, S., et al., *Successful cross-breeding of cloned pigs expressing endo-beta-galactosidase C and human decay accelerating factor*. *Xenotransplantation*, 2009. **16**(6): p. 511-21.
61. Hara, H., et al., *Initial in vitro investigation of the human immune response to corneal cells from genetically engineered pigs*. *Invest Ophthalmol Vis Sci*, 2011. **52**(8): p. 5278-86.
62. Seol, J.e.a., *Production of Transgenic Cloned Miniature Pigs with Membrane-bound Human Fas Ligand (FasL) by Somatic Cell Nuclear Transfer*. *Nature Proceedings: Pre-publication research and preliminary findings*, 2010. **hdl:10101/npre.2010.4539.1**.
63. Cho, B., et al., *Generation of soluble human tumor necrosis factor-alpha receptor 1-Fc transgenic pig*. *Transplantation*, 2011. **92**(2): p. 139-47.
64. Yeom, H.J., et al., *Generation and characterization of human heme oxygenase-1 transgenic pigs*. *PLoS One*, 2012. **7**(10): p. e46646.
65. Wheeler, D.G., et al., *Transgenic swine: expression of human CD39 protects against myocardial injury*. *J Mol Cell Cardiol*, 2012. **52**(5): p. 958-61.
66. Klymiuk, N., et al., *Xenografted islet cell clusters from INSLEA29Y transgenic pigs rescue diabetes and prevent immune rejection in humanized mice*. *Diabetes*, 2012. **61**(6): p. 1527-32.

67. Paris, L.L., et al., *Reduced human platelet uptake by pig livers deficient in the asialoglycoprotein receptor 1 protein*. *Xenotransplantation*, 2015. **22**(3): p. 203-10.
68. Wang, Z.Y., et al., *Immortalized porcine liver sinusoidal endothelial cells: an in vitro model of xenotransplantation-induced thrombocytopenia*. *Xenotransplantation*, 2012. **19**(4): p. 249-55.
69. Ran, F.A., et al., *Genome engineering using the CRISPR-Cas9 system*. *Nat Protoc*, 2013. **8**(11): p. 2281-308.
70. Kim, J.H., et al., *High cleavage efficiency of a 2A peptide derived from porcine teschovirus-1 in human cell lines, zebrafish and mice*. *PLoS One*, 2011. **6**(4): p. e18556.
71. Higginbotham, L., et al., *Pre-transplant antibody screening and anti-CD154 costimulation blockade promote long-term xenograft survival in a pig-to-primate kidney transplant model*. *Xenotransplantation*, 2015. **22**(3): p. 221-30.
72. Perkel, J.M., *Xenotransplantation makes a comeback*. *Nat Biotechnol*, 2016. **34**(1): p. 3-4.
73. Reardon, S., *New life for pig-to-human transplants*. *Nature*, 2015. **527**(7577): p. 152-4.
74. Chu, V.T., et al., *Increasing the efficiency of homology-directed repair for CRISPR-Cas9-induced precise gene editing in mammalian cells*. *Nat Biotechnol*, 2015. **33**(5): p. 543-8.
75. Schumann, K., et al., *Generation of knock-in primary human T cells using Cas9 ribonucleoproteins*. *Proc Natl Acad Sci U S A*, 2015. **112**(33): p. 10437-42.
76. Maruyama, T., et al., *Increasing the efficiency of precise genome editing with CRISPR-Cas9 by inhibition of nonhomologous end joining*. *Nat Biotechnol*, 2015. **33**(5): p. 538-42.
77. Kime, C., et al., *Efficient CRISPR/Cas9-Based Genome Engineering in Human Pluripotent Stem Cells*. *Curr Protoc Hum Genet*, 2016. **88**: p. Unit 21 4.
78. Mandal, P.K., et al., *Efficient ablation of genes in human hematopoietic stem and effector cells using CRISPR/Cas9*. *Cell Stem Cell*, 2014. **15**(5): p. 643-52.
79. Orr-Weaver, T.L. and J.W. Szostak, *Yeast recombination: the association between double-strand gap repair and crossing-over*. *Proc Natl Acad Sci U S A*, 1983. **80**(14): p. 4417-21.

80. Iizumi, S., et al., *Impact of non-homologous end-joining deficiency on random and targeted DNA integration: implications for gene targeting*. Nucleic Acids Res, 2008. **36**(19): p. 6333-42.
81. Rydberg, L., et al., *alpha-Gal epitopes in animal tissue glycoproteins and glycolipids*. Subcell Biochem, 1999. **32**: p. 107-25.
82. Cooper, D.K., *Xenotransplantation--state of the art*. Front Biosci, 1996. **1**: p. d248-65.
83. Galili, U., et al., *Interaction between human natural anti-alpha-galactosyl immunoglobulin G and bacteria of the human flora*. Infect Immun, 1988. **56**(7): p. 1730-7.
84. Oriol, R., et al., *Carbohydrate antigens of pig tissues reacting with human natural antibodies as potential targets for hyperacute vascular rejection in pig-to-man organ xenotransplantation*. Transplantation, 1993. **56**(6): p. 1433-42.
85. Bao, L., et al., *Generation of GGTA1 biallelic knockout pigs via zinc-finger nucleases and somatic cell nuclear transfer*. Sci China Life Sci, 2014. **57**(2): p. 263-8.
86. Li, P., et al., *Biallelic knockout of the alpha-1,3 galactosyltransferase gene in porcine liver-derived cells using zinc finger nucleases*. J Surg Res, 2013. **181**(1): p. e39-45.
87. Kolber-Simonds, D., et al., *Production of alpha-1,3-galactosyltransferase null pigs by means of nuclear transfer with fibroblasts bearing loss of heterozygosity mutations*. Proc Natl Acad Sci U S A, 2004. **101**(19): p. 7335-40.
88. Sharma, A., et al., *Pig cells that lack the gene for alpha1-3 galactosyltransferase express low levels of the gal antigen*. Transplantation, 2003. **75**(4): p. 430-6.
89. Kuwaki, K., et al., *Heart transplantation in baboons using alpha1,3-galactosyltransferase gene-knockout pigs as donors: initial experience*. Nat Med, 2005. **11**(1): p. 29-31.
90. Yamada, K., et al., *Marked prolongation of porcine renal xenograft survival in baboons through the use of alpha1,3-galactosyltransferase gene-knockout donors and the cotransplantation of vascularized thymic tissue*. Nat Med, 2005. **11**(1): p. 32-4.
91. Christiansen, D., et al., *Humans lack iGb3 due to the absence of functional iGb3-synthase: implications for NKT cell development and transplantation*. PLoS Biol, 2008. **6**(7): p. e172.

92. Savage, P.B., L. Teyton, and A. Bendelac, *Glycolipids for natural killer T cells*. Chem Soc Rev, 2006. **35**(9): p. 771-9.
93. Speak, A.O., et al., *Implications for invariant natural killer T cell ligands due to the restricted presence of isoglobotrihexosylceramide in mammals*. Proc Natl Acad Sci U S A, 2007. **104**(14): p. 5971-6.
94. Cheng, J.M., et al., *A divergent approach to the synthesis of iGb3 sugar and lipid analogues via a lactosyl 2-azido-sphingosine intermediate*. Org Biomol Chem, 2014. **12**(17): p. 2729-36.
95. Sanderson, J.P., et al., *CD1d protein structure determines species-selective antigenicity of isoglobotrihexosylceramide (iGb3) to invariant NKT cells*. Eur J Immunol, 2013. **43**(3): p. 815-25.
96. Dias, B.R., et al., *Identification of iGb3 and iGb4 in melanoma B16F10-Nex2 cells and the iNKT cell-mediated antitumor effect of dendritic cells primed with iGb3*. Mol Cancer, 2009. **8**: p. 116.
97. Tahiri, F., et al., *Lack of iGb3 and Isoglobo-Series Glycosphingolipids in Pig Organs Used for Xenotransplantation: Implications for Natural Killer T-Cell Biology*. J Carbohydr Chem, 2013. **32**(1): p. 44-67.
98. Diswall, M., et al., *Structural characterization of alpha1,3-galactosyltransferase knockout pig heart and kidney glycolipids and their reactivity with human and baboon antibodies*. Xenotransplantation, 2010. **17**(1): p. 48-60.
99. Diswall, M., et al., *Antigen-binding specificity of anti-alphaGal reagents determined by solid-phase glycolipid-binding assays. A complete lack of alphaGal glycolipid reactivity in alpha1,3GalT-KO pig small intestine*. Xenotransplantation, 2011. **18**(1): p. 28-39.
100. Estrada, J., et al., *Swine generated by somatic cell nuclear transfer have increased incidence of intrauterine growth restriction (IUGR)*. Cloning Stem Cells, 2007. **9**(2): p. 229-36.
101. Svennerholm, L. and P. Fredman, *A procedure for the quantitative isolation of brain gangliosides*. Biochim Biophys Acta, 1980. **617**(1): p. 97-109.
102. Diaz, T.M., et al., *Flow cytometry complement-mediated cytotoxicity assay detects baboon xenoantibodies directed to porcine epitopes undetected by hemolytic assay*. Transpl Immunol, 2004. **13**(4): p. 313-7.
103. Neville, D.C., et al., *Analysis of fluorescently labeled glycosphingolipid-derived oligosaccharides following ceramide glycanase digestion and anthranilic acid labeling*. Anal Biochem, 2004. **331**(2): p. 275-82.

104. Wing, D.R., et al., *High-performance liquid chromatography analysis of ganglioside carbohydrates at the picomole level after ceramide glycanase digestion and fluorescent labeling with 2-aminobenzamide*. *Anal Biochem*, 2001. **298**(2): p. 207-17.
105. Platt, J.L. and M. Cascalho, *New and old technologies for organ replacement*. *Curr Opin Organ Transplant*, 2013. **18**(2): p. 179-85.
106. Miyata, Y. and J.L. Platt, *Xeno--still stuck without alphaGal*. *Nat Biotechnol*, 2003. **21**(4): p. 359-60.
107. Milland, J., et al., *Carbohydrate residues downstream of the terminal Galalpha(1,3)Gal epitope modulate the specificity of xenoreactive antibodies*. *Immunol Cell Biol*, 2007. **85**(8): p. 623-32.
108. Milland, J., D. Christiansen, and M.S. Sandrin, *Alpha1,3-galactosyltransferase knockout pigs are available for xenotransplantation: are glycosyltransferases still relevant?* *Immunol Cell Biol*, 2005. **83**(6): p. 687-93.
109. Chiang, T.R., et al., *Anti-Gal antibodies in humans and 1, 3alpha-galactosyltransferase knock-out mice*. *Transplantation*, 2000. **69**(12): p. 2593-600.
110. Dor, F.J., et al., *alpha1,3-Galactosyltransferase gene-knockout miniature swine produce natural cytotoxic anti-Gal antibodies*. *Transplantation*, 2004. **78**(1): p. 15-20.
111. Posekany, K.J., et al., *Induction of cytolytic anti-Gal antibodies in alpha-1,3-galactosyltransferase gene knockout mice by oral inoculation with Escherichia coli O86:B7 bacteria*. *Infect Immun*, 2002. **70**(11): p. 6215-22.
112. Thall, A.D., H.S. Murphy, and J.B. Lowe, *alpha 1,3-Galactosyltransferase-deficient mice produce naturally occurring cytotoxic anti-Gal antibodies*. *Transplant Proc*, 1996. **28**(2): p. 556-7.
113. Zhou, D. and S.B. Levery, *Response to Milland et al.: Carbohydrate residues downstream of the terminal Galalpha(1,3)Gal epitope modulate the specificity of xenoreactive antibodies*. *Immunol Cell Biol*, 2008. **86**(8): p. 631-2; author reply 633-4.
114. Tanemura, M., et al., *Differential immune responses to alpha-gal epitopes on xenografts and allografts: implications for accommodation in xenotransplantation*. *J Clin Invest*, 2000. **105**(3): p. 301-10.
115. Butler, J.R., et al., *Recent advances in genome editing and creation of genetically modified pigs*. *Int J Surg*, 2015.

116. Menoret, S., et al., *Characterization of human CD55 and CD59 transgenic pigs and kidney xenotransplantation in the pig-to-baboon combination*. *Transplantation*, 2004. **77**(9): p. 1468-71.
117. Martin, M.J., et al., *Evolution of human-chimpanzee differences in malaria susceptibility: relationship to human genetic loss of N-glycolylneuraminic acid*. *Proc Natl Acad Sci U S A*, 2005. **102**(36): p. 12819-24.
118. Byrne, G.W., et al., *Cloning and expression of porcine beta1,4 N-acetylgalactosaminyl transferase encoding a new xenoreactive antigen*. *Xenotransplantation*, 2014. **21**(6): p. 543-54.
119. Byrne, G.W., et al., *Identification of new carbohydrate and membrane protein antigens in cardiac xenotransplantation*. *Transplantation*, 2011. **91**(3): p. 287-92.
120. Mulley, W.R. and J. Kanellis, *Understanding crossmatch testing in organ transplantation: A case-based guide for the general nephrologist*. *Nephrology (Carlton)*, 2011. **16**(2): p. 125-33.
121. Mujtaba, M.A., et al., *The strength of donor-specific antibody is a more reliable predictor of antibody-mediated rejection than flow cytometry crossmatch analysis in desensitized kidney recipients*. *Clin Transplant*, 2011. **25**(1): p. E96-102.
122. Stief, A., et al., *A nuclear DNA attachment element mediates elevated and position-independent gene activity*. *Nature*, 1989. **341**(6240): p. 343-5.
123. Brunetti, D., et al., *Transgene expression of green fluorescent protein and germ line transmission in cloned pigs derived from in vitro transfected adult fibroblasts*. *Cloning Stem Cells*, 2008. **10**(4): p. 409-19.
124. Niwa, H., K. Yamamura, and J. Miyazaki, *Efficient selection for high-expression transfectants with a novel eukaryotic vector*. *Gene*, 1991. **108**(2): p. 193-9.
125. Schmidtke, J., et al., *Treatment of atypical hemolytic uremic syndrome and thrombotic microangiopathies: a focus on eculizumab*. *Am J Kidney Dis*, 2013. **61**(2): p. 289-99.
126. Tseng, Y.L., et al., *alpha1,3-Galactosyltransferase gene-knockout pig heart transplantation in baboons with survival approaching 6 months*. *Transplantation*, 2005. **80**(10): p. 1493-500.
127. White, D.J. and N. Yannoutsos, *Production of pigs transgenic for human DAF to overcome complement-mediated hyperacute xenograft rejection in man*. *Res Immunol*, 1996. **147**(2): p. 88-94.

128. Byrne, G.W., et al., *Transgenic pigs expressing human CD59 and decay-accelerating factor produce an intrinsic barrier to complement-mediated damage*. *Transplantation*, 1997. **63**(1): p. 149-55.
129. Lublin, D.M. and K.E. Coyne, *Phospholipid-anchored and transmembrane versions of either decay-accelerating factor or membrane cofactor protein show equal efficiency in protection from complement-mediated cell damage*. *J Exp Med*, 1991. **174**(1): p. 35-44.
130. Perez de la Lastra, J.M., et al., *Pigs express multiple forms of decay-accelerating factor (CD55), all of which contain only three short consensus repeats*. *J Immunol*, 2000. **165**(5): p. 2563-73.
131. van den Berg, C.W., et al., *Role and regulation of pig CD59 and membrane cofactor protein/CD46 expressed on pig aortic endothelial cells*. *Transplantation*, 2000. **70**(4): p. 667-73.
132. Cooper, D.K., B. Ekser, and A.J. Tector, *Immunobiological barriers to xenotransplantation*. *Int J Surg*, 2015.
133. *Xenotransplantation*. *Nat Biotechnol*, 2000. **18 Suppl**: p. IT53-5.
134. Iwase, H., et al., *Pig kidney graft survival in a baboon for 136 days: longest life-supporting organ graft survival to date*. *Xenotransplantation*, 2015. **22**(4): p. 302-9.
135. McGregor, C.G., et al., *Human CD55 expression blocks hyperacute rejection and restricts complement activation in Gal knockout cardiac xenografts*. *Transplantation*, 2012. **93**(7): p. 686-92.
136. Azimzadeh, A.M., et al., *Early graft failure of GalTKO pig organs in baboons is reduced by expression of a human complement pathway-regulatory protein*. *Xenotransplantation*, 2015. **22**(4): p. 310-6.
137. Sachs, D.H., et al., *GalT-KO pigs: is the cup half empty or half full?* *Transplantation*, 2007. **84**(1): p. 12-4.
138. Ekser, B., et al., *Xenotransplantation of solid organs in the pig-to-primate model*. *Transpl Immunol*, 2009. **21**(2): p. 87-92.
139. Klintmalm, G., et al., *Cyclosporine plasma levels in renal transplant patients. Association with renal toxicity and allograft rejection*. *Transplantation*, 1985. **39**(2): p. 132-7.
140. van Kooyk, Y. and G.A. Rabinovich, *Protein-glycan interactions in the control of innate and adaptive immune responses*. *Nat Immunol*, 2008. **9**(6): p. 593-601.

141. Pham, T., et al., *Evidence for a novel human-specific xeno-auto-antibody response against vascular endothelium*. Blood, 2009. **114**(25): p. 5225-35.
142. Gong, Y.B., et al., *Experimental study of the mechanism of tolerance induction in dexamethasone-treated dendritic cells*. Med Sci Monit, 2011. **17**(5): p. BR125-31.
143. Mainali, E.S., T. Kikuchi, and J.G. Tew, *Dexamethasone inhibits maturation and alters function of monocyte-derived dendritic cells from cord blood*. Pediatr Res, 2005. **58**(1): p. 125-31.
144. Piemonti, L., et al., *Glucocorticoids affect human dendritic cell differentiation and maturation*. J Immunol, 1999. **162**(11): p. 6473-81.
145. Koshika, T., et al., *Relative efficiency of porcine and human cytotoxic T-lymphocyte antigen 4 immunoglobulin in inhibiting human CD4+ T-cell responses co-stimulated by porcine and human B7 molecules*. Immunology, 2011. **134**(4): p. 386-97.
146. Saunders, R.N., M.S. Metcalfe, and M.L. Nicholson, *Rapamycin in transplantation: a review of the evidence*. Kidney Int, 2001. **59**(1): p. 3-16.
147. Staatz, C., P. Taylor, and S. Tett, *Low tacrolimus concentrations and increased risk of early acute rejection in adult renal transplantation*. Nephrol Dial Transplant, 2001. **16**(9): p. 1905-9.
148. Rana, A., et al., *Survival benefit of solid-organ transplant in the United States*. JAMA Surg, 2015. **150**(3): p. 252-9.
149. Afzali, B., G. Lombardi, and R.I. Lechler, *Pathways of major histocompatibility complex allorecognition*. Curr Opin Organ Transplant, 2008. **13**(4): p. 438-44.
150. Deschamps, J.Y., et al., *History of xenotransplantation*. Xenotransplantation, 2005. **12**(2): p. 91-109.
151. Jerne, N.K., *The somatic generation of immune recognition*. Eur J Immunol, 1971. **1**(1): p. 1-9.
152. Moses, R.D., et al., *Xenogeneic proliferation and lymphokine production are dependent on CD4+ helper T cells and self antigen-presenting cells in the mouse*. J Exp Med, 1990. **172**(2): p. 567-75.
153. Oostingh, G.J., et al., *Comparison of allogeneic and xenogeneic in vitro T-cell proliferative responses in sensitized patients awaiting kidney transplantation*. Xenotransplantation, 2003. **10**(6): p. 545-51.

154. Swain, S.L., et al., *Xenogeneic human anti-mouse T cell responses are due to the activity of the same functional T cell subsets responsible for allospecific and major histocompatibility complex-restricted responses*. J Exp Med, 1983. **157**(2): p. 720-9.
155. Scalea, J., et al., *T-cell-mediated immunological barriers to xenotransplantation*. Xenotransplantation, 2012. **19**(1): p. 23-30.
156. Yamada, K., D.H. Sachs, and H. DerSimonian, *Human anti-porcine xenogeneic T cell response. Evidence for allelic specificity of mixed leukocyte reaction and for both direct and indirect pathways of recognition*. J Immunol, 1995. **155**(11): p. 5249-56.
157. Benichou, G., A. Valujskikh, and P.S. Heeger, *Contributions of direct and indirect T cell alloreactivity during allograft rejection in mice*. J Immunol, 1999. **162**(1): p. 352-8.
158. Purcell, A.W., I.R. van Driel, and P.A. Gleeson, *Impact of glycans on T-cell tolerance to glycosylated self-antigens*. Immunol Cell Biol, 2008. **86**(7): p. 574-9.
159. Varki, A. and P. Gagneux, *Multifarious roles of sialic acids in immunity*. Ann N Y Acad Sci, 2012. **1253**: p. 16-36.
160. Ikehara, Y., S.K. Ikehara, and J.C. Paulson, *Negative regulation of T cell receptor signaling by Siglec-7 (p70/AIRM) and Siglec-9*. J Biol Chem, 2004. **279**(41): p. 43117-25.
161. Buchlis, G., et al., *Enhanced T cell function in a mouse model of human glycosylation*. J Immunol, 2013. **191**(1): p. 228-37.
162. Crocker, P.R., J.C. Paulson, and A. Varki, *Siglecs and their roles in the immune system*. Nat Rev Immunol, 2007. **7**(4): p. 255-66.
163. Brinkman-Van der Linden, E.C., et al., *Loss of N-glycolylneuraminic acid in human evolution. Implications for sialic acid recognition by siglecs*. J Biol Chem, 2000. **275**(12): p. 8633-40.
164. Cooper, D.K., et al., *Progress in pig-to-non-human primate transplantation models (1998-2013): a comprehensive review of the literature*. Xenotransplantation, 2014. **21**(5): p. 397-419.
165. Cozzi, E., et al., *Alterations in the coagulation profile in renal pig-to-monkey xenotransplantation*. Am J Transplant, 2004. **4**(3): p. 335-45.

166. Robson, S.C., D.K. Cooper, and A.J. d'Apice, *Disordered regulation of coagulation and platelet activation in xenotransplantation*. *Xenotransplantation*, 2000. **7**(3): p. 166-76.
167. Iwase, H., et al., *Pig kidney graft survival in a baboon for 136 days: longest life-supporting organ graft survival to date*. *Xenotransplantation*, 2015.
168. Paris, L.L., et al., *ASGR1 expressed by porcine enriched liver sinusoidal endothelial cells mediates human platelet phagocytosis in vitro*. *Xenotransplantation*, 2011. **18**(4): p. 245-51.
169. Ierino, F.L., et al., *Disseminated intravascular coagulation in association with the delayed rejection of pig-to-baboon renal xenografts*. *Transplantation*, 1998. **66**(11): p. 1439-50.
170. Schmelzle, M., J. Schulte Esch, 2nd, and S.C. Robson, *Coagulation, platelet activation and thrombosis in xenotransplantation*. *Curr Opin Organ Transplant*, 2010. **15**(2): p. 212-8.
171. Shimizu, A., et al., *Thrombotic microangiopathic glomerulopathy in human decay accelerating factor-transgenic swine-to-baboon kidney xenografts*. *J Am Soc Nephrol*, 2005. **16**(9): p. 2732-45.
172. Cowan, P.J., D.K. Cooper, and A.J. d'Apice, *Kidney xenotransplantation*. *Kidney Int*, 2014. **85**(2): p. 265-75.
173. Burlak, C., et al., *The fate of human platelets perfused through the pig liver: implications for xenotransplantation*. *Xenotransplantation*, 2010. **17**(5): p. 350-61.
174. Mazzucato, M., et al., *Porcine von Willebrand factor binding to human platelet GPIb induces transmembrane calcium influx*. *Thromb Haemost*, 1996. **75**(4): p. 655-60.
175. Schulte Am Esch, J., 2nd, et al., *O-linked glycosylation and functional incompatibility of porcine von Willebrand factor for human platelet GPIb receptors*. *Xenotransplantation*, 2005. **12**(1): p. 30-7.
176. Wu, Q.Y., et al., *Differential distribution of von Willebrand factor in endothelial cells. Comparison between normal pigs and pigs with von Willebrand disease*. *Arteriosclerosis*, 1987. **7**(1): p. 47-54.
177. Cowan, P.J., S.C. Robson, and A.J. d'Apice, *Controlling coagulation dysregulation in xenotransplantation*. *Curr Opin Organ Transplant*, 2011. **16**(2): p. 214-21.

178. Meehan, S.M., et al., *Thrombotic microangiopathy and peritubular capillary C4d expression in renal allograft biopsies*. Clin J Am Soc Nephrol, 2011. **6**(2): p. 395-403.
179. Ezzelarab, M.B., et al., *Systemic inflammation in xenograft recipients precedes activation of coagulation*. Xenotransplantation, 2014.
180. Byrne, G.W., et al., *Increased immunosuppression, not anticoagulation, extends cardiac xenograft survival*. Transplantation, 2006. **82**(12): p. 1787-91.
181. Byrne, G.W., et al., *Cloning and expression of porcine beta1,4 N-acetylgalactosaminyl transferase encoding a new xenoreactive antigen*. Xenotransplantation, 2014.
182. Salomon, D.R., et al., *AST/ASTS workshop on increasing organ donation in the United States: creating an "arc of change" from removing disincentives to testing incentives*. Am J Transplant, 2015. **15**(5): p. 1173-9.
183. Ekser, B., et al., *Impact of thrombocytopenia on survival of baboons with genetically modified pig liver transplants: clinical relevance*. Am J Transplant, 2010. **10**(2): p. 273-85.
184. Iwase, H., et al., *The role of platelets in coagulation dysfunction in xenotransplantation, and therapeutic options*. Xenotransplantation, 2014. **21**(3): p. 201-20.
185. Bongoni, A.K., et al., *Porcine extrahepatic vascular endothelial asialoglycoprotein receptor 1 mediates xenogeneic platelet phagocytosis in vitro and in human-to-pig ex vivo xenoperfusion*. Transplantation, 2015. **99**(4): p. 693-701.
186. Ezzelarab, M.B., et al., *Systemic inflammation in xenograft recipients precedes activation of coagulation*. Xenotransplantation, 2015. **22**(1): p. 32-47.
187. Buhler, L., et al., *Pig kidney transplantation in baboons: anti-Gal(alpha)1-3Gal IgM alone is associated with acute humoral xenograft rejection and disseminated intravascular coagulation*. Transplantation, 2001. **72**(11): p. 1743-52.
188. Soin, B., et al., *Physiological aspects of pig-to-primate renal xenotransplantation*. Kidney Int, 2001. **60**(4): p. 1592-7.
189. Ashwell, G. and A.G. Morell, *The role of surface carbohydrates in the hepatic recognition and transport of circulating glycoproteins*. Adv Enzymol Relat Areas Mol Biol, 1974. **41**(0): p. 99-128.

190. Grewal, P.K., et al., *The Ashwell receptor mitigates the lethal coagulopathy of sepsis*. Nat Med, 2008. **14**(6): p. 648-55.
191. Grozovsky, R., K.M. Hoffmeister, and H. Falet, *Novel clearance mechanisms of platelets*. Curr Opin Hematol, 2010. **17**(6): p. 585-9.
192. van't Veer, C. and T. van der Poll, *Keeping blood clots at bay in sepsis*. Nat Med, 2008. **14**(6): p. 606-8.
193. Varki, A., *Glycan-based interactions involving vertebrate sialic-acid-recognizing proteins*. Nature, 2007. **446**(7139): p. 1023-9.
194. Gay, L.J. and B. Felding-Habermann, *Contribution of platelets to tumour metastasis*. Nat Rev Cancer, 2011. **11**(2): p. 123-34.
195. Butler, J.R., et al., *Silencing porcine genes significantly reduces human-anti-pig cytotoxicity profiles: an alternative to direct complement regulation*. Transgenic Res, 2016. **25**(5): p. 751-9.
196. Dickson, L.E., et al., *The proximal tubule and albuminuria: really!* J Am Soc Nephrol, 2014. **25**(3): p. 443-53.
197. Sandoval, R.M. and B.A. Molitoris, *Quantifying glomerular permeability of fluorescent macromolecules using 2-photon microscopy in Munich Wistar rats*. J Vis Exp, 2013(74).
198. Butler, J.R., et al., *The fate of human platelets exposed to porcine renal endothelium: a single-pass model of platelet uptake in domestic and genetically modified porcine organs*. J Surg Res, 2016. **200**(2): p. 698-706.
199. Nielsen, R., et al., *Characterization of a kidney proximal tubule cell line, LLC-PK1, expressing endocytotic active megalin*. J Am Soc Nephrol, 1998. **9**(10): p. 1767-76.

CURRICULUM VITAE

James R. Butler

Education

Indiana University- PhD; Molecular Genetics 2013-
2017
Indiana University School of Medicine, M.D. Honors program in Surgery
2011 *Davidson College*, A.B. Hons: cum laude.
2007
Oxford University, St. Catherine's College 2005-
2006
Harvard University, undergraduate physics
2005

Editorial Positions

Xenotransplantation –ad hoc reviewer 2016-
present
Journal of Surgical Research –ad hoc reviewer 2015-
present
International Journal of Surgery –ad hoc reviewer 2015-
present
Transplantation- ad hoc reviewer 2016-
present
Elsevier Publishing- external referee for text books 2007-
present
-*Handbook of Human Genome Editing (Elsevier 2017)*
The Oxford University Owl- Managing Science Editor. 2005-
2007
The Harvard Crimson - section editor 2005-
2006

External Funding

Butler JR. Improving transgene expression on porcine endothelium through identification of endogenous promoters: a strategy to drive human complement regulatory proteins. *2015 Association for Academic Surgery Research Fellowship Award*. February 3, 2015, Las Vegas NE. \$20,000.

Butler JR. Defining the co-stimulatory properties of vascular endothelium in a porcine model: a strategy to promote anergy in clinical xenografts. *2015 American Society of Transplant Surgeons Scientist Scholarship Award*. May 3, 2015, Philadelphia, PA. \$45,000.

Positions and Appointments

Indiana University Department of Surgery July 2011 -
present

General Surgery Resident.

SSAT Resident Education Committee; elected member May 2014 - May
2016

Organize fellowship information sessions. Work to refine national curriculum for general surgery resident education.

Indiana University Transplantation Laboratory; Research Fellow July 2013- June
2016

My passion within science is using nuclease-based genomic editing tools to create new models of cellular-mediated response pathways in transplant rejection. Working towards a xenotransplant model that alleviates the current problem with organ shortage, we have recently produced porcine organs that are immunological comparable to a human allograft. With my thesis complete, my focus for the past year –when not in clinic- has been to mentor medical and undergraduate students in their lab experience and together, to efficiently create transgenic models of transplant immunology that investigate the pathways of T-cell co-stimulation.

Anaclim, LLC; Clinical research researcher Organizer August-October 2005

Drawn to the need for increased representation of minority data in clinical trials, I assisted coordinating and enrolling multicenter clinical pharmaceutical research projects for Eli Lilly. Anaclim is a minority-focused contract research organization that seeks to increase minority-patient data in clinical trials.

Journal Publications

1. Kannan P Samy, **James R Butler**, Ping Li, David C.K. Cooper, Burcin Ekser. *The role of costimulation blockade in solid organ and islet xenotransplantation*. Journal of Immunology Research. Vol 2017 (2017) DOI:10.1155/2017/8415205
2. Joseph M Ladowski, Luz M Reyes, Gregory R Martens, **James R. Butler**, Zheng-Yu Wang, Devin E Eckhoff, Matt Tector, A. Joseph Tector: *Swine Leukocyte Antigen (SLA) Class II is a Xenoantigen*. Transplantation, August 24, 2017 PMID: 28846555
3. **James R. Butler**, Rafael M.N. Santos, Gregory R. Martens, Joseph M. Ladowski, Zheng-Yu Wang, Ping Li, Matthew Tector, A. Joseph Tector: *Efficient generation of targeted and controlled mutational events in porcine cells using nuclease-directed homologous recombination*. Journal of Surgical Research 01/2017;, DOI:10.1016/j.jss.2017.01.025
4. Gregory R Martens, Luz M Reyes, **James R Butler**, Joseph M Ladowski, Jose L Estrada, Richard A Sidner, Devin E Eckhoff, Matt Tector, A Joseph Tector: *Humoral Reactivity of Renal Transplant-Waitlisted Patients to Cells from GGTA1/CMAH/B4GalNT2, and SLA Class I Knockout Pigs*. Transplantation 01/2017;, DOI:10.1097/TP.0000000000001646
5. Adam S A Gracon, Tiffany W Liang, Thomas S Easterday, Daniel J Weber, **James Butler**, James E Slaven, Gary W Lemmon, Raghu L Motaganahalli: *Institutional Cost of Unplanned 30-Day Readmission Following Open and Endovascular Surgery*. Vascular and Endovascular Surgery 08/2016; 50(6)., DOI:10.1177/1538574416666227
6. **James R. Butler**: *Peer review report 2 on "Adipocytes enhance murine pancreatic cancer growth via a hepatocyte growth factor (HGF)-mediated mechanism"*. International Journal of Surgery 06/2016; 25(1)., DOI:10.1016/j.ijss.2016.03.009
7. **James R Butler**, Gregory R Martens, Jose L Estrada, Luz M Reyes, Joseph M Ladowski, Cesare Galli, Andrea Perota, Conor M Cunningham, Matthew Tector, A Joseph Tector: *Silencing porcine genes significantly reduces human-anti-pig cytotoxicity profiles: an alternative to direct complement regulation*. Transgenic Research 04/2016;, DOI:10.1007/s11248-016-9958-0
8. **James R. Butler**, Nicholas J. Skill, David L. Priestman, Frances M. Platt, Ping Li, Jose L. Estrada, Gregory R. Martens, Joseph M. Ladowski, Matthew Tector, A. Joseph Tector: *Silencing the porcine iGb3s gene does not affect Gal α 3Gal levels or measures of anticipated pig-to-human and pig-to-primate acute rejection*. Xenotransplantation 03/2016; 23(2)., DOI:10.1111/xen.12217
9. **James R. Butler**, Zheng-Yu Wang, Gregory R. Martens, Joseph M. Ladowski, Ping Li, Matthew Tector, A. Joseph Tector: *Modified glycan models of pig-to-human*

xenotransplantation do not enhance the human-anti-pig T cell response.
Transplant Immunology 02/2016; 35., DOI:10.1016/j.trim.2016.02.001

10. **James R. Butler**, Syed A. Ahmad, Matthew H. Katz, Jessica L. Cioffi, Nicholas J. Zyromski: *A systematic review of the role of periadventitial dissection of the superior mesenteric artery in affecting margin status after pancreatoduodenectomy for pancreatic adenocarcinoma.* HPB 02/2016; 18(4)., DOI:10.1016/j.hpb.2015.11.009
11. Zheng-Yu Wang, Ping Li, **James R. Butler**, Ross L. Blankenship, Susan M. Downey, Jessica B. Montgomery, Shunji Nagai, Jose L. Estrada, Matthew F. Tector, A. Joseph Tector: *Immunogenicity of Renal Microvascular Endothelial Cells From Genetically Modified Pigs.* Transplantation 01/2016; 100(3)., DOI:10.1097/TP.0000000000001070
12. **James R. Butler**, Leela L. Paris, Ross L. Blankenship, Richard A. Sidner, Gregory R. Martens, Joseph M. Ladowski, Ping Li, Jose L. Estrada, Matthew Tector, A. Joseph Tector: *Silencing Porcine CMAH and GGTA1 Genes Significantly Reduces Xenogeneic Consumption of Human Platelets by Porcine Livers.* Transplantation 01/2016; 100(3)., DOI:10.1097/TP.0000000000001071
13. **James R. Butler**, Tanyi M. Fohtung, Kumar Sandrasegaran, Eugene P. Ceppa, Michael G. House, Attila Nakeeb, C. Max Schmidt, Nicholas J. Zyromski: *The Natural History of Pancreatic Lipoma: Does it Need Observation.* Pancreatology 11/2015;, DOI:10.1016/j.pan.2015.11.005
14. **James R Butler**, Gregory R Martens, Ping Li, Wang Zheng-Yu, Jose L Estrada, Joseph M Ladowski, Matt Tector, A Joseph Tector: *The Fate of Human Platelets Exposed to Porcine Renal Endothelium: A Single-Pass Model of Platelet Uptake in Domestic and Genetically Modified Porcine Organs.* Journal of Surgical Research 09/2015; 200., DOI:10.1016/j.jss.2015.08.034
15. **James R Butler**, Joseph M Ladowski, Greg R Martens, Matthew Tector, A. Joseph Tector: *Recent Advances in Genome Editing and Creation of Genetically Modified Pigs.* International Journal of Surgery (London, England) 07/2015; 23., DOI:10.1016/j.ijssu.2015.07.684
16. **James R Butler**, Tyrone Rogers, George Eckart, Gregory R Martens, Eugene P Ceppa, Michael G House, Attila Nakeeb, C Max Schmidt, Nicholas J Zyromski: *Is Antisecretory Therapy After Pancreatoduodenectomy Necessary? Meta-analysis and Contemporary Practices of Pancreatic Surgeons.* Journal of Gastrointestinal Surgery 02/2015; 19(4)., DOI:10.1007/s11605-015-2765-8
17. Leela L. Paris, Jose L. Estrada, Ping Li, Ross L. Blankenship, Richard A. Sidner, Luz M. Reyes, Jessica B. Montgomery, Christopher Burlak, **James R. Butler**, Susan

- M. Downey, Zheng-Yu Wang, Matthew Tector, A. Joseph Tector: *Reduced human platelet uptake by pig livers deficient in the asialoglycoprotein receptor 1 protein*. *Xenotransplantation* 02/2015; 22(3)., DOI:10.1111/xen.12164
18. Jose L. Estrada, Greg Martens, Ping Li, Andrew Adams, Kenneth A. Newell, Mandy L. Ford, **James R. Butler**, Richard Sidner, Matt Tector, Joseph Tector: *Evaluation of human and non-human primate antibody binding to pig cells lacking GGTA1/CMAH/4GalNT2 genes*. *Xenotransplantation* 02/2015; 22(3)., DOI:10.1111/xen.12161
19. Ping Li, Jose L. Estrada, Christopher Burlak, Jessica Montgomery, **James R. Butler**, Rafael M. Santos, Zheng-Yu Wang, Leela L. Paris, Ross L. Blankenship, Susan M. Downey, Matthew Tector, A. Joseph Tector: *Efficient generation of genetically distinct pigs in a single pregnancy using multiplexed single-guide RNA and carbohydrate selection*. *Xenotransplantation* 09/2014; 22(1)., DOI:10.1111/xen.12131
20. **James R. Butler**, Eugene P. Ceppa, Michael G. House, Attila Nakeeb, C. Max Schmidt, Nicholas J. Zyromski: *Mo1625 Is Antacid Therapy After Pancreatoduodenectomy Necessary? Contemporary Global Practice of Pancreatic Surgeons*. *Gastroenterology* 05/2014; 146(5)., DOI:10.1016/S0016-5085(14)63898-1
21. **James R Butler**, George J Eckert, Nicholas J Zyromski, Michael J Leonardi, Keith D Lillemoe, Thomas J Howard: *Natural history of pancreatitis-induced splenic vein thrombosis: A systematic review and meta-analysis of its incidence and rate of gastrointestinal bleeding*. *HPB* 12/2011; 13(12)., DOI:10.1111/j.1477-2574.2011.00375.x

Book Chapters

1. Nicholas J. Zyromski, **James R. Butler**: *Management of Postoperative Bile Duct Stricture*. *Difficult Decisions in Hepatobiliary and Pancreatic Surgery*, 01/2016; ISBN: 978-3-319-27363-1, DOI:10.1007/978-3-319-27365-5_21
2. **James R Butler**, Nicholas J. Zyromski, *Primary Sclerosing Cholangitis*. The SCORE Portal. The Surgical Council on Resident Education. July 2009

Published Abstracts

1. Ladowski, JL, Santos RMN, Reyes L, Margtens GR, Butler JR, Sidner RA, Wang ZY, Cunningham C, Tector M, Tector AJ. A Swine for Human MHC Class I Swap: Implications for Xenotransplantation. *American Journal of Transplantation*. 2017(4)1: 613-614
2. Li, P., Smith, L.R., **Butler J.R.**, Irwin S.T., Kubal, C.A, Fridell, J.A, Ekser B. Scaddold-free 3D-bioprinting (3DBP) of genetically-engineered pig cells. *Xenotransplantation* 24(5):56. September 2017
3. Martens, G.R., Estrada, J., Sidner R.A., **Butler, J.R.**, Reyes, L., Ladowski, J., Kim, S., Tector, M, Adams, A., Tector AJ. Porcine GGTA1/B4GalNT2 gene knockout reduces antibody binding and achieves one year life-supporting renal xenograft in pig-to-rhesus model. *Xenotransplantation* 24(5):56. September 2017
4. Martens, G.R., Reyes, L., Sidner R.A **Butler, J.R.**, Ladowski, J., Tector, M, Tector AJ. Swine leukocyte antigen cross reactive group antigens. *Xenotransplantation* 24(5):56. September 2017
5. **Butler, J. R.**, E. P. Ceppa, M. G. House, A. Nakeeb, C. M. Schmidt and N. J. Zyromski (2014). "Mo1625 Is Antacid Therapy After Pancreatoduodenectomy Necessary? Contemporary Global Practice of Pancreatic Surgeons." *Gastroenterology* 146(5): S-1069.
6. Wang, Z.-Y., M. Tector, S. Nagai, **J. Butler**, R. Blankenship, S. Downey, J. Estrada, P. Li and A. Tector (2015). Effects of Immunosuppressives On Porcine Renal Microvascular Endothelial Cell-Activated Human T Cell Proliferation: A Cellular Model of Kidney Xenotransplantation In Vitro. *American Journal of Transplantation*, WILEY-BLACKWELL 111 RIVER ST, HOBOKEN 07030-5774, NJ USA.
7. Martens, G. R., P. Li, L. M. Reyes, J. L. Estrada, **J. R. Butler**, Z.-y. Wang, J. Ladowski, R. A. Sidner, M. Tector and J. A. Tector (2015). "Ggta1/cmah/ β 4galnt2 knockout porcine cells have reduced human antibody binding and achieved near background thresholds for most transplant patients and remaining antibody binding is partially attributable to swine leukocyte antigen." *Xenotransplantation* 22: S84.
8. Martens, G. R., P. Li, L. M. Reyes, J. L. Estrada, **J. R. Butler**, Z.-Y. Wang, J. Ladowski, R. A. Sidner, M. Tector and A. J. Tector (2015). GGTA1/CMAH/B4GALNT2 Knockout porcine cells have reduced human antibody binding and achieved near background thresholds for most transplant patients and remaining antibody binding is partially attributable to swine leukocyte antigen. *Transplantation*, LIPPINCOTT WILLIAMS & WILKINS TWO COMMERCE SQ, 2001 MARKET ST, PHILADELPHIA, PA 19103 USA.

9. Paris, L., R. Blankenship, R. Sidner, **J. Butler**, S. Downey, J. Estrada, M. Tector and A. Tector (2014). "Deletion of Cytidine Monophospho-N-Acetylneuraminic Acid Hydroxylase in Pigs Decreases Human Xenogeneic Platelet Uptake." *American Journal of Transplantation* 14: 415-416.
10. **Butler, J. R.**, N. J. Skill, D. Priestman, F. Platt, P. Li, J. L. Estrada, G. R. Martens, J. M. Ladowski, M. Tector and A. J. Tector (2016). "Porcine iGb3s gene silencing provides minimal benefit for clinical xenotransplantation." <http://dx.doi.org/10.1111/xen.12217>
11. Ladowski, J. M., **J. Butler**, G. Martens, L. Reyes, Z.-Y. Wang, J. Tune, M. Tector and A. J. Tector (2016). "A Novel Assay to Screen Porcine MHC Class II Antibodies in Potential Xenotransplant Recipients." *The FASEB Journal* 30(1 Supplement): 701.706-701.706.

Podium Presentations

1. **Butler JR**, Kays JK, House MG, Ceppa EP, Nakeeb A, Schmidt CM, Zyromski NJ. Outcomes of Pancreatoduodenectomy in the cirrhotic patient: risk stratification and meta-analysis. Presentation at the Americas Hepato-Pancreato-Biliary Congress. March 12, 2018. Miami FL.
2. **Butler JR**, Gene engineering: ethical and legal implications in the translational laboratory. Invited lecture to Indiana University School of Law, program in medical law. October 7th 2016.
3. Martens GR **Butler JR**, Estrada JL, Reys LM, , Ladowski JL, Tector M, Tector AJ. Porcine glycan gene inactivation reduces antibody binding for patients awaiting kidney transplant to clinically acceptable allotransplant levels. International Xenotransplantation Meeting. November 3rd 2015. Melbourne Australia.
4. **Butler JR**, Estrada JL, Reys LM, Martens GR, Ladowski JL, Tector M, Tector AJ. Efficient generation of targeted mutation using nuclease-directed homologous recombination. Podium Presentation at the 11th annual Accademic Surgical Congress February 8th 2016. Jacksonville FL.
5. Ladowski JL, Tchervenkov J, **Butler JR**, Martens GR, Blum J, Tector AJ. Effect of Swine Leukocyte Antigen Class II on Human PBMCs in a Mixed Cell Reaction. Podium Presentation at the 11th annual Accademic Surgical Congress February 8th 2016. Jacksonville FL.
6. **Butler JR**, Martens GR, Ladowski JL, Estes BW, Wang ZY, LI P, Tector M, Tector AJ. Silencing Porcine Carbohydrate Genes Significantly Reduces Human-Anti-Pig Cytotoxicity Profiles: An Alternative To Direct Complement Regulation.

Podium Presentation at the Western Surgical Association Scientific Session.
November 8th 2015. Nappa Valley, CA.

7. **Butler JR**, Estrada JL, Reys LM, Martens GR, Ladowski JL, Tector M, Tector AJ. Improving models of xenotransplantation: improving nuclease-based editing to create a clinical application. Invited lecture to Indiana University Department of Medical and Molecular Genetics. May 7th 2015.
8. **Butler JR**, LI P, Estrada J, Burlak C, Paris L, Tector M, Tector JA. Creation of Pigs Lacking of iGb3 and Isoglobo Glycosphingolipids: the Implication to Xenotransplantation. Podium presentation at the Indiana University General Surgery Research Conference. May 23, 2014. Indianapolis IN. Winner of the “Indiana University Best Translational Science 2014 Award.”
9. **Butler JR**, House MG, Ceppa EP, Nakeeb A, Schmidt CM, Zyromski NJ. The case for prophylactic antisecretory medication after pancreaticoduodenectomy. Podium Presentation at the 10th annual Academic Surgical Conference. February 5th 2015. LasVegas NV.
10. **Butler JR**, Paris LP, Blankenship R, Estrada J, Li P, Burlak C, Tector M, Tector AJ. The Fate of Human Platelets Exposed to Porcine Renal Endothelium: A Single-Pass Model of Platelet Uptake in Domestic and Genetically Modified Pig Kidneys. Podium Presentation at the American College of Surgeons Indiana Chapter Conference April 4th 2015. Indianapolis IN. Winner of the “R. Molton Broadman Award” for excellence in research.
11. **Butler JR**, Paris LP, Blankenship R, Estrada J, Li P, Burlak C, Tector M, Tector AJ. The Interaction between human platelets and porcine endothelium, effecting change through carbohydrate modification. Podium presentation at the Indiana University General Surgery Research Conference. May 5th, 2015. Indianapolis IN. Winner of the “Best Translational Science 2014 Award.”
12. **Butler JR**, House MG, Ceppa EP, Nakeeb A, Schmidt CM, Zyromski NJ. Marginal Ulcer after Pancreaticoduodenectomy: What can we be Doing Better? Podium Presentation at the American College of Surgeons Indiana Chapter Conference April 23 2014. Indianapolis IN. Winner of the “R. Molton Broadman Award” for excellence in research.
13. **Butler JR**, LI P, Estrada J, Burlak C, Montgomery J, Santos RM, Tector M, Tector JA. Efficient generation of genetically distinct pigs in a single pregnancy using multiplexed single-guide RNA and carbohydrate selection. Podium Presentation. American College of Surgeons Indiana Chapter Conference April 23 2014. Indianapolis IN.
14. **Butler JR**, Eckert GJ, Zyromski NJ, Leonardi MJ, Lillemoe KD, Howard TJ. The Natural History of Pancreatitis-Induced Splenic Vein Thrombosis: A Systematic

Review with Meta-Analysis of Incidence and Rate of GI Bleed. Presentation at the Americas Hepato-Pancreato-Biliary Congress. March 12, 2011. Miami FL.

15. Patel JB, Chauhan A, Howard TJ, **Butler JR**, Nakeeb A, Schmidt CM, Pitt HA, House MG, Lillemoe KD, Zyromski NJ. Pancreatoduodenectomy In Patients with Hepatic Cirrhosis: Is it Worthwhile? Presentation at the Americas Hepato-Pancreato-Biliary Congress. March 13, 2011. Miami FL.

Poster Presentations

1. **Butler JR**, Syed A. Ahmad, Matthew H. Katz, Jessica L. Cioffi, Nicholas J. Zyromski. A systematic review of the role of periaortitis in affecting margin status after pancreatoduodenectomy for pancreatic adenocarcinoma. Poster presentation at The Pancreas Club, May 6, 2017. Chicago IL.
2. **Butler JR**, Schmidt CM, Ceppa EP, House MG, Nakeeb A, Zyromski NJ. Is Antacid Therapy after Pancreatoduodenectomy Necessary? Contemporary Global Practice of Pancreatic Surgeons. Poster of Distinction. SSAT Digestive Disease Week Conference May 3, 2014. Chicago IL.
3. **Butler JR**, Ceppa EP, House MG, Nakeeb A, Schmidt CM, Zyromski NJ. Is Antacid Therapy after Pancreatoduodenectomy Necessary? Contemporary Global Practice of Pancreatic Surgeons. Poster presentation at The Pancreas Club, May 2, 2014. Chicago IL.

Membership

Alpha Omega Alpha- Member since 2017

The Society for Surgery of the Alimentary Tract. – Member since 2013

-Elected Member of SSAT Resident Education Committee May 2014-present.

American Association of Transplant Surgeons- Member since 2013

Association for Academic Surgery- Member since 2013

American Medical Association- Member since 2007

American College of Surgeons – Member since 2010

Indiana University General Surgery Residency Council. -Elected Member May 2014

Omicron Delta Kappa- Honorary society; Elected Member 2007, under the merits of leadership and scholarship, with consistent placement within the top 10 percent of the class.

Alpha Epsilon Delta- Honorary society; Elected Member 2007,

The Oxford Union Debating Society- Elected Member 2006.

Interests and Activities

Men's Lacrosse

2006 World Cup- Competed for Team Finland in the 2006 World Games.

Oxford University Men's Lacrosse- Selected to Southern England All-Star Team.

USA Team South- Competed in the 2005 Beijing international Tournament.

Davidson Lacrosse- All-American Honorable Mention, Two-time Academic All-Conference.